Pathogenic *Escherichia coli* hijack the host immune response

by

Kathrin Tomasek

October, 2021

A thesis submitted to the
Graduate School
of the
Institute of Science and Technology Austria
in partial fulfillment of the requirements
for the degree of
Doctor of Philosophy

Committee in charge:
Mario de Bono, Chair
Michael Sixt
Calin Guet
Daria Siekhaus
Urs Jenal

The thesis of Kathrin Tomasek, titled *Pathogenic Escherichia coli hijack the host immune response*, is approved by:

Supervisor: Michael Sixt, IST Austria, Klosterneuburg, Austria

Signature: _____

Co-supervisor: Calin Guet, IST Austria, Klosterneuburg, Austria

Signature: _____

Committee Member: Daria Siekhaus, IST Austria, Klosterneuburg, Austria

Signature: _____

Committee Member: Urs Jenal, University Basel, Basel, Switzerland

Signature: _____

Defense Chair: Mario de Bono, IST Austria, Klosterneuburg, Austria

Signature: _____

Signed page is on file

IST Austria Thesis, ISSN: 2663-337X

I hereby declare that this thesis is my own work and that it does not contain other people's work without this being so stated; this thesis does not contain my previous work without this being stated, and the bibliography contains all the literature that I used in writing the dissertation.

I declare that this is a true copy of my thesis, including any final revisions, as approved by my thesis committee, and that this thesis has not been submitted for a higher degree to any other university or institution.

I certify that any republication of materials presented in this thesis has been approved by the relevant publishers and co-authors.

Signature: _____

Kathrin Tomasek

October, 2021

Signed page is on file

Abstract

Bacteria-host interactions represent a continuous trade-off between benefit and risk. Thus, the host immune response is faced with a non-trivial problem – accommodate beneficial commensals and remove harmful pathogens. This is especially difficult as molecular patterns, such as lipopolysaccharide or specific surface organelles such as pili, are conserved in both, commensal and pathogenic bacteria. Type 1 pili, tightly regulated by phase variation, are considered an important virulence factor of pathogenic bacteria as they facilitate invasion into host cells. While invasion represents a *de facto* passive mechanism for pathogens to escape the host immune response, we demonstrate a fundamental role of type 1 pili as active modulators of the innate and adaptive immune response.

Acknowledgments

I am truly grateful to my supervisors Calin Guet and Michael Sixt for the scientific freedom they granted to me, allowing me to explore whatever I came up with – from the very initial idea of the project to the final version of the thesis. Both always critically questioned how my findings fit into the bigger context and encouraged me to think outside the box. Their constant mentorship and boundless support has helped me to become the scientist I am today.

I am very grateful for the members of my thesis committee, Urs Jenal and Daria Siekhaus. I especially want to thank Daria for her insightful comments on my research and the manuscript, and for encouraging me to take the next step in my career.

I am grateful to have had the possibility to spend my years at IST with many great group members and scientists, who eventually became my friends. In particular, I want to thank the following: Alex Leithner and Frank Assen, for their help in the lab; Ivana Glatzova for being a fantastic first student under my supervision (*#richandfamous*) and her patience with cell culture experiments (*"final_final_please work_experiment"*); Michi Lukesch for his protein-protein docking magic and the endless brainstorming sessions about CD14 during our enjoyable coffee breaks; Max Görtz and Vlad Gavra for being great students and for their patience with bacterial cloning; Bor Kavčič for being the master of *galk* selection/counter selection, for always reminding me how quick & dirty my bacterial cloning became over the years, and for always making time to read my texts (*"Would you mind if I just change a tiny aspect of it?", "Which one?", "The words."*); Jakob Wallner from BOKU for endless trials at the Octet and his great idea for the dot blot assay; Ingrid deVries for keeping the cell culture lab running; Tobi Bergmiller for being my mentor during my master thesis internship and for indirectly pushing me into my PhD research topic; Bella Tomanek for her critical questions and supportive chats throughout all these years; Anna Staron for showing me how to stay strong and calm during the sometimes long and painful submission process; "The youngsters" (Katya "The Tough" Krasnopeeva, Kirti "The Coffee Head Counter" Jain and Nathalie "Our Sunshine" Gruber) for making come to lab each day a pleasure; Rodi Römhild for being brave enough to become "magic banf jr." and for his amazing baking skills; Mike Hennessey-Wesen for always correcting my Denglisch and his encouraging words whenever they are needed; Mato Lagator for forwarding me articles about how patients with recurrent UTIs suffer both physically and psychologically, thereby showing me how important my research could be; Julian Stopp for endless chats on the bridge and all the cuddles in pre-pandemic times; Robert Hauschild and Saren Tasciyan for their magic hands in script writing; Freyja Langer from the Preclinical Facility, not only for her support during mouse experiments, but also for chats on other topics; Judit Singer from the BioImaging Facility for rescuing my flow cytometry experiments whenever the Canto misbehaved; Vanessa Zheden from the EM Facility for always borrowing me her forceps.

My final thanks go to my family and Mario for letting me explore my scientific curiosity and being supportive throughout many years of studies and research, and for at least pretending to understand what I talk about when I come home from a long day in the lab.

About the Author

Already early on, in school almost 18 years ago, microbiology and the tiny microbial world fascinated Kathrin Tomasek. Following her passion about microbiology, combined with a great interest in human genetics, Kathrin completed a BSc and MSc in Molecular Biotechnology at the University of Applied Sciences in Vienna (FH Campus Wien).

Her journey at IST Austria started already in January 2013 in the Group of Calin Guet where she performed her Master thesis research in the field of systems biology, supervised by Tobias Bergmiller. Although Calin was previously not convinced by the concept of a "Fachhochschule", he offered Kathrin a limited contract as a lab technician. However, the day Calin was supposed to sign her contract, Kathrin had to admit some bad news. Looking closely at her data and controls, she found that the bimodality she was studying during her internship was due to some issue with the buffer she used and thus what she had identified as bistability of the *mar* regulon in *E. coli* was an artifact. The results of this "artifact" were published in the *Journal of Biotechnology* few years later. From July 2013 till August 2015 Kathrin stayed in the Group of Calin as a research technician and worked on various projects together with different group members, two leading to successful publications in *Science* (Bergmiller et al) and *eLife* (Staron et al).

Finally, in 2015, Calin convinced Kathrin to start her PhD journey and she decided to do so at IST Austria. She came up with a project on pathogen-host interactions as she wanted to understanding how the two worlds, the prokaryotic and the eukaryotic, interact with each other how and how opportunistic pathogens cause persistent infectious in the presence of the immune system. Kathrin managed to convince Calin and Michael Sixt, who is working in the field of immune cell migration, to co-affiliated her. During her PhD studies, Kathrin presented her research at several conferences (16th International Conference on Innate Immunity (poster) – Greece 2019, Actualities and perspectives in invasive medicine (invited speaker) – Romania 2019, EMBO symposium – New Approaches and Concepts in Microbiology (poster, virtual) – Germany 2021 and CSHL meeting – Microbial Pathogenesis & Host Response (poster, virtual) – USA 2021).

List of Publications

Tomasek K, Leithner A, Glatzova I, Lukesch MS, Sixt M and Guet CC. Type 1 piliated uropathogenic *E. coli* hijack the host immune response by binding to CD14 – https://doi.org/10.1101/2021.10.18.464770

Table of Contents

List of Figures

List of Tables

List of Abbreviations

DC dendritic cell

LPS lipopolysaccharide

MHCII major histocompatibility complex II

UPEC uropathogenic *Escherichia coli*

UTI urinary tract infection

1 Introduction

1.1 Ecology and evolution of Escherichia coli and what it needs to become a pathogen

Even though *Escherichia coli* is by far the best studied model organism, we are just now grasping deeper insights into its ecology and evolution, particularly in terms of bacteria-host interaction. Although *E. coli* has not undergone massive changes in morphology during its evolution, it exhibits a large degree of genetic diversity across strains. This diversity includes also accessory genetic material (genes not present in all strains) which continuously and considerably alter the specific regulatory networks of each strain (Touchon et al. 2009). Strains of *E. coli* are as diverse genetically as are the diseases they cause, ranging from diarrhea to meningitis, from asymptomatic bacteriuria to lethal urosepsis (Donnenberg 2013). However, not every *E. coli* strains cause disease; some reside in the mammalian gut as commensals, existing in symbiosis with their host (Souza et al. 2002).

In principle, any commensal *E. coli* has the potential to evolve into a pathogen following *virulence traits* (Wirth et al. 2006). For a long time it was thought that pathogenic *E. coli* exhibit a higher mutation rate than non-pathogenic strains, allowing these strains to combat the challenges faced during pathogenesis (Souza et al. 2002). However, the mutational frequency is similar between commensal and pathogenic *E. coli* in humans. This high level of genetic plasticity allows the bacterium to adapt rapidly to different environments and ecological niches.

1.1.1 *Evolved* to perform a specific function in a specific environment – the adapted virulence trait

Adapted virulence traits evolved specifically to increase the fitness of a pathogen during the infection (Donnenberg 2013).

An example of an adapted virulence trait is the acquisition of foreign genetic material through horizontal gene transfer (Oelschlaeger et al., 2002). The genetic material can be exchanged within or even across species and the genetic information shared can encode for antibiotic resistance or various virulence factors (Souza et al. 2002). These include toxins or adhesion filaments, but even prophages or even bigger groups of genes, so called pathogenicity islands (Donnenberg 2013).

Another example is that of pathoadaptive mutations which alter the existing genome, rather than the evolution of new genes or gene functions (Donnenberg 2013). Such mutations are, for example, found in the lipopolysaccharide (LPS) structure, the flagellum or pili components (Weissman et al., 2006; Donnenberg, 2013). These mutations include point-mutations to amplifications and even loss of function mutations.

1.1.2 *Fit* to perform a specific function in a specific environment – the pre-adapted virulence trait

Pre-adapted virulence traits, although originally evolved for a non-virulent function, increase the fitness of the pathogen (Donnenberg 2013).

A prime example of a pre-adapted trait is that of certain adhesion filaments, such as type 1 pili which I will address throughout this thesis. Both commensal and pathogenic *E. coli* use type 1 pili to adhere to host epithelial cells in their respective host niche (Wiles et al. 2008; Spaulding et al. 2017). Type 1 pili are encoded in the genome of almost all *E. coli* strains – pathogenic and non-pathogenic alike (Vigil et al. 2011) and were shown to increase fitness of the pathogenic strains (Mulvey et al. 1998; Connell et al. 1996; Weissman et al. 2006; Wright et al. 2007).

Type 1 pili are encoded in the *fim* operon that harbors all genes responsible for synthesis, assembly and regulation of the pilus organelle (Schwan 2011). Expression of the operon is regulated by a mechanism called phase variation: site-specific recombinases place the *fimA* promoter either in the phase-ON or phase-OFF orientation, resulting in the piliated or non-piliated phenotype of the bacteria, respectively. Most non-pathogenic *E. coli* express two site-specific recombinases but some pathogenic ones express additional recombinases that affect type 1 pili expression – for example the uropathogenic *E. coli* strain, CFT073, expresses three additional recombinases (Bryan et al. 2006).

1.2 Opportunistic pathogens and how they have mastered the balance between a "commensally" and pathogenic lifestyle

Pathogenic *E. coli* are divided into three pathogenic linages – professional, accidental, and opportunistic pathogens (Donnenberg 2013). The category into which a strain falls depends on the ability of the strain to cause disease, contributing to its continued survival in nature.

Professional pathogens such as *Shigella*, enteroinvasive *E. coli* (EIEC), enterotoxic *E. coli* (ETEC), and enteropathogenic *E. coli* (EPEC), need to cause diseases to continue circulating in nature (Donnenberg 2013). While these pathogens can colonize humans asymptomatically, they depend on symptomatic individuals to spread from host to host. Professional pathogens are highly adapted to the pathogenic lifestyle by adapted virulence traits, making them highly infectious and easily transmissible.

For accidental pathogens, such as enterohemorrhagic *E. coli* (EHEC), their virulence can be seen as an ecological accident and an evolutionary dead-end, as symptomatic infections usually do not promote their transmission between hosts (Donnenberg 2013). Additionally, these pathogens are also unable to repopulate their original host environment. Virulence factors found among those pathogens are mainly of pre-adapted nature.

Opportunistic pathogens, such as extraintestinal-pathogenic *E. coli* (ExPEC), can continuously circulate in humans as asymptomatic colonizers almost *"commensally"* and cause symptomatic infections only occasionally (Donnenberg 2013). These pathogens are able to

recolonize their original host environment, but are also shed in high numbers during infections which causes a spread between hosts. Both types of virulence traits, adapted and pre-adapted, are found among opportunistic pathogens.

Uropathogenic *E. coli* (UPEC) are a prime example of opportunistic pathogens and they use type 1 pili as pre-adapted virulence traits to increase their fitness in the urinary tract (Mulvey et al. 1998; Connell et al. 1996; Weissman et al. 2006; Wright et al. 2007). The tight and coordinated expression of type 1 pili by phase variation seems to be an important component in the adaptation to their pathogenic lifestyle (Bayliss 2009). In their original niche, UPECs adhere to epithelial cells in the upper portion of crypts and small villi in the colon using type 1 pili (Spaulding et al. 2017). In the host intestine, these *E. coli* manage to persist for long periods of time in an almost commensal state (Grant and Hung 2013; Donnenberg 2013). However, in order to populate a different host niche, such as the bladder, the bacteria need to downregulate type 1 pili expression in favor of flagella expression, to switch from a sessile lifestyle to a motile one (Lane et al. 2007). In urine, type 1 pili expression is also locked in the phase-OFF state (Greene et al. 2015), whereas contact to epithelial cells in the bladder switches expression on and even locks it in the phase-ON state, which allows the pathogens to adhere to the host cells (Greene et al. 2015; Lim et al. 1998). In this early stage of infection, UPECs circumvent clearance by the host immune system using type 1 pili to invade into epithelial cells where they replicate (Hunstad and Justice 2010). From these protective niches, the pathogens can reestablish the infection leading to persistent or recurrent infections (Grant and Hung 2013; Hunstad and Justice 2010). The unique potential to blur the lines between commensal and pathogenic lifestyle makes opportunistic pathogens, in particular UPECs, a very interesting model organism to study persistent or recurring infections.

1.3 The host immune system – several lines of defense against infections

The immune system consists of innate and adaptive immunity. The innate immune system represents the first line of defense against invading pathogens, whereas the adaptive immune system leads to the development of an immunological memory (Chaplin 2010). The immune system not only consists of cells, but also includes proteins and small molecules, such as cytokines, chemokines and reactive free radical species and these proteins are secreted by infected cells but also by the immune cells themselves.

The innate immune system already starts at the physical barriers of the body, such as epithelial cell layers and the mucus layer overlaying the epithelium (Chaplin 2010). Innate immune cells, such as neutrophils, macrophages and monocytes, are the major phagocytic cells and engulf microbes, digest them and represent processed antigens to other immune cells, mainly from the adaptive immune system. Therefore, these cells play a key role in activation of the adaptive immune response.

The adaptive immune response performs specific actions against the target antigen and therefore against the invading pathogen (Chaplin 2010). The response of the adaptive immune system can be split into the antibody response, carried out by B lymphocytes, and the cell-mediated response, carried out by T lymphocytes. B and T cells reside in the secondary lymphoid tissues, such as lymph nodes, and once they encounter an antigen

processed and presented by another immune cell they become activated. Although B cells are the antibody producing cell type, T cells provide help for B cell maturation and antibody class switch (Chaplin 2010). Additionally, T cells also identify and neutralize infected host cells to control the infection.

Recruitment of cells of the innate as well as the adaptive immune system to lymph nodes but also to the sites of pathogen invasion in the periphery is essential for the antimicrobial defense (Chaplin 2010) (Figure 1-1). Chemokines, cytokines and cellular adhesion molecules mediate this process of migration and adhesion.

The complex interplay of the innate and the adaptive immune system highlights the difficulty to tailor a specific response against an invading pathogen (Chaplin 2010). Any disturbance of the system might lead to a tipped balance between action and reluctance, leading to either massive tissue damage if the immune response exaggerates or to persistent infections if the response is too weak.

1.4 The molecular mechanism behind pathogen recognition

The innate and adaptive immune systems of the host recognize infections and react to them in fundamentally different ways, given how differently the cells of each system trade with the molecular diversity of microorganisms (Medzhitov 2007).

Recognition of an infection by the adaptive immune cells is mediated by the antigen receptors (Medzhitov 2007). These receptors are highly diverse with random, yet still narrow specificities against each microbial antigen. This specificity is achieved by somatic recombination and clonal expansion of pathogen-specific receptors, building the basis for the immunological memory of the adaptive immune response.

Recognition of an infection by innate immune cells is mediated by pattern recognition receptors (PRRs) which have broad specificities, yet detecting conserved molecular structures of groups of microorganisms (eg. LPS of Gram negative bacteria) (Medzhitov 2007). These conserved features are referred to as pathogen-associated molecular patterns (PAMPs), although they can be found on pathogenic and non-pathogenic microorganisms. The best characterized PPRs are Toll-like receptors (TLRs) which recognize a broad spectrum of microbial ligands, with TLR4 being the key receptor recognizing LPS (Vaure and Liu 2014). TLRs are transmembrane receptors eliciting inflammatory and antimicrobial responses by activating tissue-residing immune cells to produce pro-inflammatory cytokines or antimicrobial proteins or peptides.

PRRs couple the innate and adaptive immune response, as recognition and activation of innate immune cells via PRRs leads to activation of adaptive immune cells (Medzhitov 2007). For example, T cells in the lymph node are activated by dendritic cells (DCs) (Figure 1-1): DCs reside in most peripheral tissues and constantly monitor their close environment for invading pathogens. Upon pathogen encounter through PRRs binding PAMPs on the bacterial surface, DCs engulf the bacteria by phagocytosis and process antigenic peptides on their surface in the

major histocompatibility complex II (MHC II) molecules. This leads to activation and maturation of DCs, accompanied by production of cytokines and upregulation of specific cell-surface signals. Matured DCs migrate from the site of infection to the closest lymph node through lymph vessels following chemokine gradients in the tissue and lymph vessels themselves. In the lymph node, the DCs entering also activate lymph-node residing DCs leading to a potentiation of the signal (Lindquist et al. 2004; Inaba et al. 1998). The DCs present the pathogen-derived antigen in the MHC II and upregulated cell-surface molecules, such as co-stimulatory molecules, to T cells in the lymph node, finally leading to activation of the adaptive immune response.

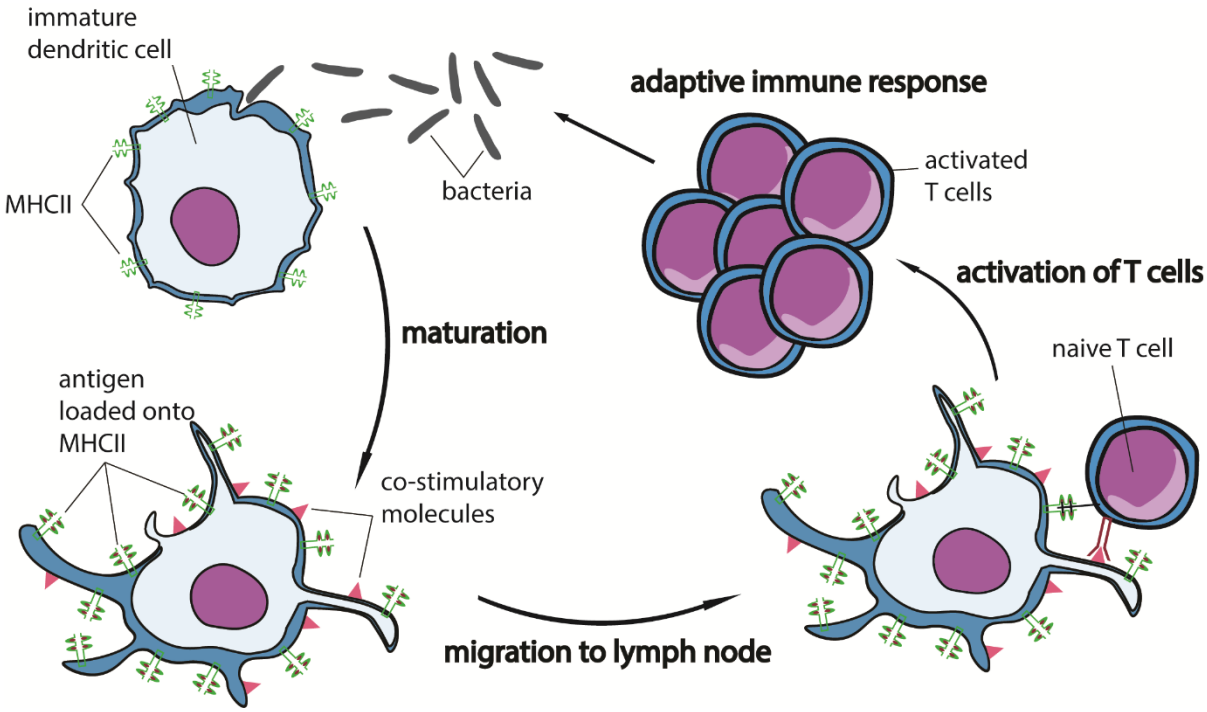

Figure 1-1**:** *Antimicrobial defense illustrated at the interaction of dendritic cells and T cells.*

Immature dendritic cells (DCs, innate immune cells) phagocytose invading bacteria in the periphery and mature by loading processed bacterial peptides into the major histocompatibility complex II (MHCII) and by upregulation of co-stimulatory molecules. Matured DCs migrate to the lymph node to interact with and activate naïve T cells (adaptive immune cells). Activated T cells proliferate into high numbers to mount an adaptive immune response against the invading pathogen.

1.5 Persistent or recurring infections and the role of the host immune response

Several factors contribute to persistent or recurring bacterial infections, some can be attributed to the pathogenic bacteria, others to the response of the host immune system.

Upon bacterial invasion epithelial cells secrete cytokines, soluble signal molecules capable of attracting and activating cells of the host immune system including polymorphonuclear leukocytes, macrophages and dendritic cells. Additionally, highly infected epithelial cells undergo exfoliation, a process consisting of apoptosis followed by detachment from the bladder surface to remove those cells with the flow of urine (Hunstad, Justice 2010). However, exfoliation not only removes infected superficial cells from the bladder surface but it also leaves the underlying cells exposed to extracellular UPEC. Although the invasion of epithelial cells by UPECs is a relatively rare event (Mysorekar and Hultgren 2006), it allows pathogens to limit exposure to the host immune system and to establish a protected niche from which they can cause symptomatic infections and reestablish the infection, leading to persistence (Hunstad and Justice 2010; Grant and Hung 2013).

Additionally, other pathogenic *E. coli* utilize several strategies to subvert innate immunity, thereby avoiding clearance by the host and enabling sustained persistence (Donnenberg 2013). For example, EPEC suppress activation of the transcription factor nuclear factor-κB (NF-κB) and thereby prevent the production of pro-inflammatory chemokines and cytokines (Vossenkämper et al. 2010). The pathogen *Shigella* can efficiently evade autophagy, a mechanism used by eukaryotic cells to degrade their own defect organelles as well as intracellular pathogens (Ogawa et al. 2005). UPECs were even found to interfere at the interface between innate and adaptive immunity: during urinary tract infections (UTIs), tissue-resident mast cells secrete high amounts of interleukin-10 (IL-10), an immuno-suppressive cytokine (Chan et al. 2013) that drives the differentiation of regulatory T cells (Hsu et al. 2015).

Additionally, the host immune response may unintentionally create protected niches, leading to persistent or recurring infections. For example, bladder-residing macrophages sequester UPECs before antigen-presenting cells, such DCs, come into action (Mora-Bau et al. 2015). Additionally, the distinction between commensal and pathogenic bacteria might not always be obvious to the host immune system, given that some bacteria express the same surface molecules, such as LPS, irrespective of their pathogenicity. The host therefore evolved towards commensal bacteria by the compartmentalization of receptors recognizing such surface molecules and by ignoring commensal microbial products or by attenuating pro-inflammatory signaling (Magalhaes et al. 2007). Also antibodies, usually part of the humoral adaptive immune response to pathogens, were shown to coat commensal bacteria of the microbiota in the intestinal lumen to stabilize the commensals ability to colonize the intestine (Caruso et al. 2020). Typically, T cell dependent or independent IgA antibodies bind with low affinity to microbial LPS, DNA or flagellar antigens of gut microbiota. However, these polyreactive IgA antibodies may also enable cross-reactivity to pathogens, potentially contributing to protective immunity during infections (Bunker and Bendelac 2018).

The combined effects of subverting the host immune response and establishing a protected niche inside the host, either intentionally by the pathogen or unintentionally by the host, increase the pathogen's chance to establish persistent infections.

1.6 Questions addressed in this thesis

In this thesis, I asked whether type 1 pili play a role in manipulating host immunity and thereby facilitate persistent or recurring infections by dissecting the underlying molecular mechanism between the interaction of UPECs and dendritic cells.

In chapter two of this thesis, I will show how type 1 piliated UPECs target all three functional keystones of DCs that are critical for the activation of naïve T cells – migration of DCs to the lymph node, the physical interaction with T cells, and the ability to activate T cells by expressing co-stimulatory molecules. I identified the CD14 receptor on DCs as a previously undescribed binding partner of FimH, the protein located at the tip of the type 1 pilus. The FimH amino acids involved in CD14 binding are highly conserved across pathogenic and non-pathogenic *E. coli*, making this interaction a potential target for interfering with persistent and recurrent infections.

In chapter three of this thesis, I will show that type 1 pilated UPECs lead to a strong non-cell autonomous effect. This non-cell autonomous effect was observed between differentially stimulated DCs by activation of the NFAT pathway and secretion of immuno-modulating cytokines, but also when DCs stimulated with type 1 piliated UPECs were re-introduced into the non-tolerogenic environment of the host. Interestingly, it seems that type 1 piliated UPECs activate the humoral immune response but non-piliated UPEC dampen the response.

In chapter four of this thesis, I will show that the immune modulatory effects of type 1 piliated pathogens strongly depend on the genetic background of the pathogen. This dependency on the genetic background is not only true *inter-special*, for example between *E. coli* and *Klebsiella*, but also *intra-special*, meaning between different clinical isolates of UPECs. Additionally, given that FimH is necessary but not sufficient to affect behavior of DCs, I was interested in identifying the "other factor(s)" needed to dampen the immune response during UTIs.

2 Type 1 piliated uropathogenic *E. coli* hijack the host immune response by binding to CD14

This chapter was prepared as a manuscript by Tomasek K, Leithner A, Glatzova I, Lukesch MS, Sixt M and Guet CC. Type 1 piliated uropathogenic *E. coli* hijack the host immune response by binding to CD14 – https://doi.org/10.1101/2021.10.18.464770

Supplementary Figures can be found at the Appendix of the thesis. Supplementary Tables and Files will be put online on the IST repository by the time the manuscript is accepted for publication.

2.1 Introduction

Cells of metazoan organisms constantly interact with a wide diversity of bacterial species that populate the host organism internally as well as externally. Therefore the host immune response is faced with a non-trivial problem – accommodate beneficial commensals and remove harmful pathogens (Hooper and Macpherson 2010). The difficulty of this task lies in the fact that most of the molecular patterns, such as lipopolysaccharide (LPS) or surface organelles such as pili and flagella, are conserved between commensal and pathogenic bacteria. The main difference between commensal and pathogenic strains is the ability of the latter to hijack host cell functions for their own benefit (Magalhaes et al. 2007). Consequently, the host immune system uses complex discrimination strategies, such as spatial compartmentalization of the receptors recognizing pathogen signatures and concurrent sensing of molecular patterns associated with host-damage. The host discrimination ability is not always perfect, as pathogens can persist asymptomatically in the host for long periods of time or cause symptomatic acute or chronic infections in some individuals, but not in others (Grant and Hung 2013). For example, the commensal bacterium *Escherichia coli*, one of the main residents of the mammalian intestine, occasionally causes clinical infections, especially when the bacteria acquire virulence traits and thus manage to populate extraintestinal host niches (Magalhaes et al. 2007). Usually disease progression does not pose a dead end to such opportunistic pathogens, since bacteria are shed in high numbers during the infection, allowing the pathogen to populate new environments, a new host or even recolonize their original host niche – the intestine (Donnenberg 2013).

In principle, any commensal *E. coli* has the potential to evolve into a pathogen by acquiring virulence traits (Wirth et al. 2006). Those traits can be either adapted, namely evolved specifically to increase the fitness of a pathogen during the infection, or pre-adapted, meaning even though they increase the fitness of the pathogen they were originally evolved for a non-virulent function (Donnenberg 2013). Examples of adapted traits are the acquisition of pathogenicity islands through horizontal gene transfer (Oelschlaeger et al., 2002) or pathoadaptive mutations, such as changes in the LPS, flagellum or pili components (Weissman et al., 2006; Donnenberg, 2013). A prime example of a pre-adapted trait are type 1 pili. Both commensal and pathogenic *E. coli* (Shawki and McCole 2017; Croxen and Finlay 2010), but also other *Enterobacteriaceae* (Struve et al. 2008; Kolenda et al. 2019), use type 1 pili to adhere to host cells in their respective ecological niches (Spaulding et al. 2017). Type 1 pili undergo a constant and reversible change in their expression due to phase variation which

allows populations of isogenic bacteria to exhibit controlled genotypic and phenotypic variation (Bayliss 2009). In the case of type 1 pili, site-specific recombinases place the *fimA* promoter either in the phase-ON or phase-OFF orientation, resulting in piliated or non-piliated bacteria (Schilling et al. 2001). UPECs have mastered the use of phase variation as a remarkable genetic mechanism of plasticity for their advantage, since type 1 pili expression is tightly regulated by the host environment. For example, growing UPECs *in vitro* in human urine locks expression in the phase-OFF state (Greene et al. 2015), whereas adhesion to host cells has been shown to lock expression in the phase-ON state (Greene et al. 2015; Lim et al. 1998). Phase variation greatly adds to the virulence and fitness of UPECs by generating heterogeneity among the bacterial population where individual cells switch back and forth between the type 1 piliated and non-piliated phenotype (Bayliss 2009; Wright et al. 2007). Type 1 pili are necessary for the persistent and therefore recurring infection of the bladder (Hunstad and Justice 2010; Wright et al. 2007), but also other persistent bacterial infections (Shawki and McCole 2017).

Several mechanisms are known to contribute to persistent or recurring infections, one of which is the residing of pathogenic bacteria within a protected niche (Grant and Hung 2013). Such niches can be physical structures when the pathogen invades host cells to hide from the immune response (Grant and Hung 2013; Donnenberg 2013). For example, UPECs invade host epithelium cells in the bladder using type 1 pili, propagate intracellularly and compromise the host defense barriers (Hunstad and Justice 2010; Martinez et al. 2000). Strikingly, also the host immune response may unintentionally create protected niches. For example, bladder residing macrophages sequester UPECs before antigen-presenting cells, such as dendritic cells (DCs), come into action (Mora-Bau et al. 2015).

DCs are the key cell type connecting the innate and adaptive immune response (Mellman and Steinman 2001). Distinct subtypes of DCs, expressing different surface receptors (Merad et al. 2013), reside in every tissue of the host and DCs were also identified at the epithelial junction of the bladder (Schilling et al. 2003). In response to an infection, these resident DCs together with newly recruited inflammatory DCs sense and ingest pathogens. Subsequently, they start to secrete immune modulatory cytokines and migrate from the site of infection to the draining lymph nodes where they present acquired and processed antigens to T cells, thus triggering the adaptive immune response. However, even if the host immune system manages to detect the pathogen, eradication of the infection is not guaranteed. Pathogens utilize several strategies to subvert innate and adaptive immunity, thereby avoiding clearance by the host and establishing persistent infections (Donnenberg 2013). For example, UPECs were shown to interfere at the interface between innate and adaptive immunity: after contact with UPECs during urinary tract infections (UTIs), tissue resident mast cells secrete high amounts of interleukin-10 (IL-10), an immuno-suppressive cytokine (Chan et al. 2013), that drives the differentiation of regulatory T cells (Hsu et al. 2015). The combined effect of subverting the host immune response and establishing a protected niche inside the host greatly increases the ability of pathogens to cause persistent infections.

Here, we asked whether type 1 pili play a role in manipulating host immunity and thereby facilitate recurring bacterial infections by dissecting the underlying molecular mechanism between the interaction of uropathogenic *E. coli* and dendritic cells.

2.2 Results

2.2.1 Type 1 piliated UPEC inhibit T cell activation and proliferation by decreasing expression of co-stimulatory molecules on dendritic cells

To study the influence of type 1 pili on the adaptive immune system, we engineered bacteria with and without pili. The *fim* genes that produce the molecular components of the type 1 pilus are part of an operon on the *E. coli* chromosome (Figure 2-1A and B) whose expression is regulated by phase-variation. We generated stable phase-locked bacterial mutants by locking the fim switch (*fimS*) either in the phase-ON orientation, resulting in constitutive expression of the type 1 pilus, or in the phase-OFF orientation, blocking expression of the pilus (hereafter simply termed ON and OFF, respectively). To achieve this, we deleted the 9 bp long recognition site for the site-specific recombinases FimB and FimE in the internal repeat region upstream of the *fimS* element in either orientation (Figure 2-1C). The presence and absence of type 1 pili was confirmed by electron microscopy and yeast-agglutination assay (Figure 2-1D). Additionally, electron microscopy indicates absence of any other pili, such as p fimbriae, under the chosen growth conditions since the OFF mutant appears bald (Figure 2-1D, right panel).

Since the adaptive immune response seems to be limited during persistent or recurring infections (Magalhaes et al. 2007), such as recurring bladder infections (Abraham and Miao 2015), we asked if activation and proliferation of naïve T cells *in vitro* is altered upon stimulating DCs with the genetically constructed UPEC ON or OFF mutants. The activation of Ovalbumin (OVA) specific $CD4^+$ T cells (Barnden et al., 1998), as assessed by CD69 receptor upregulation and CD62L receptor downregulation, was massively reduced when DCs were stimulated with OVA and UPEC ON mutants, compared to OVA and UPEC OFF mutants (Figure 2-1E). Accordingly, the number of proliferating T cells was also strongly decreased (Figure 2-1F).

Cellular identity, such as the CD11c surface marker and surface levels of MHCII, the hallmark of DC activation, was only very mildly altered upon exposure to UPEC ON (Supplementary Figure 1C and D). Beyond presentation of MHCII, the expression of co-stimulatory molecules on DCs is decisive for effective T cell priming and differentiation into effector cells (Banchereau and Steinman 1998). We therefore analyzed surface expression of CD40, CD80 and CD86 after ON and OFF stimulation and found significantly decreased levels after ON stimulation (Figure 2-1G).

These data suggest that type 1 piliated UPECs prevent effective activation of the adaptive immune response by decreasing expression of co-stimulatory molecules on DCs and thus restrict their ability to activate T cells.

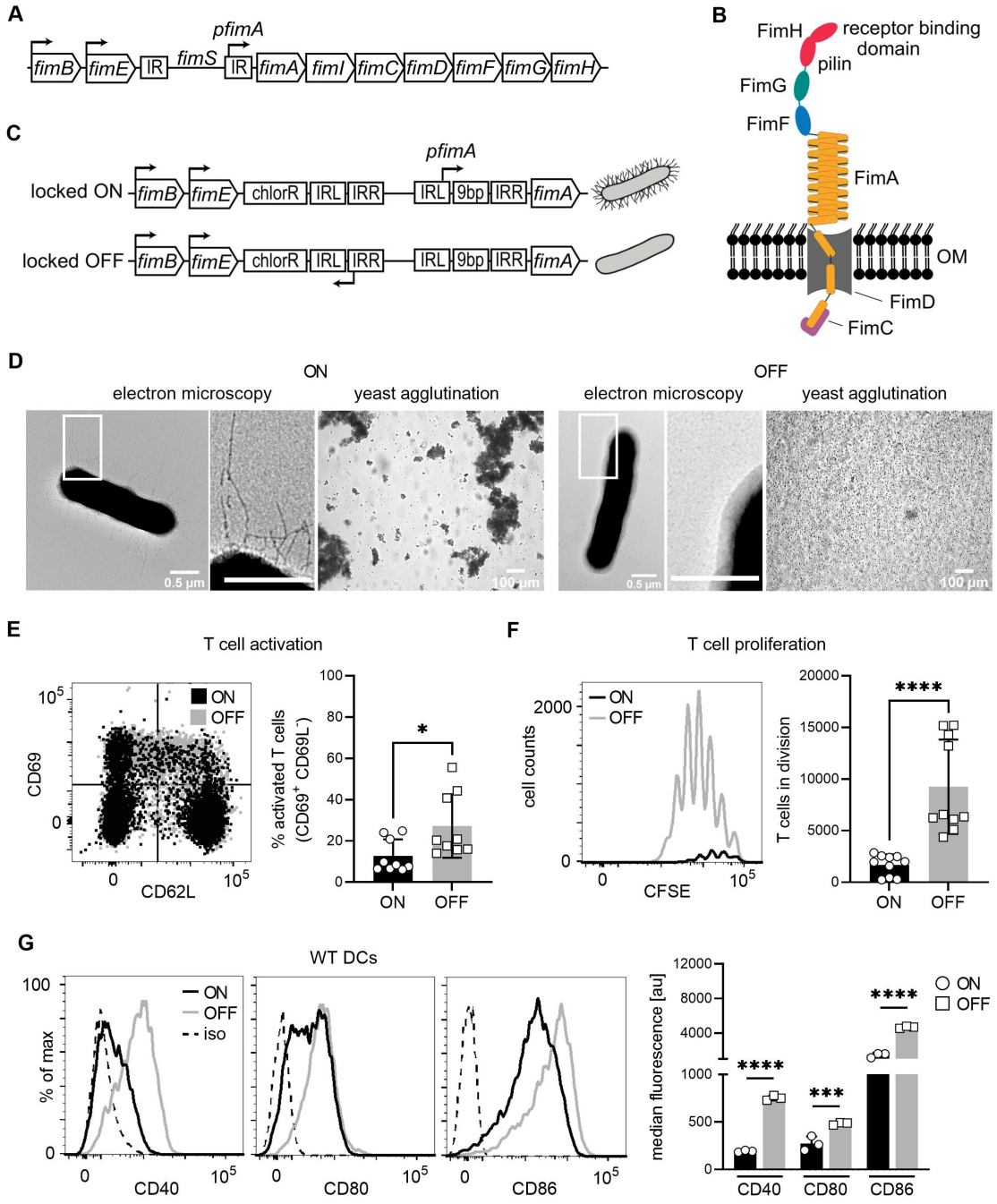

Figure 2-1: *Type 1 piliated UPECs inhibit T cell activation and proliferation by decreasing co-stimulatory molecules on DCs.*

A. *Type 1 pili genes are expressed from the fim operon. Phase variation of the fim switch (fimS) harboring fimA promoter (pfimA) drives expression. fimB and fimE genes express site-specific recombinases, FimB and FimE respectively, inverting the fimS region by binding to the inverted repeats (IR).* ***B.*** *Type 1 pili consist of several repeating units of the rod protein FimA, two adaptor proteins FimF and FimG, and the tip protein FimH. Fimbrial- and a receptor-binding domain of the two-domain FimH protein are shown. FimD, outer membrane usher. FimC, chaperone.* ***C.*** *Phase-locked mutants were generated by deleting the 9 bp recognition site for the site-specific recombinases in the left inverted repeat region of the fimS in either ON or OFF orientation by introducing FRT sites resulting in piliated and non-piliated bacteria (see Methods).* ***D.*** *ON (left panel) and OFF mutants (right panel). Electron microscopy images, with zoomed in regions (white boxes) marked in inlays, and yeast agglutination assay.* ***E.*** *Dot plot of CD69 and CD62L expression on T cells after co-culture with ON (black) and OFF (grey) stimulated DCs (left panel). Quantification of $CD69^+$ $CD62L^-$ T cell frequencies (right panel).* ***F.*** *CFSE dilution profile of T cells after 96h of co-culture with ON (black) and OFF (grey) stimulated DCs (left). Quantification of T*

cells in division (right panel). ***G.*** *Expression level of co-stimulatory molecules (CD40, CD80, CD86) of WT DCs after stimulation with ON (black) and OFF mutants (grey) (left panel; iso – isotype control). Quantification of median fluorescence values of co-stimulatory molecules (right panel).*

2.2.2 Type 1 piliated UPEC decrease dendritic cell migratory capacity and increase T cell contact times by triggering integrin activation

Beyond presentation of the antigen in the context of co-stimulatory factors, two additional cell biological parameters are essential for the priming of T cells. First, DCs have to migrate from the site of antigen encounter and uptake (usually peripheral tissues) to the site of antigen presentation (e.g. lymph nodes), where they meet T cells. This migration step is directionally guided by chemokines and highly efficient even in the absence of adhesive interactions with the extracellular matrix (Lämmermann et al. 2008). Second, T cells have to physically interact with DCs in order to probe their surface for antigen presentation and co-stimulation. Hence, the contact dynamics between DCs and T cells are essential parameters determining T cell activation and proliferation (Bousso 2008).

We first investigated DC-T cell contacts using live cell microscopy and found that UPEC ON mutants increased the antigen specific contact times between DCs and naïve $CD4^+$ T cells, compared to UPEC OFF mutants. Even after 6 h of co-culture a large fraction of T cells was unable to dissociate from DCs (Figure 2-2A). This was specific to antigen-bearing DCs, as in the absence of OVA contact times were short and indistinguishable between ON and OFF stimulation. Activation of β2 integrins, specifically CD11b, on DCs was shown to increase the duration of cell-cell contacts by binding to its counter receptor ICAM-1 on T cells, leading to a decrease in the activation of T cells (Varga et al. 2007). We therefore investigated if the activation status of CD11b on DCs was affected after stimulation with ON mutants. We analyzed total and active levels of CD11b using the activation-independent antibody M1/70 and CBRM1/5 antibody, which recognizes the active conformation of human, but also mouse CD11b ((Oxvig et al. 1999) and (Supplementary Figure 2-2A)). We found that UPEC ON stimulation shifted CD11b to the active conformation when compared to UPEC OFF or LPS stimulation (Figure 2-2B and Supplementary Figure 2A).

In line with the finding that type 1 piliated UPEC enhanced CD11b activity, ON mutants triggered tight adhesion of DCs to serum-coated surfaces (Figure 2-2C). This surface immobilization was integrin mediated, as for *β2* integrin knockout DCs the differential adhesion was lost (Figure 2-2C and Supplementary Figure 2C). (Notably, *β2* integrin deficient DCs showed increased β1 integrin-mediated background-binding (Supplementary Figure 2B)). We next asked whether UPEC ON stimulation interferes with the migratory capacity of DCs. We performed *in vitro* migration assays where DCs migrate in cell derived matrices (Kaukonen et al. 2017) and found diminished migration after stimulation with ON mutants when compared to OFF mutants (Figure 2-2D). The same effect on the migratory capacity we observed in crawl out assays in physiological tissue (Stösel et al. 1997). Here, the ventral halves of explanted mouse ears were repeatedly exposed to either UPEC ON or OFF bacteria during 48 h. After stimulation with ON mutants, fewer endogenous DCs were found inside lymph vessels as compared to OFF stimulation (Figure 2-2E). In ears harvested from β2

knockout mice the migration defect was rescued and similar levels of *β2*$^{-/-}$ DCs migrated into the lymph vessels after ON and OFF stimulation (Figure 2-2E and Supplementary Figure 2D). These data suggest that hyperactive CD11b hinders both migration and T cell activation of DCs by immobilizing them to extracellular matrix proteins like fibrinogen or cellular ligands like ICAM-1. This integrin gain of function phenotype is in line with findings that pharmacological approaches which activate integrins have stronger *in vivo* effects on leukocyte migration than approaches to inhibit integrin function (Maiguel et al. 2011). To test if immobilization by hyperactive CD11b is indeed causative for the loss of migration upon UPEC ON stimulation, we measured migration of DCs in 3D collagen gels. Here, DCs efficiently migrate in an integrin-independent manner (Lämmermann et al. 2008) and hyperactive CD11b, which does not bind to collagen 1, should not be able to immobilize the cells. We found that the migration speed of ON and OFF stimulated DCs in a 3D collagen assay was indistinguishable (Supplementary Figure 2E).

Finally, we asked if activation of β2 integrins maps upstream of the observed detrimental effect on co-stimulatory molecule expression after stimulation with UPEC ON mutants. *β2*$^{-/-}$ DCs still expressed lowered levels of co-stimulatory molecules after ON stimulation when compared to OFF stimulation (Figure 2-2F), suggesting that downregulation of co-stimulatory molecules does not depend on integrin activation.

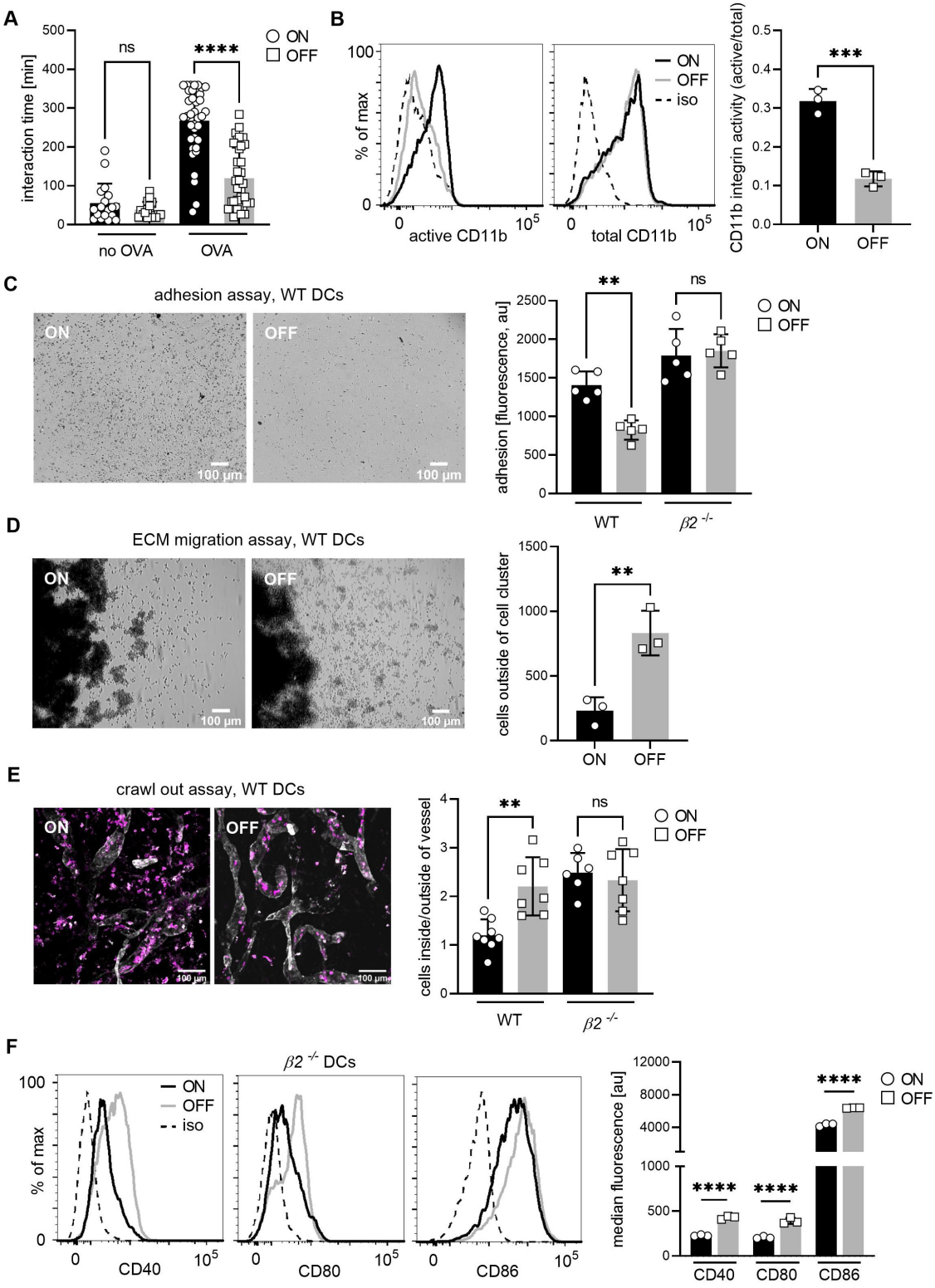

Figure 2-2: *Over-activation of integrins increases DC-T cell contact time and adhesion of DCs to extracellular matrixes leading to decreased migratory capacity.*

A. *Interaction time between ON and OFF stimulated DCs and T cells in the presence and absence of OVA peptide.* ***B.*** *Histograms of active and total CD11b integrin after ON (black) and OFF (grey) stimulation of DCs (left panel; iso – isotype control). Quantification of CD11b activity (active/total levels of CD11b) (right panel).* ***C.*** *Adhesion assay of WT DCs after ON and OFF stimulation (left panel). Quantification of fluorescence signals, proxy for adherent cells, after ON (black) and OFF (grey) stimulation of WT and β2$^{-/-}$ DCs (right panel).* ***D.*** *Extracellular matrix (ECM) migration assay of WT DCs after ON and OFF stimulation (left panel). Quantification of individual*

cells outside of cell cluster (right panel). ***E.*** *Ear crawl out assay of WT DCs after ON and OFF stimulation. Endogenous DCs stained with anti-MHCII (magenta). Lymph vessels stained with anti-LYVE-1 (white) (left panel). Quantification of cells inside over outside of lymph vessel after ON (black) and OFF (grey) stimulation of WT and β2$^{-/-}$ DCs (right panel).* ***F.*** *Expression level of co-stimulatory molecules (CD40, CD80, CD86) of β2$^{-/-}$ DCs after stimulation with ON (black) and OFF mutants (grey) (left panel; iso – isotype control). Quantification of median fluorescence values of co-stimulatory molecules (right panel).*

Taken together, type 1 piliated UPEC increase integrin activity on DCs leading to increased cell-cell and cell-matrix attachment. This causes prolonged interaction times with T cells and impaired migratory capacity. Together, with the above finding of reduced co-stimulatory molecule expression, these data demonstrate that type 1 piliated UPEC target three functional hallmarks of DCs that are critical for the activation of naïve T cells – (i) migration of DCs to the lymph node, (ii) the physical interaction with T cells and (iii) the expression of co-stimulatory molecules.

2.2.3 The GPI-anchored glycoprotein CD14 binds FimH, making it a novel target for type 1 pili

To find the interaction partner on the host cell that leads to integrin activation, we first investigated the role of the major immune cell receptor TLR4 which has been previously suggested as a receptor for the FimH protein of type 1 pili (Mossman et al. 2008). We analyzed the adhesion and migration behavior of *tlr4*$^{-/-}$ DCs after stimulation with UPEC ON mutants and found that both behaviors were still affected (Figure 3A-B and Supplementary Figure 2-3A). Our results, together with recent findings in *Salmonella* (Uchiya et al. 2019), suggest that other receptors besides TLR4 could serve as molecular targets of type 1 pili.

We then focused on CD14, a GPI anchored glycoprotein and co-receptor of TLR4, since a strong correlation has been reported between CD14 expression, integrin activity, and cell adhesion (Wright et al. 1991). We therefore performed adhesion and crawl out migration assays stimulating *cd14*$^{-/-}$ DCs with UPEC ON and OFF mutants and found that behavior of DCs was fully restored (Figure 2-3C andD and Supplementary Figure 3B). *cd14*$^{-/-}$ DCs also showed almost full rescue of the levels of co-stimulatory molecules after ON stimulation, compared to OFF stimulation (Figure 2-3E). We conclude that CD14 is required for the increases in integrin activity and decreases in co-stimulatory molecule expression after stimulation with type 1 piliated UPECs.

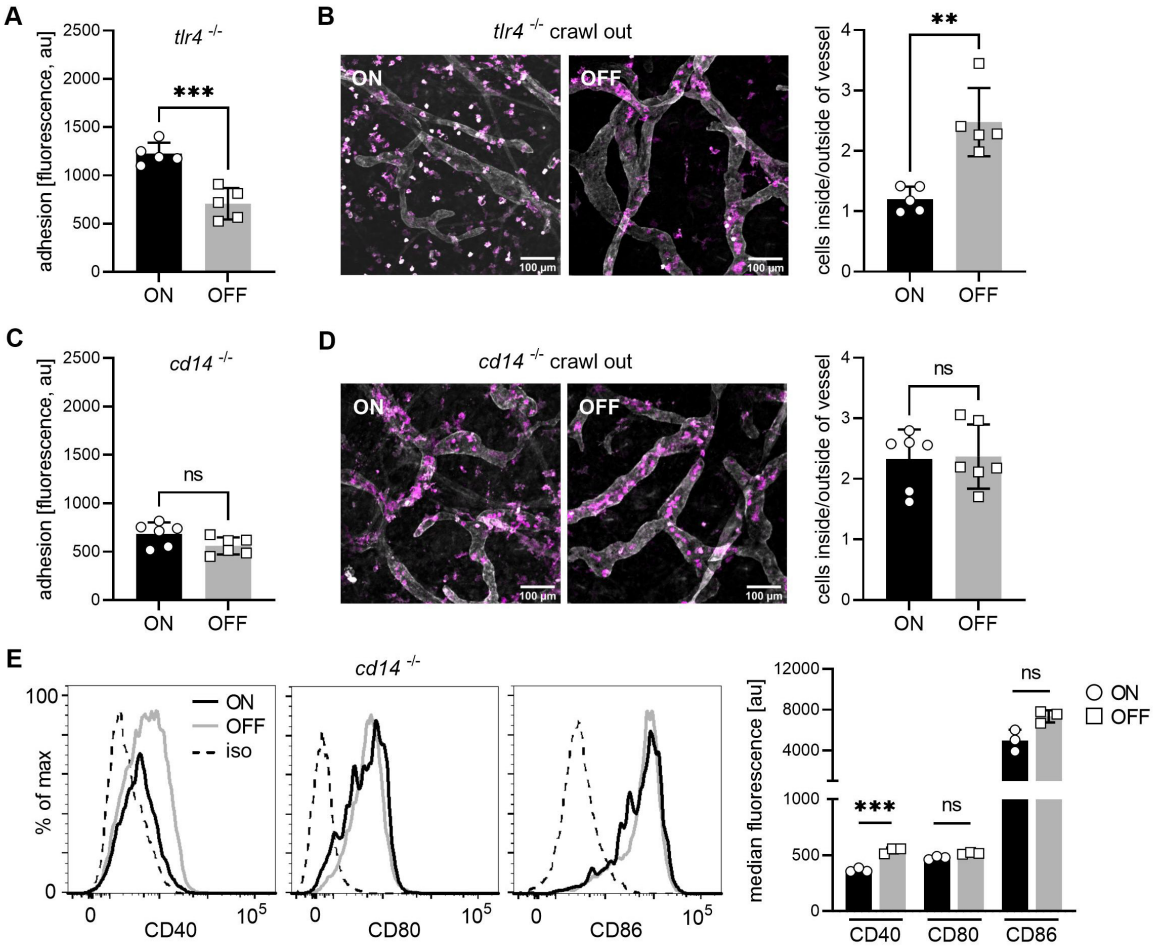

Figure 2-3**:** *Interaction of type 1 piliated UPEC with CD14, but not TLR4, is important for the observed phenotypes.*

A. *Adhesion assay of tlr4$^{-/-}$ and cd14$^{-/-}$ DCs. Quantification of fluorescence signal after ON (black) and OFF (grey) stimulation.* ***B.*** *Ear crawl out assay of tlr4$^{-/-}$ DCs after ON and OFF stimulation. Endogenous DCs stained with anti-MHCII (magenta). Lymph vessels stained with anti-LYVE-1 (white) (left panel). Quantification of cells inside over outside of lymph vessel after ON (black) and OFF (grey) stimulation tlr4$^{-/-}$ DCs (right panel).* ***C.*** *Quantification of the adhesion assay of cd14$^{-/-}$ DCs after ON (black) and OFF (grey) stimulation (5 biological replicates).* ***D.*** *Ear crawl out assay of cd14$^{-/-}$ DCs after ON and OFF stimulation. Endogenous DCs stained with anti-MHCII (magenta). Lymph vessels stained with anti-LYVE-1 (white) (left panel). Quantification of cells inside over outside of lymph vessel after ON (black) and OFF (grey) stimulation cd14$^{-/-}$ DCs (right panel).* ***E.*** *Expression level of co-stimulatory molecules (CD40, CD80, CD86) of cd14$^{-/-}$ DCs after stimulation with ON (black) and OFF mutants (grey) (left panel; iso – isotype control). Quantification of median fluorescence values of co-stimulatory molecules (right panel).*

We next asked how type 1 pili interact with the CD14 receptor. *In silico* protein-protein docking analysis predicted strong binding of -56.98 kcal/mole between FimH (PDB: 6GTV; (Sauer et al. 2019)) and CD14 (PDB: 1WWL; (Kim et al. 2005)) (Table S2; File S1), which is stronger than the -49.81 kcal/mole between FimH and TLR4 (PDB: 3VQ2; (Ohto et al. 2012)) or the -35.55 kcal/mole for CD48 (PDB: 2PTV; (Velikovsky et al. 2007)), another FimH receptor (McArdel et al. 2016) (Table S2). Binding sites in FimH were located in its N-terminal domain and in CD14 within the central region of the crescent shaped monomer (Figure 2-4A), in an area not involved in LPS binding (Table S3) (Kim et al. 2005). Since CD14 of mouse (PDB: 1WWL) and human (PDB: 4GLP; (Kelley et al. 2013)) have highly similar secondary structures, but differ in their amino acid sequence (Kelley et al. 2013), we performed docking analysis

with human CD14. We found predicted strong FimH binding (-55.95 kcal/mole) to be conserved in similar regions of both proteins but mediated by different amino acids (Table S2 and Table S4). This indicates that the difference in amino acid sequence between mouse and human CD14 seems negligible for the otherwise conserved strategy of how FimH of type 1 pili binds to CD14 receptor.

To verify the predicted binding of FimH to CD14 *in vitro*, we generated UPEC ON mutants lacking the *fimH* gene (ON *ΔfimH*). Compared to *Salmonella*, where a *fimH* is necessary for the biosynthesis of type 1 fimbriae (Zeiner et al. 2012), *E. coli* mutants lacking *fimH* still express type 1 pili which are, however, non-functional (Maurer and Orndorff 1985; Klemm and Christiansen 1987; Jones et al. 1995). We confirmed that the ON *ΔfimH* mutants still express type 1 pili but lack the ability to agglutinate with yeast (Supplementary Figure 4A). We performed an immunoprecipitation-type approach using magnetic Protein A beads, a CD14-Fc chimeric protein and the bacterial mutants. First, the CD14-Fc chimera was coupled to the magnetic Protein A beads (Supplementary Figure 5A). Next, we introduced a constitutively expressed *yfp* fluorescent marker into the chromosome of the UPEC ON and ON *ΔfimH* mutants for tracking. Using fluorescence microscopy, we found abundant ON mutants bound per CD14-coupled bead, whereas binding of the *fimH* deletion mutants was scarce (Figure 2-4B). Binding of ON mutants was not due to unspecific binding of FimH to the bead matrix, as uncoupled beads also showed very scarce binding. Additionally, we analyzed the binding of bacteria to beads by flow cytometry by gating on the size parameters and fluorescence signal of the bacteria event population (see Supplementary Figure 5B for gating strategy and methods section for further technical details). ON mutants showed increased binding to CD14-coupled beads, when compared to the *fimH* deletion mutants or to ON mutants binding to uncoupled beads (Figure 2-4C). To further test if only FimH is necessary for binding to CD14, and not interactions with LPS on the bacterial membrane, we extracted type 1 pili (Sheikh et al. 2017) from UPEC ON and ON *ΔfimH* mutants and performed a dot blot assay using biotinylated CD14 and Streptavidin-HRP (Figure 2-4D). Biotinylated CD14 only bound to type 1 pili extracts from ON mutants, whereas no binding was observed to type 1 pili extracts from ON mutants lacking the FimH protein.

We next tested if binding of FimH to CD14 is causative for the increase in adhesion of DCs and the decrease in co-stimulator molecules on their membrane after UPEC ON stimulation. Indeed, deleting *fimH* from UPEC ON mutants fully rescued the adhesion and the expression of all co-stimulatory molecules when compared to stimulation with the UPEC ON mutants (Figure 2-4E and F).

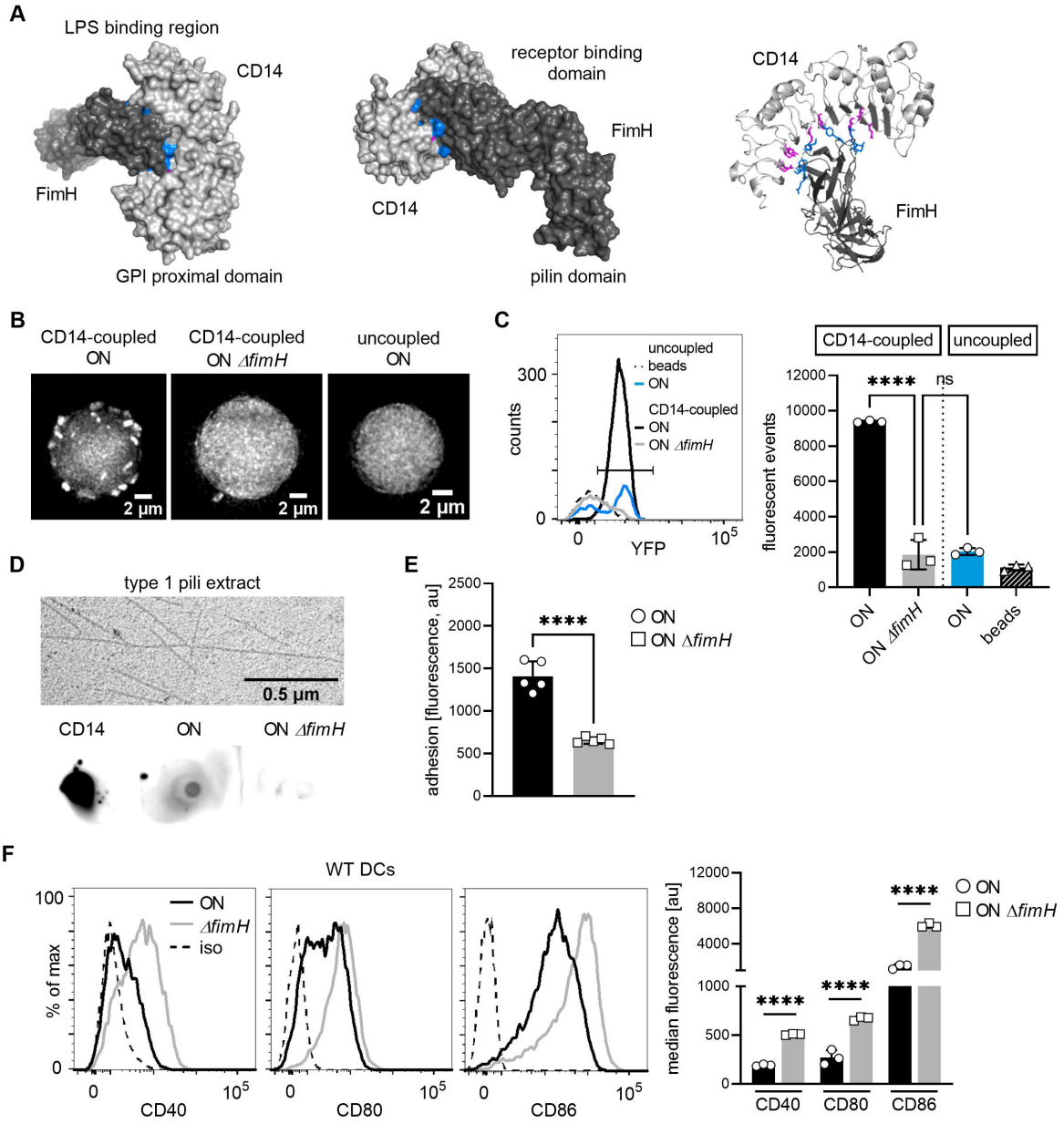

Figure 2-4: *FimH binds to CD14 via protein-protein interactions and deletion of fimH rescues adhesion and expression of co-stimulatory molecules.*

A. *In silico protein-protein docking analysis for FimH and CD14 (see also file S1 and Table S2). FimH is shown in dark grey and CD14 in light grey. Left panel shows surface plot of docked proteins from the view of CD14 on the membrane of the cell. Middle panel shows surface plot of docked proteins from the view of FimH on the membrane of E. coli. GPI proximal domain, LPS-binding, lectin and pilin domains are indicated. Right panel shows secondary structures of proteins. Top 10 amino acids predicted to interact during the binding are highlighted in blue for FimH and magenta for CD14.* ***B.*** *Microscopy images of bead binding assay. ON or ON ΔfimH mutants expressing a constitutive yfp fluorescent marker bound to CD14-coupled or uncoupled beads are shown.* ***C.*** *Flow cytometry analysis of bead binding assay. Histogram of fluorescence events in the bacteria gate (left panel). Uncoupled beads (dashed black), ON mutants bound to uncoupled beads (blue), ON mutants bound to CD14-coupled beads (black), ON ΔfimH bound to CD14-coupled beads (grey). Quantification of fluorescent events in the bacterial gate (right panel).* ***D.*** *Type 1 pili extracts and dot blot assay. Electron microscopy images of type 1 pili extracts from ON mutants (upper panel). Dot blot assay of type 1 pili extracts with biotinylated CD14 (lower panel). Pre-blotted biotinylated CD14 served as positive control. Bound CD14 was visualized with Streptavidin-HRP antibody.* ***E.*** *Adhesion assay of WT DCs after ON and ON ΔfimH stimulation. Quantification of fluorescence signals after ON (black) and ON ΔfimH (grey) stimulation.* ***F.*** Expression level of co-stimulatory

molecules (CD40, CD80, CD86) of WT DCs after stimulation with ON (black) and ON *ΔfimH* mutants (grey) (left panel; iso – isotype control). Quantification of median fluorescence values of co-stimulatory molecules (right panel) (3 biological replicates). ON data are the same as in Figure 1G.

Finally, we asked if expression of pathogenic FimH in an otherwise non-pathogenic bacterial background is sufficient to affect expression of co-stimulatory molecules on DCs. We constructed a locked-ON mutant of *E. coli* W, a non-pathogenic *E. coli* strain, and replaced the endogenous *fimH* gene with the pathogenic *fimH* variant of UPEC CFT073 strain. This non-pathogenic ON $fimH_{CFT073}$ mutant was able to agglutinate with yeast, confirming the correct insertion of the pathogenic *fimH* gene (Supplementary Figure 4B). However, expression of co-stimulatory molecules on DCs after stimulation with non-pathogenic *E. coli* W ON mutants or the non-pathogenic ON $fimH_{CFT073}$ mutant was barely affected (Supplementary Figure 4C).
Based on these experimental observations, we propose that CD14 is a novel target for the FimH protein of type 1 pili and that direct protein-protein interaction is the underlying mechanism of binding. FimH is necessary for the modulatory effects seen on DCs after stimulation with UPEC ON mutants, whereas expressing the pathogenic *fimH* gene alone is not sufficient to cause these effects in an otherwise non-pathogenic background.

2.2.4 FimH amino acids predicted to bind are highly conserved and are partially located in the mannose-binding domain

The two-domain FimH protein consists of a receptor-binding domain and a pili-binding domain (Choudhury et al. 1999). The receptor-binding domain not only interacts with host receptors, like uroplakin Ia on bladder epithelial cells, but also highly specifically binds D-mannose which due to this specific interaction has been used in the treatment of UTIs (Wiles et al. 2008). The amino acids responsible for binding mannose are located in the mannose-binding pocket (P1, N46, D47, D54, Q133, N135, D140 and F142; Table S3) (Hung et al. 2002) and the tyrosine gate (Y48, I52, Y137; Table S3) (Touaibia et al. 2017). These residues are highly conserved among pathogenic and non-pathogenic *E. coli* strains (Figure 5A), whereas other amino acids that affect the flexibility of the FimH protein and therefore facilitate host colonization were found to be mutated in pathogenic *E. coli* (Chen et al. 2009; Sokurenko et al. 1998; Kalas et al. 2017). Interestingly, the most important amino acids of FimH we predicted to be responsible for binding to CD14 are highly conserved among several different *E. coli* strains, whether they are pathogenic or not (Figure 2-5A).
To verify their significance for binding to CD14, we introduced mutations into the three most important amino acids. We exchanged amino acids R98 (binding energy -7.23 kcal/mole), T99 (binding energy -4.92 kcal/mole) and Y48 (binding energy -4.29 kcal/mole) individually to alanine or all three at the same time creating a triple mutant. All four FimH mutants were still able to bind to CD14-coupled beads and only the triple mutant showed some decrease in binding (Figure 2-5B). Stimulating DCs with the FimH amino acid mutants showed partial rescue for co-stimulatory molecule expression levels (Figure 2-5C). This suggests that not only these individual amino acids mediate binding to CD14, but most likely several other amino acids and thus the supporting secondary structure of the FimH protein are involved.

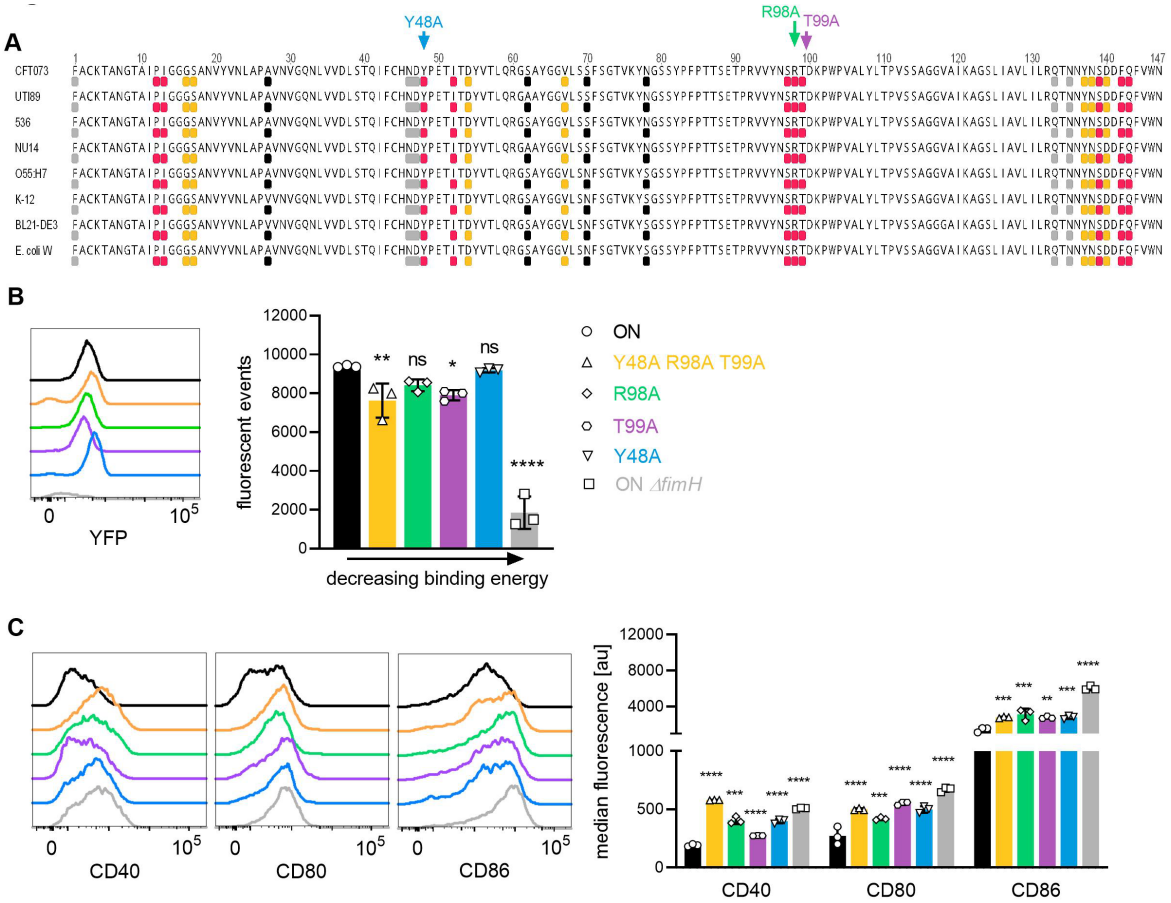

Figure 2-5: *FimH binds to CD14 via highly conserved amino acid residues partially located in the mannose-binding domain.*

A. *Receptor-binding domain of FimH from different E. coli strains is shown (UPEC: CFT073, UTI89, 536, NU14, EPEC: O55:H7; non-pathogenic; K-12, BL21-DE3, E. coli W). The top 10 amino acids on FimH showing strongest binding energy towards mouse CD14 (PDB: 1WWL) are shown in pink and towards human CD14 (PDB: 4GLP) are shown in orange. Amino acids I13, P12 and F42 are involved in both, mouse and human CD14, and therefore only shown in pink. Amino acids located in mannose-binding pocket and tyrosine gate are shown in grey. Amino acids I13, Y48, I52, Y137 and F142 are involved in mannose and CD14 binding and therefore only shown in pink. Common pathoadaptive mutations that differ between UPEC and non-pathogenic E. coli are shown in black. Amino acids mutated to generate FimH amino acid mutants were Y48 (binding energy -4.29 kcal/mole), T99 (binding energy -4.92 kcal/mole) and R98 (binding energy -7.23 kcal/mole) (see also Table S2 and S4). B. Bead binding assay of FimH amino acid mutants. Overlaid fluorescence events in the bacteria gate (left panel). ON (black), ON ΔfimH (grey), Y48A (blue), T99A (violet), R98A (green) and Y48A R98A T99A (yellow). Quantification of fluorescent events in the bacterial gate (right panel). ON and ON ΔfimH data are the same as in Figure 4C. C. Overlaid expression levels of co-stimulatory molecules (CD40, CD80, CD86) of WT DCs after stimulation with ON (black), ON ΔfimH mutants (grey), and FimH amino acid mutants Y48A (blue), T99A (violet), R98A (green) and Y48A R98A T99A (yellow) (left panel). Quantification of median fluorescence values of co-stimulatory molecules (right panel).*

Since Y48 and other identified FimH amino acids with weaker binding energies for CD14 (Table S3) are located in the mannose binding pocket, we were interested whether FimH antagonists, such as D-mannose or the low molecular weight mannose derivate M4284 (Schönemann et al. 2019), disrupt the interaction. Additionally, we tested a blocking CD14 antibody (M14-23) (Tsukamoto et al. 2010) for its ability to inhibit binding of FimH to CD14. Our experiments showed that 175 µM D-mannose was not sufficient to block binding of UPEC ON bacteria to CD14, whereas 1 mM D-mannose and M4284 at 10 µM were able to inhibit

binding of ON mutants to CD14-coupled beads (Figure 2-6A). The blocking CD14 antibody reduced bacteria binding to beads by roughly 25 % but was the most effective at rescuing expression of co-stimulatory molecules on DCs among all tested components (Figure 2-6B).

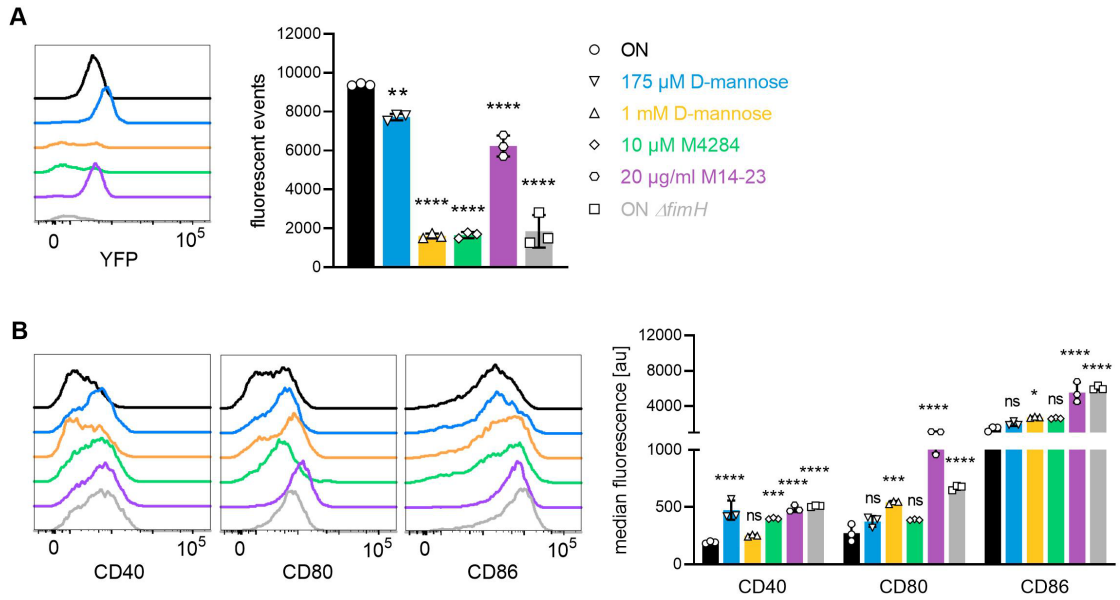

Figure 2-6: *FimH antagonists and a blocking CD14 antibody (partially) block binding and rescue expression of co-stimulatory molecules on DCs.*

A. *Bead binding assay of ON mutants in the presence of FimH antagonists and blocking CD14 antibody. Overlaid fluorescence events in the bacteria gate (left panel). ON (black), ON ΔfimH mutants (grey), 175 µM D-mannose (blue), 1 mM D-mannose (yellow), 10 µM M4284 (green) and 20 µg/ml M14-23 antibody (violet). Quantification of fluorescent events in the bacterial gate (right panel).* ***B.*** *Overlaid expression levels of co-stimulatory molecules (CD40, CD80, CD86) of WT DCs after stimulation with ON (black), ON ΔfimH mutants (grey), and ON stimulation in presence of 175 µM D-mannose (blue), 1 mM D-mannose (yellow), 10 µM M4284 (green) and 20 µg/ml M14-23 antibody (violet) (left panel). Quantification of median fluorescence values of co-stimulatory molecules (right panel).*

Thus, existing FimH antagonists as well as blocking CD14 antibodies show certain potential to treat recurring or persistent infections caused by type 1 piliated pathogens.

2.3 Discussion

Here, we uncovered that type 1 piliated UPECs target the CD14 glycoprotein on the surface of DCs to shut down the migratory capacity of DCs and their ability to interact with and activate T cells.

It has been proposed that the tight regulation of UPECs type 1 pili expression has evolved to limit exposure to the host immune system, allowing the pathogen to establish a persistent infection (Donnenberg 2013). In this study we uncovered and characterized a different fundamental role of type 1 pili, as modulators of the innate and adaptive immune response. We found that type 1 piliated UPECs decreased the migratory capacity of DCs by increasing their adhesion to other cells, such as T cells, and the extracellular matrix by over-activation of integrins. The effective and timely transition from adhesion to the migration phenotype is

essential for DCs to migrate from the site of the actual infection to the lymph node in order to interact with lymphocytes. To achieve these migratory and signaling tasks, DCs need to dynamically regulate integrin mediated adhesion, and we found that over-activation of integrins triggered by type 1 piliated UPECs leads to effective immobilization to the extracellular matrix and decreased turnover of cell-cell interactions. Over-activation of integrins, by hijacking integrin-linked kinases leading to decreased turnover of focal adhesions, was already shown to subvert innate immunity during *Shigella* and enterohemorrhagic *E. coli* (EHEC) infections (Kim et al. 2009; Shames et al. 2010), however UPECs do not express the responsible genes. Moreover, we found that type 1 piliated UPECs also decreased the expression of co-stimulatory molecules, which are essential for T cell activation and proliferation.

We identified CD14, a GPI-anchored glycoprotein, as the direct target for the FimH protein of type 1 pili. In analogy, a previous study showed that the *fimA*-encoded major type V fimbriae of the oral pathogen *Porphyromonas gingivalis* also bind CD14 and thereby increase integrin-mediated adhesion by activating CD11b integrin (Harokopakis and Hajishengallis 2005). Using in silico protein-protein docking analysis we found strong predicted binding between CD14 and FimH through specific amino acids in both proteins. Interestingly, the respective FimH amino acids are highly conserved not only among pathogenic, but also non-pathogenic *E. coli* strains. However, although we found FimH to be necessary, we did not find the simple presence of pathogenic FimH in an otherwise non-pathogenic genetic background to be sufficient for suppression of the immune response. We therefore hypothesize that the predicted amino acids are mainly important for the pathogens to interact with and thereby to dampen the activation of immune cells and thus the immune response in the host to persist "commensally" for prolonged times. However, it is unknown which other gene(s) work together with *fimH*, as the UPEC strain CFT073 carries accessory genes encoded by 13 pathogenicity islands (Lloyd et al. 2007). Generally, the pathogenic potential of UPECs does not seem to be the result of a defined virulence gene, but rather a combination of effects by several genes (Touchon et al. 2009).

Given how pathogenic bacteria circumvent the host immune response by generating protected niches (Grant and Hung 2013) and the constantly growing presence of multi-drug resistant strains (Boucher et al. 2009), treatment of persistent or recurring infections is increasingly challenging. Although vaccination approaches against FimH (Eldridge et al. 2020) or non-conventional treatments, such as small mannosides (Schönemann et al. 2019; Mydock-McGrane et al. 2016), showed promising results, treatments of infections caused by type 1 piliated pathogens remains difficult. Our findings underscore the importance of the mannose-binding domain, and several conserved amino acid residues in this domain, in the interaction between FimH and CD14. For example, R98, showing the strongest binding to CD14 in our predictions, was identified to be important to stabilize the protein-ligand interaction (Han et al. 2010). However, targeting this residue only, was not sufficient to boost affinity of FimH antagonists (Tomašič et al. 2021). Given our results, we hypothesize that this could be because not individual amino acids, but the overall secondary structure of the mannose-binding domain of FimH is important for the interaction with host receptors. Blocking CD14 antibodies, such as the human anti-CD14 antibody IC14 (Axtelle and Pribble 2001), could represent an alternative way to treat recurring infections caused by type 1 piliiated pathogens, such as UTIs or inflammatory bowel diseases like Crohn's disease

(Sivignon et al. 2017), given that CD14 is expressed by hematopoietic but also non-hematopoietic cells (Zanoni and Granucci 2013).

Although opportunistic pathogens continuously circulate in humans as asymptomatic colonizers, they occasionally cause symptomatic acute or even chronic infections in some individuals (Donnenberg 2013). Opportunistic pathogens use type 1 pili to adhere to and invade into host epithelial cells. While the cellular invasion represents a *de facto* passive mechanism for the pathogens to hide from the immune system and to establish persistent or recurring infections, we found that UPECs use type 1 pili to actively manipulate the behavior of innate immune cells, and thus also the adaptive immune response, by direct interaction of FimH and CD14 receptor on DCs. Since CD14 is a multi-functional co-receptor of several immune cell types (Zanoni and Granucci 2013) and type 1 pili are expressed not only by pathogenic but also by non-pathogenic *E. coli* (Shawki and McCole 2017; Croxen and Finlay 2010), our findings add a new layer of complexity to the physiological relevance of type 1 pili – as modulators of the immune response in general and specifically during persistent and recurring infections.

2.4 Methods

2.4.1 Animals

Mice were bred and maintained at the local animal facility in accordance with the IST Austria ethics commission. All experiments were conducted in accordance with the Austrian law for animal experiments. Permission (BMWFW-66.018/0010-WF/V/3b/2016) was granted by the Austrian federal ministry of science, research and economy.

2.4.2 Cell culture

R10 medium, RPMI 1640 + 10 % FCS, 2 mM L-Glutamine, 50 µM beta-mercaptoethanol, 100 U/ml Penicillin and 100 µg/ml Streptomycin, was used as basic medium. Stem cell medium was supplemented with 10 ng/ml IL-3, 20 ng/ml IL-6 and 1 % stem cell factor (SCF) supernatant produced by B16 melanoma cells. Hoxb8 medium was supplemented with 125 ng/ml Flt3 and 1 µM estradiol. iCD medium was supplemented with 2 ng/ml GM-CSF and 75 ng/ml Flt3. GM-CSF and Flt3 supernatants were produced by hybridoma cells and concentration of cytokines was measured by ELISA. All media were used pre-warmed. Cells were grown routinely at 37 °C with 5 % CO_2. For infection and subsequent assays, cells were cultured in R10 medium without antibiotics and buffered with 20 mM Hepes (R10H20) in the absence of CO_2.

2.4.3 WT, *β2*$^{-/-}$, *tlr4*$^{-/-}$ and *cd14*$^{-/-}$ Hoxb8 cell generation

5-week-old wild type C57BL/6J, *β2*$^{-/-}$ (B6.129S7-Itgb2^{tm1Bay}/J), *tlr4*$^{-/-}$ (B6(Cg)-Tlr4$^{tm1.2Karp}$/J) and *cd14*$^{-/-}$ (B6.129S4-Cd14^{tm1Frm}/J) mice were obtained from the Jackson Laboratory. Immortalization of bone marrow cells was performed as described previously (Leithner et al. 2018; Redecke et al. 2013). In brief, bone marrow was isolated from the femur and tibia by centrifugation and cells were precultured in stem cell medium for 3 days to enter the cell cycle. $1*10^5$ cells were spin-infected with Hoxb8-MSCV retrovirus using lipofectamine at 1000 g for 1 h in Hoxb8 medium. Cells were fed and split every few days for 3-4 weeks until all uninfected cells died off and only Hoxb8 infected, immortalized, cells were left.

2.4.4 Dendritic cell differentiation

iCD103 DCs, expressing CD103, were differentiated from Hoxb8 progenitor cells as described previously for bone marrow cells with minor modifications (Mayer et al. 2014). In brief, Hoxb8 cells were seeded at a density of $3*10^5$ cells into 10 cm bacterial culture dishes in 10 ml iCD medium. On day 3 cells were split 1:2 and toped up with fresh iCD medium to 10 ml. On day 6, cells were fed with 10 ml iCD medium and non-adherent iCD103 DCs were frozen on day 9. For images of immature and matured cells, as well as flow cytometry staining of different surface markers see Supplementary Figure 1.

Frozen DCs were allowed to recover after thawing for at least 4 h before infection. Non-adherent cells were counted and seeded at a density of $1\text{-}2*10^5$/ml in R10H20 medium. Assays were performed with DCs that were either stimulated with bacteria or recombinant LPS at 200 ng/ml. *β2*$^{-/-}$ DCs were purified from potential other cells using the EasySep™ mouse Pan-DC enrichment kit and allowed to rest for 1 h before the infection assay.

2.4.5 Bacterial strain construction

For cloning, strains were grown routinely in LB medium. Plasmids were maintained at 100 µg/ml ampicillin or 50 µg/ml kanamycin. Single copy integration was performed at 12 µg/ml chloramphenicol or 25 µg/ml kanamycin. For experiments, strains were grown at 37 °C in R10H20 medium without antibiotics or in medium containing 0.5 % casamino acids, 1x M9 salts, 1 mM $MgSO_4$, 0.1 mM $CaCl_2$ and 0.5 % glycerol (CAA M9 glycerol). Primers used for cloning are listed in Table 1.

2.4.5.1 Locked mutants

E. coli W ((Archer et al. 2011); ATCC 9637) and clinical isolate CFT073 ((Welch et al. 2002); ATCC 7000928; a kind gift of Ulrich Dobrindt) were used as well as derivatives of those strains. Phase-locked mutants were generated by replacing the 9 bp long recognition site for the site-specific recombinases FimB and FimE in the internal repeat region on the left site of the fim switch (*fimS*) with an FRT site (Figure 2-1C). The fimS region was amplified either in the ON (primers 132 and 110) or OFF (primers 133 and 112) orientation from the chromosome of the wild type strain but omitting the 9 bp recognition site on the left site. An FRT-removable chloramphenicol resistance marker was amplified from pKD3 plasmid using primers 128 and 134 (Datsenko and Wanner 2000). The resistance marker was assembled left of the amplified fimS regions using NEBuilder assembly kit (NEB). The assembled DNA fragments were PCR amplified using primers 130 and 131 and integrated into the chromosome of the respective strains instead of the endogenous *fimS* using lambda red recombination (Datsenko and Wanner 2000). In brief, *E. coli* W or CFT073 wild type bacteria were transformed with pSIM6 plasmid expressing thermal inducible Red genes under control of the native λ phage pL (Datta et al. 2006) and selected with ampicillin at 30 °C. After inducing expression of lambda red genes at 42 °C for 15 min, bacteria were made electrocompetent and transformed with 100 ng of the cleaned PCR fragments. Bacteria were allowed to recover in LB medium for 1 h at 37 °C before spreading on LB plates containing chloramphenicol.

After verifying single copy integration using primers 119, 120, cam_test_R and 3_SphI_pKD3_test, the resistance marker was subsequently removed using pCP20 plasmid (Cherepanov and Wackernagel 1995). The mutated *fimS* region was sequenced to confirm deletion of the 9 bp long recombinase recognition site on the left site, but a fully intact recognition site on the right site. Presence or absence of the type 1 pilus on the bacterial outer membrane was confirmed by electron microscopy and yeast agglutination assay. Resulting

locked mutants were: CFT073 locked-ON – KT179, CFT073 locked-OFF – KT180 and *E. coli* W locked-ON – KT232.

2.4.5.2 *FimH* deletion mutant

fimH gene from CFT073 locked-ON mutants (KT179) was deleted by lambda red recombination. The FRT-flanked chloramphenicol resistance marker from pKD3 plasmid was amplified using primers 146 and 148 and integrated into the chromosome of KT179 strain. Successful deletion was confirmed by PCR (primers 157 and 158). Resistance was flipped using pCP20 plasmid resulting in CFT073 locked-ON *ΔfimH* mutant – KT193. Presence of type 1 pili was confirmed by electron microscopy. Absence of *fimH* was confirmed by sequencing and yeast agglutination assay.

2.4.5.3 Chromosomal *yfp* marker

mVenus driven by the right site of the lambda P_O was integrated in the lambda phage attachment site on the chromosome of CFT073 locked-ON (KT179) and CFT073 locked-ON *ΔfimH* (KT193) mutants using CRIM integration (Haldimann and Wanner 2001). In brief, KT179 and KT193 strains were transformed with pInt-ts helper plasmid and selected on ampicillin plates at 30 °C. Bacteria were made electrocompetent and transformed with P_R-mVenus carrying pAH120-frt-cat integration plasmid. After recovery in LB medium for 1 h at 37 °C, expression of lambda red genes was induced at 42 °C for 15 min before spreading on LB plates containing chloramphenicol.
Single copy integration of the CRIM plasmid was verified with PCR as mentioned previously (Haldimann and Wanner 2001). Since pAH120-frt-cat was designed to have a FRT flanked chloramphenicol resistance marker (Nikolic et al. 2018), resistance was subsequently removed using pCP20 plasmid (Cherepanov and Wackernagel 1995). Resulting mutants were: CFT073 locked-ON *attλ* P_R-mVenus – VG003 and CFT073 locked-ON *ΔfimH attλ* P_R-mVenus – KT257.

2.4.5.4 *FimH* replacement mutant

The endogenous *fimH* gene of the non-pathogenic *E. coli* W strain was exchanged scar-less with *fimH* of the pathogenic UPEC strain CFT073 using *galK* selection/counter-selection (Kavčič et al. 2020). The FRT-flanked kanamycin resistance marker from gDNA harboring *ΔgalK::kan* (gift of Bor Kavčič) was amplified using primers galK-ver-F and galK-ver-R (gift of Bor Kavčič) and integrated into the *galK* gene of *E. coli* W locked-ON (KT232). Loss of *galK* gene was confirmed by PCR using primers FarChro *galK* UO and galK-KpnI-r (gift of Bor Kavčič). Resistance was flipped using pCP20 plasmid. *galK* under constitutive J23100 promoter was amplified from pKD13-PcgalK plasmid using primers 296 and 297 and transformed to replace the endogenous *fimH* gene using lambda red recombination. After recovery, any residual carbohydrate residues were removed by washing the cells several times with M9 buffer (Tomasek et al. 2018) before plating on M9 minimal medium containing 0.1 % galactose as only carbohydrate source for positive selection. Integration of *galK* gene into *fimH* was confirmed by PCR using primers 157 and 158. CFT073 *fimH* gene was amplified from a gblock (IDT) carrying the *fimH* sequence from CFT073 using primers 198 and 276 and integrated instead of the constitutive *galK* gene. After recovery, cells were washed several times as before. Transformants were counter-selected on artificial urine medium agar plates ((AU-Siriraj; (Chutipongtanate and Thongboonkerd 2010)) supplemented with 20 µg/ml L-aspartate and 20 µg/ml L-isoleucine (Bouvet et al. 2017), and containing 0.2 % 2-deoxy-D-

galactose (DOG) and 0.2 % glycerol for the counter-selection. Pathogenic *fimH* integration was confirmed by PCR using primers 157 and 158. Resulting mutant was *E. coli* W locked-ON fimH::fimH$_{CFT073}$ – MG002.

2.4.5.5 FimH amino acid mutants

Single and triple point mutants of amino acids predicted to be most involved in binding to CD14 were generated using *galK* selection/counter-selection as mentioned above. Briefly, *galK* was deleted from CFT073 locked-ON mutants (KT179). Thereafter constitutive expressed *galK* was inserted in the endogenous *fimH* of this strain for selection. 100 µg gblocks (IDT) carrying either Y48A, R98A, T99A or the triple mutation (Y48A, R98A, T99A) in the *fimH* sequence from strain CFT073 were integrated instead of the constitutive *galK* gene. Correct integration of *fimH* having mutated amino acid residues was confirmed by sequencing. Resulting mutants were CFT073 locked-ON *fimH*$_{Y48A\ R98A\ T99A}$ – KT260, CFT073 locked-ON *fimH*$_{Y48A}$ – KT261, CFT073 locked-ON *fimH*$_{R98A}$ – KT262 and CFT073 locked-ON *fimH*$_{T99A}$ – KT263.

2.4.6 Inhibitors used

Since the suggested upper daily limit of orally applied D-mannose to treat UTIs is 9 g, leading to blood mannose levels of roughly 175 µM (Alton et al. 1997), we decided to compare this concentration to a strongly increased one of 30-60 g D-mannose resulting in 1 mM blood mannose levels. The small mannoside M4284 was used at 10 µM. The blocking CD14 antibody M14-23 was used at 20 µg/ml (Tsukamoto et al. 2010). Inhibitors were added as the same time as the bacteria, no pre-incubation steps were carried out.

2.4.7 Yeast agglutination assay

Saccharomyces cerevisiae was grown in YPD medium at 30 °C for 2 days. After centrifugation, cells were resuspended in M9 buffer to an OD_{600} of 1 and stored in the fridge. An aliquot of the yeast was transferred to glass slides and bacterial colonies were directly mixed into the yeast solution. Agglutination occurred within few seconds to 1 min. Pictures of agglutinated yeast and bacteria cells were taken on a brightfield microscope at 10x magnification and images were processed with Fiji.

2.4.8 Growth curve assay and doubling time estimation

Single bacterial colonies were inoculated in 160 µl R10H20 in 96-well plates and grown overnight at 220 rpm at 37 °C. The next day, cultures were diluted 1 in 1,000 in R10H20 supplemented with 0.0005 % triton-X and grown at 37 °C with shaking. Optical density was measured every 30 min at 600 nm at a Synergy H1 plate reader for a total of 7 h. The data were blank normalized, and the doubling time (dt) was calculated from exponential data using following formula $dt = \frac{t2-t1}{\left(3.3*\log\left(\frac{OD_{600}{}^{2}}{OD_{600}{}^{1}}\right)\right)}$.

For all assays, bacteria were grown to early- to mid-exponential phase (OD_{600} 0.25; *E. coli* W 4 h, CFT073 3 h 20 min; see Supplementary Figure 6A) in 1 ml R10H20 medium, if not indicated otherwise, at 37 °C in deep well plates.

2.4.9 Minimal inhibitory concentration (MIC) assay

Cultures were grown to OD_{600} of 0.25 and approximately 10^6 bacteria were used for MIC assays. Serial dilutions of gentamicin were performed in a microdilution manner using 96-well

plates and OD_{600} was measured after 18 h incubation at 37 °C with shaking. The threshold to calculate the MIC was set to detectable growth above the blank background after normalization. CFT073 locked-ON (KT179) and locked-OFF (KT180) mutants had similar MIC to gentamicin in R10H20 medium (see Supplementary Figure 6B). 5x the MIC was used to prevent extracellular growth of bacteria in the infection assays (7.5 µg/ml).

2.4.10 Electron microscopy

Bacteria were grown to mid-exponential phase in CAA M9 glycerol medium, fixed with glutaraldehyde (EM grade, final concentration 2.5 %) for 30 min at 4 °C, washed twice with PBS and concentrated in water. Formvar-coated copper grids were glow discharged for 2 min and $5*10^6$ bacteria were loaded for 5 min. Excess liquid was removed with filter papers and bacteria were stained with Uranyless for 2 min. After removal of excess liquid, the grids were washed 10 times in water and dried. EM images were taken at TEM T10 microscope at 80 kV. Images were processed with Fiji.

2.4.11 Predicted protein-protein interaction

Crystal structures of FimH (PDB: 6GTV), mouse CD14 (PDB: 1WWL), human CD14 (PDB: 4GLP), mouse TLR4 (PDB: 3VQ2) and mouse CD48 (PDB: 2PTV) were obtained from rscb.org, cleaned from solvents and other co-precipitated molecules using PyMol and run on HawkDock server to predict protein binding (Weng et al. 2019). Additional MM/GBSA analysis was run to predict free binding energy (Hou et al. 2011).

2.4.12 Bead binding assay

5 µl of 10 µm bead slurry (PureProteom Protein A magnetic beads, Merck) were used per reaction. Beads were washed 3x with PBS containing 0.005 % tween (PBS-T). Beads were collected using a magnetic stand. 5 µg CD14-Fc recombinant protein in a total of 10 µl of PBS-T was coupled to the beads for 1 h at 4 °C with rotation. After washing the beads, 100 µl of bacteria grown to early- to mid-exponential phase in CAA M9 glycerol medium (~$1*10^7$ bacteria) were incubated in the presence of tween with the CD14-coupled beads for 1 h at 4 °C with rotation. After washing, this time with M9 glycerol medium containing tween, bead-bound bacteria were fixed with 0.5 % PFA in M9 buffer for 10 min at 4 °C.
For flow cytometry, samples were diluted in M9 buffer and analyzed on a FACS Canto II (BD). 10,000 events gated on FSC-A and SSC-A to exclude debris were recorded at medium flow rate and data were analyzed using FlowJo software. Three things should be noted: First, we observed that due to the high force applied in the sample injection tube during acquisition, the bacteria were separated from the magnetic beads they previously were bound to, leading to a single detectable fluorescent peak only. Second, due to their size, the magnetic beads are also detected in the gating range specific for the bacterial population (see Supplementary Figure 5C). Third, as can also be seen in the fluorescent images, the magnetic beads have weak auto-fluorescence in the FITC channel. We therefore quantified the amount of fluorescent events applying the same gating strategy as for the bacterial population only (Supplementary Figure 5B and C).
For fluorescent microscopy, samples were embedded in mounting buffer and spread on a cover slip. Images were taken with 100x magnification on a custom-built Olympus widefield microscope with Hamamatsu Orca Flash4.0v2 camera and LED-based fluorescence illuminator using YFP (x513/22,m543/22) fluorescence channel (Chait et al. 2017). Images were processed with Fiji and deconvoluted with Huygens software.

2.4.13 Type 1 pili extracts

Type 1 pili extracts were generated as described previously (Sheikh et al. 2017) with minor modifications. Briefly, CFT073 locked-ON (KT179) and CFT073 locked-ON *ΔfimH* (KT193) were grown overnight in CAA M9 glycerol medium and harvested at 4,000 g for 1 h. The cell pellet was resuspended in 1 mM Tris-HCl (pH 8.0) and incubated at 65 °C for 1 h with occasional vortexing. After pelleting the cells at 15,000 g for 10 min, type 1 pili were precipitated from the supernatant overnight in the presence of 300 mM NaCl and 100 mM $MgCl_2$ at 4 °C. Type 1 pili were concentrated at 20,000 g for 10 min, washed once with 1 mM Tris-HCl and snap frozen in a small volume of 1 mM Tris-HCl.

2.4.14 Dot blot assay

The recombinant chimera CD14-Fc protein was biotinylated using the EZ-Link Sulfo NHS-LC-LC-Biotin kit (Thermofisher) and a 5-fold molar excess of biotin. In brief, CD14-Fc was dissolved in PBS at 1 mg/ml and biotinylated with a 5-fold molecular excess of biotin for 30 min at room temperature (RT). The biotinylation reaction was stopped with 3 mM Tris-HCl (pH 7.0).

The PVDF membrane was activated for 5 min with MeOH, washed for 5 min in water and allowed to dry for 5 min. 20 ng biotinylated CD14 and roughly 20 µg type 1 pili extract from CFT073 ON (KT179) and CFT073 ON *ΔfimH* (KT193) mutants were loaded onto the membrane. Protein spots were allowed to dry for 10 min and then the membrane was blocked in 3 % BSA in PBS for 30 min at 37 °C. 40 ng biotinylated CD14 in 3 % BSA in PBS and 0.05 % tween was blotted on the membrane and incubated for 1 h at 37 °C. Then the membrane was washed 3x in PBS with tween for 5 min each. Streptavidin-HRP antibody was pre-diluted 1:100 in 3 % BSA in PBS with tween and diluted once more 1:5,000 in PBS with tween. The membrane was incubated with Streptavidin-HRP for 1 h at RT. After washing again 3x as before, chemiluminescence was detected using clarity ECL substrates (Biorad).

2.4.15 Infection assays

DCs were seeded at a density of 1-2*10^5 cells/ml in R10H20 medium (for adhesion assays black 24-well tissue-treated dishes were used, for any other assay non-treated dishes were used). DCs were matured either by addition of 200 ng/ml recombinant LPS or bacteria at a multiplicity of infection (MOI) of 10 (10 bacteria per 1 DC). 1 h post infection (pi) gentamicin was added at 7.5 µg/ml to prevent extracellular growth of bacteria. 18-20 h pi subsequent assays were performed.

2.4.16 Adhesion assay

Non-adherent DCs were removed, and adherent cells were washed twice with 500 µl PBS. Adherent cells were stained with Hoechst 33342 (NucBlue reagent, 2 drops/ml) in R10H20 medium for 30 min at 37 °C. Cells were washed twice and 1 ml Live Cell Imaging solution (140 mM NaCl, 2.5 mM KCl, 1.8 mM $CaCl_2$, 1.0 mM $MgCl_2$, 20 mM HEPES, pH 7.4) was added to the wells. Fluorescence was measured with a Synergy H1 plate reader (excitation 490 nm, emission 520 nm, bottom reading without lid, 50 data points per well). Pictures of adherent cells were taken on a brightfield microscope at 4x magnification and images were processed with Fiji.

2.4.17 Flow cytometry staining

DCs were collected and incubated in FACS buffer (1x PBS, 2 mM EDTA, 1 % BSA; RT) or Tyrode´s buffer (used for active CD11b and β1 staining, on ice) with Fc receptor block for 20 min. Cells were stained for 30 min with antibodies using the respective buffer with Fc receptor block. Cells were washed twice with PBS and resuspended in the respective buffer for analysis on FACS Canto II (BD). 10,000 events gated on FSC-A and SSC-A to exclude debris were recorded at medium flow rate. Data were analyzed using FlowJo software by performing doublet discrimination.

2.4.18 Ex vivo ear crawl out assays

Ear crawl out assays were performed similar as published previously with minor modifications (Kopf et al. 2020). In brief, ears from 5-week-old female C57Bl/6J WT mice were first UV sterilized for 10 min and then split into dorsal and ventral halves. Ventral halves were placed in R10H20 medium, ventricles facing down. Ears were incubated with 10^6 CFT073 locked-ON (KT179) or OFF (KT180) bacteria for 48 h, renewing the infection stimulus after 24 h. 1 h after every infection 7.5 µg/ml gentamicin was added to the medium. Ears were fixed using 4 % PFA and immersed using 0.2 % triton-X. After blocking in 1 % BSA in PBS, lymphatics were stained for 90 min using rat anti-Lyve-1 antibody and DCs were stained using biotinylated anti-MHCII antibody. Secondary antibodies, anti-rat $F(ab')_2$-AF488 and Streptavidin-AF647, were used subsequently for 45 min each. Ears were fixed on cover slips with ventricles facing up using cover glasses. 10 µm z-stacks were taken on inverted LSM800 confocal microscope with 488 and 640 nm LED-laser light source. Images were taken from 3 biological replicates (except *tlr4*$^{-/-}$ where 2 biological replicates were imaged) analyzing at least 2 field of views each. Maximum intensity projection images were processed with Fiji. Images were analyzed using custom-made scripts in Fiji. Pre-processing was done using lymphatics script and analysis using LVmeanDCarea script.

2.4.19 In vitro 3D collagen migration assay

3D collagen chemotaxis assays were performed as described previously (Leithner et al. 2016), with minor modifications. Assays were performed in PureCol bovine collagen with a final collagen concentration of 1.6 mg/ml in 1x minimum essential medium eagle (MEM) and 0.4 % sodium bicarbonate using 1-2*10^5 DCs. The collagen-cell mixture was cast to custom-made migration chambers and polymerized for 1 h at 37 °C. CCL19 chemokine in R10 (0.625 µg/ml) was pipetted on top of the gel and the chambers were sealed with paraffin. Images were taken every 30 sec for a total of 5 h on bright field microscopes using 4x magnification and an exposure of 20 ms. Data were analyzes using custom-made Fiji scripts: images were pre-processed using Tracking_pre-processing_for_brightfield script and analyzed using migrationspeedREP script.

2.4.20 In vitro extracellular matrix migration assay

Cell-derived matrixes (CDM) were produced as described previously (Kaukonen et al. 2017). In brief, round shaped coverslips were coated with 0.2 % gelatin in PBS in 24-well dishes for 1 h at 37 °C. Gelatin was crosslinked with 1 % glutaraldehyde in PBS for 30 min at RT and quenched with 1 M glycine in PBS for 20 min at RT. After washing the coverslips twice with PBS, 5*10^4 3T3 mouse fibroblasts in DMEM, GlutaMAX, supplemented with 10 % FCS, 100 U/ml penicillin and 100 µg/ml streptomycin were seeded per well. After 48 h 3T3 fibroblasts reached confluency and were treated daily with ascorbic acid for better

crosslinking of the extracellular matrix. Old medium was gently removed and fresh medium with 50 µg/ml sterile ascorbic acid was added for 10-14 days. 3T3 fibroblasts were extracted with extraction buffer (0.5 % Triton-X, 20 mM NH_4OH in PBS) for 2 min and washed twice with PBS containing 1 mM $CaCl_2$ and 1 mM $MgCl_2$ (PBS/Ca/Mg). DNA was digested with 100 µg/ml DNaseI in PBS/Ca/Mg for 1 h at 37 °C and CDM were washed twice with PBS/Ca/Mg before storage in PBS/Ca/Mg supplemented with 100 U/ml penicillin and 100 µg/ml streptomycin at 4 °C.

Before use, CDM were placed onto custom-made imaging chambers and incubated with R10 medium for 1 h at 37 °C. The medium was removed and a 1 µl CCL21 chemokine (25 µg/ml) spot was injected into the CDM and incubated for 10 min. 1 ml R10 medium was added on top and the CDM was incubated for 1 h at 37 °C to allow a chemokine gradient to form. After washing twice gently with R10 medium, CFT073 locked-ON (KT179) and locked-OFF (KT180) stimulated DCs were concentrated by centrifugation and the dense cell pellet was pipetted into the CDM at the opposite site to the chemokine spot. 2 ml of R10 medium was added and images were taken every minute for a total of 6 h on a bright field microscope using 10x magnification and an exposure of 20 ms. Single cells outside of the cell cluster were counted after 5 h. Images were processed with Fiji.

2.4.21 In vitro T cell assay

T cell assays were performed as described previously (Leithner et al. 2021). In brief, primary naïve $CD4^+$ T cells were isolated from the spleen of OT-II mice (B6.Cg-Tg(TcraTcrb)425Cbn/J) using EasySep Mouse $CD4^+$ T cell isolation kit (Stemcell Technologies) after homogenization with a 70 µm cell strainer and resuspending the cells in PBS supplemented with 2 % FCS and 1 mM EDTA. T cells were co-cultured with DCs matured with CFT073 locked-ON (KT179) or OFF (KT180) at a ratio of 5:1 ($5*10^4$ T cells:$1*10^4$ DCs) in 96-well round bottom well plates in R10 medium.

2.4.21.1 T cell activation

After 24 h co-culture in the presence of 0.1 µg/ml ovalbumin (OVA), medium was removed by spinning. Cells were incubated with Fc receptor block in FACS buffer and stained with anti-CD4, anti-CD69 and anti-CD62-L antibodies for 15 min at 4 °C. After resuspending cells in FACS buffer, 100 µl were recorded on FACS Canto II (BD) and the ratio of CD69 to CD62L expression of $CD4^+$ T cells was analyzed by FlowJo software.

2.4.21.2 T cell priming

T cells were stained with 5 µM CFSE stain in 5 % FCS in PBS for 5 min at RT. After 30 min recovery in R10 medium at 37 °C, cells were routinely checked for fluorescence.

After co-culturing with DCs for 4 days in the presence of 0.1 µg/ml OVA, medium was removed by spinning. Cells were stained with anti-CD4 antibody for 10 min at 4 °C. After resuspending cells in FACS buffer and 7AAD viability stain, 100 µl were recorded on FACS Canto II (BD). Dividing T cells were analyzed with FlowJo software.

2.4.22 DC-T cell interaction time

Interaction time of DCs and T cells was measured as described previously (Leithner et al. 2021). In brief, glass bottom dishes were plasma cleaned for 2 min and coated with 1x poly-L-lysine in water for 10 min at RT. Dishes were washed two times with water and dried overnight. $1.5*10^5$ DCs, pre-loaded with 0.1 µg/ml OVA for 1 h 30 min, were mixed with $3*10^5$

T cells and loaded onto the coated dishes in a total volume of 300 µl. Images were taken every 30 sec for a total of 6 h on bright field microscope using 20x magnification and an exposure of 20 ms. Images were processed with Fiji.

2.4.23 Quantification and Statistical Analysis

Data are represented as means ± standard deviations. Statistics were performed using GraphPad Prism version 9.0.2 for Windows. Statistical details for each experiment can be found in the respective Figure legends. Significance was defined as follows: * $p<0.1$, ** $p<0.05$, *** $p<0.01$, **** $p<0.001$.

3 The unexpected effect of non-cell autonomy

Experiments in this chapter were performed by Tomasek K, Leithner A and Assen F. Tomasek K performed crawl in assays and all experiments shown in 3.2.2. Tomasek K and Leithner A together performed the in vivo assays, with Leithner A doing the footpad injections, lymph node dissections and follow up cell staining. Assen F performed retro-orbital T cell injections for in vivo T cell priming assays. Tomasek K performed the B cell assay with technical assistance of Leithner A. The results in this chapter are not published.

3.1 Introduction

The interactions between host and microbe are best studied in vivo using for example mouse infection models. The urinary tract, as a model to study persistent or recurring infections, offers a simplified tool to study these interactions as the microbial flora is less complex as in the colon or on the skin (Beutler 2016). In UTI models, pathogenic bacteria are introduced into the bladder or even the kidney of mice by catheterization and the infection process can be monitored by determining bacterial loads or imaging explanted bladder or kidney at different time points (Hung et al. 2009). Moreover, the regulation of immune response to the bacteria can be studied by analyzing immune cell counts, levels of serum antibodies, cytokine levels and even gene expression profiles of individual immune cell types (Chan et al. 2013). However, such mouse infection models require not only very skilled personnel, but also ethical approval and many replicates. Additionally, any infection, no matter if simulated in the lab using infection models or during an infection in the wild, involves not only one cell type, but many different cells inside the host. For example, bladder epithelial cells are the first cells a bacterium inside the host interacts with and neutrophils are among the first innate immune cells invading into the urine during the early state of bladder infections (Bien et al. 2012). During the later stage of infection, when the pathogens subvert the innate immune response of neutrophils, macrophages and DCs residing in the underlying tissue take action and subsequently activate the adaptive immune response. Hence, no cell inside the host can be studied in isolation. Each cell is in a constant exchange with many other cells, either directly or indirectly by cell-signaling molecules, such as cytokines. Therefore, the dynamic response of all host cells during the early and late infection process might complicate the interpretation of an experimental outcome. To still study the response to infections in a more physiological context than just the Petri dish, different approaches were implemented to not lose the context dependency of cell-cell interactions but still reduce the overall complexity: ex vivo ear assays (Lämmermann et al. 2008), footpad injection models (Lämmermann et al. 2008; Leithner et al. 2016), organoid models (Sharma et al. 2021a) and recently even organ-on-a-chip models (Sharma et al. 2021b).

Given the results described in chapter two, where we found type 1 piliated UPEC acting as modulators of innate and adaptive immunity by affecting migration and co-stimulatory molecules of DCs, we were interested how in vitro stimulated DCs behave once they are challenged in competition assays with differently stimulated DCs or when they are re-introduced into their in vivo niche, the tissue of the host. The re-introduced DCs inside the host undergo interactions with many other host cells, either directly by cell-cell contacts or indirectly by cell-signaling molecules. This interactions can have great influence on both cell

types, the re-introduced DCs and the non-tolerogenic host cells. Using this rather simplistic approach of re-introducing stimulated DCs into the host tissue, we bypass the early state of infection but still gain insights into the late state of the infection process during persistent or recurring infections.

3.2 Results

3.2.1 Dendritic cells stimulated with type 1 piliated UPEC experience, but also generate, non-cell autonomous effects

Here, we used ear crawl in assays and footpad injections to analyze the invasion and migration behavior of DCs after in vitro stimulation with UPEC ON or OFF mutants. Either individually stimulated DCs were assayed or the stimulated DCs were mixed in equal amount ("mixing models or competitive assays") and assayed. Additionally, we investigated the ability of the in vitro stimulated DCs to activate T cells in vivo.

The difference between the ex vivo ear crawl out assay presented in chapter two and the crawl in assay in this chapter is the following: in the crawl out assay, tissue-residing (endogenous) DCs migrate into lymph vessels, whereas in the crawl in assay, exogenous DCs first need to invade into the ear tissue and then migrate into the lymph vessels. Migration of endogenous WT DCs out of the tissue into the lymph vessels was reduced after incubating the mouse ears with UPEC ON mutants (Figure 2-2E). The same results were obtained when analyzing migration of exogenously stimulated DCs in a crawl in assay: less UPEC ON stimulated DCs migrated into the lymph vessel, as compared to OFF stimulated ones (Figure 3-1A, non-mixed). Using in vivo migration assays, by injecting DCs into the footpad of mice and assaying migration into the popliteal lymph node, showed a similar effect: less UPEC ON stimulated DCs reached the lymph node, as compared to UPEC OFF stimulated ones (Figure 3-1B, non-mixed). However, the pronounced difference between ON and OFF in the ex vivo assays is weakened in vivo.

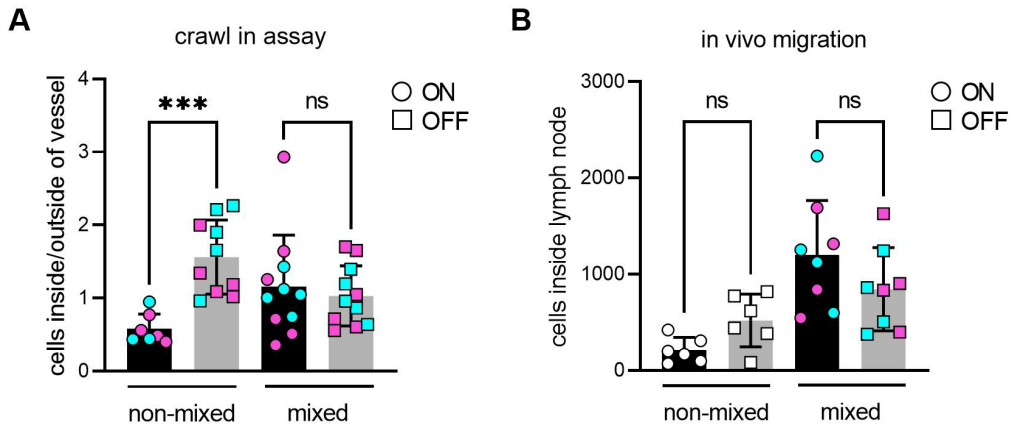

Figure 3-1: *DCs experience a strong non-cell autonomous effect, affecting their migration behavior.*

A. *Crawl in assay of ON and OFF stimulated WT DCs in WT mouse ears. Quantification of cells inside over outside of lymph vessel after ON (black) and OFF (grey) stimulation. Exogenous DCs were stained with Oregon green (cyan) or TAMRA (magenta) and applied individually or mixed in a 1:1 ratio onto the ear sheets. ON or OFF*

stimulated DCs in the individually performed assays were also stained with both dyes, to exclude any dye-specific effects. ***B.*** *Amount of DCs inside the lymph node after ON (black) and OFF (grey) stimulation. Exogenous DCs were stained with Oregon green (cyan) or TAMRA (magenta) and injected individually or mixed in a 1:1 ratio into the footpad of WT mice.*

Strikingly, competition assays between UPEC ON and OFF stimulated DCs revealed an unexpected non-cell autonomous effect. OFF stimulated DCs migrated less efficiently into the lymph vessels when co-applied with ON stimulated DCs in the crawl in assays (Figure 3-1A, ON:OFF mixed). The same effect was observed when co-injecting UPEC ON and OFF stimulated DCs into the footpad of mice and assaying the in vivo migration into the popliteal lymph node (Figure 3-1B, ON:OFF mixed). Additionally, the competition assays also revealed a general increase in migration of ON stimulated DCs in the presence of OFF stimulated DCs (Figure 3-1A and B).

It therefore seems that first, the non-tolerogenic environment inside the mouse affects migration of ON stimulated DCs leading to a less pronounced migration difference after ON and OFF stimulation (Figure 3-1B, individual) and second, ON and OFF stimulated DCs experience a reciprocally affecting non-cell autonomous effect in competition assays (Figure 3-1A and B, ON:OFF mixed).

Next, we asked if the non-cell autonomous effect observed in the non-tolerogenic environment of the mouse would allow ON stimulated DCs to activate and thus prime T cells. Contrary to the results we observed in vitro, where we observed a striking defect in T cell priming after UPEC ON stimulation (Figure 2-1F), ON stimulated DCs reaching the popliteal lymph node were able to prime OVA specific $CD4^+$ T cells in vivo as efficiently as OFF stimulated ones (Figure 3-2A). We were able to link the ability to prime T cells in vivo to a regain in expression of the co-stimulatory molecule CD86 on ON stimulated DCs (Figure 3-2B).

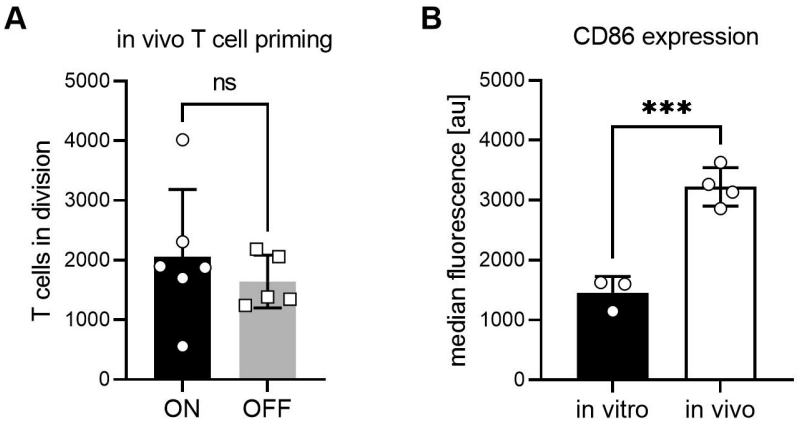

Figure 3-2**:** *The non-tolerogenic mouse environment increases the expression of co-stimulatory molecules on injected DCs leading to effective T cell priming.*

A. *Amount of dividing $CD4^+$ OT-II T cells in the popliteal lymph node after injecting ON or OFF stimulated DCs into the footpad of mice.* ***B.*** *Levels of CD86 on the membrane of DCs after stimulation with UPEC ON in vivo and in vitro.*

To this end, we found that DCs stimulated with type 1 piliated UPEC experience a non-cell autonomous effect in the presence of other DCs but also in the non-tolerogenic environment

of the mouse – both leading to restored migration capacity of the DCs and even restored ability to activate T cells in vivo.

3.2.2 Type 1 piliated UPEC alter the cytokine profile of dendritic cells by over-activating the NFAT pathway

We were interested in the underlying molecular mechanism for the non-cell autonomous effect seen in the competition assay between UPEC ON and OFF stimulated DCs. We speculated that binding of type 1 piliated UPEC to CD14 receptor, a GPI anchored protein, indirectly activates downstream signaling altering the cytokine profile of ON stimulated DCs. Since the NFAT (nuclear factor of activated T cells) pathway was shown to be activated by CD14-mediated Ca^{2+} influx (Zanoni et al. 2009), we used the inhibitor FK506 to block calcineurin prior to stimulation with bacteria. Blocking the NFAT pathway partially rescued the expression of co-stimulatory molecules after ON stimulation, compared to OFF stimulation (Figure 3-3A).

Given that NFAT acts as a transcription factor for several cytokines (Fric et al. 2012), and for example G-CSF (CSF3) was shown to be upregulated during UTIs (Ingersoll et al. 2008), we asked if UPEC ON stimulation triggers expression and secretion of immuno-modulating cytokines from DCs. We performed RNA-seq analysis and cytokine assays to analyze differences in cytokine expression and secretion after stimulation with ON and OFF mutants. Combining the expression and secretion data, we found several cytokines to be upregulated, both transcriptionally and translationally, by ON stimulated DCs (Figure 3-3B).

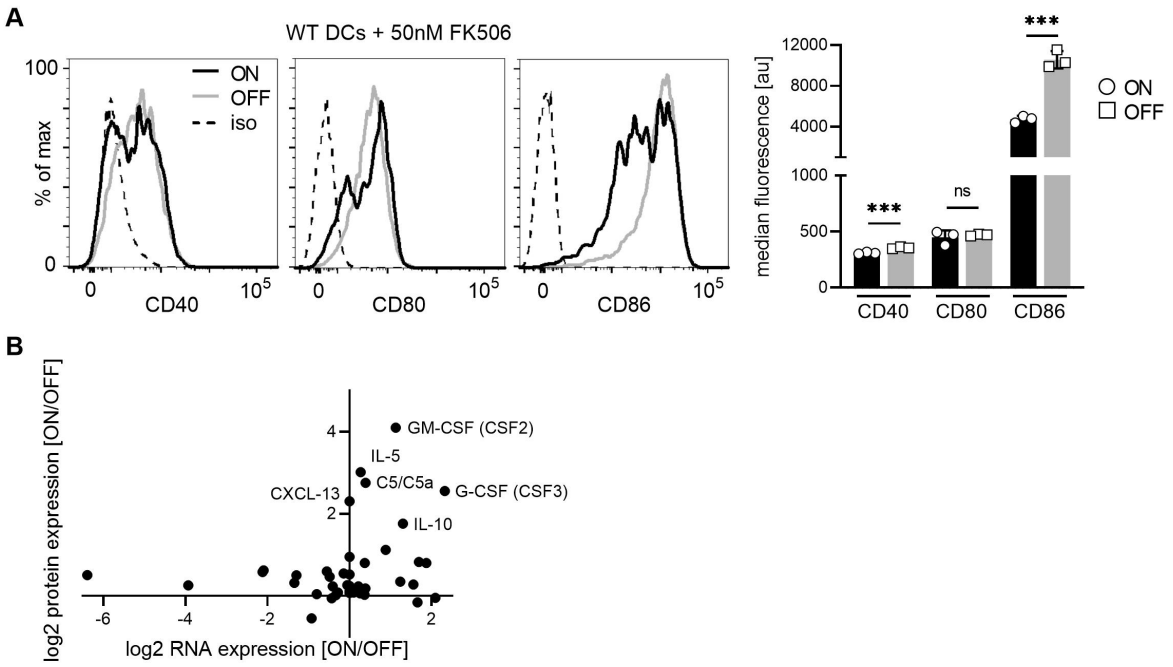

Figure 3-3: *Type 1 piliated UPEC alter expression of immuno-modulating cytokines by over-activating the NFAT pathway.*

A. *Levels of co-stimulatory molecules (CD40, CD80, CD86) on the membrane of DCs after stimulation with UPEC ON (black) and UPEC OFF mutants (grey) after pre-incubating DCs 20min prior to stimulation with the calcineurin*

inhibitor FK506 at 50nM (left; dashed black line = isotype controls). Quantification of the median fluorescence signal. ***B.*** *ON-stimulated DCs express and secrete higher levels of cytokines modulating inflammation and adhesion, like GM-CSF, IL-5, C5, G-CSF, CXCL-13 and IL-10.*

Among G-CSF, we also found GM-CSF (granulocyte-macrophage colony stimulating factor, CSF2) and other immuno-modulating cytokines, such as IL-10, IL-5, C5/C5a and CXCL-13 to be increased after UPEC ON stimulation (Figure 3-3B). We were interested if secretion of those immuno-modulating cytokines could affect other DCs in trans by a paracrine mode of action. Since we identified the importance of CD14 receptor for the interaction with type 1 piliated bacteria in chapter two of this thesis, and since WT and *cd14*$^{-/-}$ DCs can be easily distinguished in flow cytometry by staining for CD14, we decided to co-culture WT and CD14 knockout DCs and stimulate them with ON mutants. Since we found previously that DCs lacking the CD14 receptor were themselves not affected by UPEC ON stimulation (Figure 2-3E), we were asking if secretion of immuno-modulating cytokines, such as IL-10, by WT DCs would affect expression of co-stimulatory molecules on *cd14*$^{-/-}$ DCs in trans.

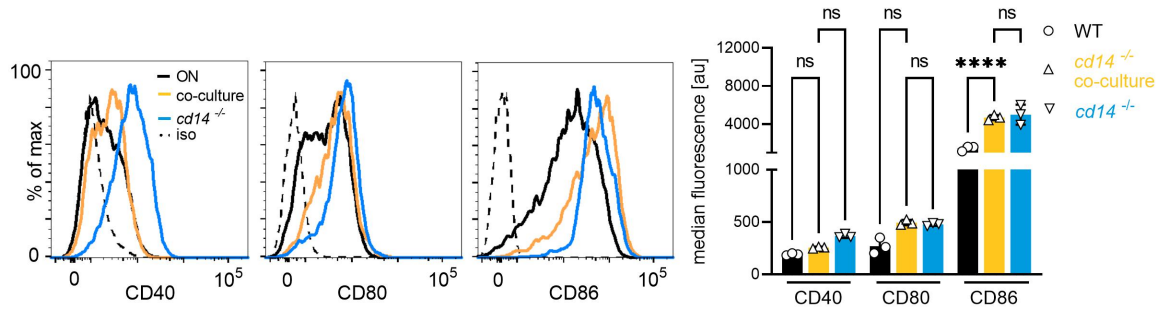

Figure 3-4**:** *DCs stimulated with type 1 piliated UPEC partially alter expression of co-stimulatory molecules on other cells in trans.*

Levels of co-stimulatory molecules (CD40, CD80, CD86) on the membrane of DCs after stimulation with UPEC ON mutants. Expression levels of WT DCs only (black), cd14 -/- DCs after co-culture with WT DCs (orange) and cd14 -/- only (blue) are shown (left; dashed black line = isotype controls). Quantification of the median fluorescence signal (right).

The secretion of immuno-modulating cytokines by WT DCs indeed affected expression of CD40 on CD14 knockout DCs, but had only little effect on the other co-stimulatory molecules (Figure 3-4). We assume that the physical contact of the bacteria by their type 1 pili and the CD14 receptor is needed to affect expression of all co-stimulatory molecules and the non-cell autonomous effect in vitro might not be sufficient to affect cells in trans entirely.

3.2.3 Type 1 piliated UPEC induce the antibody response of B cells, whereas non-piliated UPEC seem to dampen the antibody production

The adaptive immune response consists of two arm: the cell-mediated immunity, mediated by T cells, and the humoral immunity, which is the antibody-mediated response (Chaplin 2010). Since we found activation of T cells strongly reduced after UPEC ON stimulation in vitro (Figure 2-1F), and given that antibodies are secreted by plasma cells after differentiation from

naïve B cells with the help of T cells, we were wondering if also the antibody-mediated arm of the adaptive immune response is affected after ON stimulation.

Therefore, we performed a B cell helper assay to determine the antibody production after interaction with activated T cells. Strikingly, ON stimulation induced IgM antibody production by B cells, whereas OFF stimulation did not increase IgM levels over the baseline level (Figure 3-5). Additionally, OFF stimulation even decreased the amount of secreted IgG and IgA antibodies, compared to the baseline level.

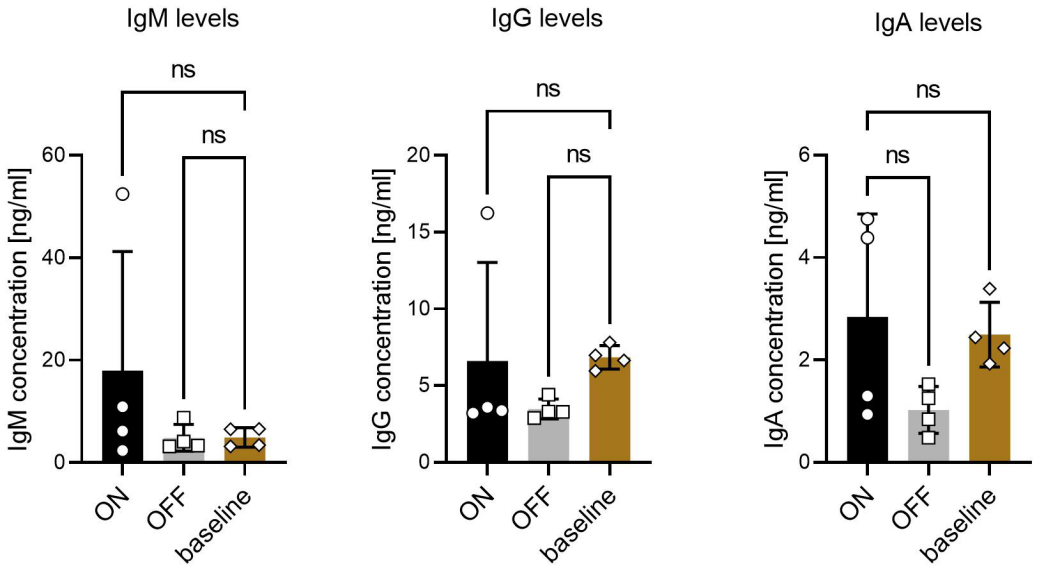

***Figure 3-5**: Type 1 piliated bacteria induce IgM production, whereas non-piliated bacteria dampen IgG and IgA production by B cells.*

Antibody levels of IgM, IgG and IgA were analyzed after 10 days of co-culture of B cells and activated $CD4^+$ T cells. T cells were activated by co-culture with UPEC ON and OFF stimulated DCs. The basal level of antibody production was established with naïve T cells.

We found that type 1 piliated bacteria induce IgM antibody production, but do not induce IgG or IgA antibodies. Interestingly, non-piliated bacteria seem to actively dampened production of IgG and IgA antibodies.

3.3 Discussion

Although (mouse) infection models are useful and necessary to understand infection processes and the regulation of the immune response to commensals and pathogens in vivo, the high complexity of these model system is often a “black box”. Simpler models, such as explanted tissues or organs, can therefore reduce the complexity and help in understanding how different cells of the host or immune system interact with each other in still a rather physiological context. Using such models, we found that exogenously stimulated DCs experience a pronounced non-cell autonomous effect in the presence of other DCs and in the non-tolerogenic environment of the mouse. This effect is most likely caused by cytokines, the signaling molecules of the cell. We found several immuno-modulating cytokines, driven by activation of the NFAT pathway, upregulated after stimulation with type 1 piliated bacteria: G-CSF was previously found to increase neutrophil migration into the bladder during UTIs

(Ingersoll et al. 2008) and GM-CSF was previously found to increase adhesion of monocytes (Gamble et al. 1989) most likely by increasing expression of CD11b integrins (Socinski et al. 1988). Increased expression of GM-CSF could be the underlying mechanism for the increased activity of CD11b integrin observed after stimulation with type 1 piliated bacteria (see chapter two of this thesis). Additionally, we found IL-10 to be upregulated after stimulation with type 1 piliated bacteria and IL-10 is known to act as an autocrine immunosuppressant: it decreases expression of co-stimulatory molecules on DCs (Mittal and Roche 2015) and also drives differentiation of regulatory T cells (Hsu et al. 2015). Moreover, IL-10 is a hallmark cytokine produced by tolerogenic DCs (Domogalla et al. 2017). However, it most likely be that the NFAT pathway is not the only pathway altered after stimulation with type 1 pilited UPEC, as CD14 interacts with several co-receptors and therefore potentially triggers many different pathways inside the cell (Zanoni and Granucci 2013).

Limited response of the adaptive immune system seems to be one major reason behind persistent or recurring infection (Magalhaes et al. 2007; Abraham and Miao 2015). We found cell-mediated adaptive immune response, as means of T cell activation and proliferation, almost absent after stimulation with type 1 piliated bacteria in vitro, but not in vivo. This pronounced difference might be due to the non-cell autonomous effects and the non-tolerogenic environment inside the mouse model. Interestingly, we did not find the humoral arm of the adaptive immunity to be absent during stimulation with type 1 piliated bacteria. However, we found a pronounced difference in the antibody production between piliated and non-piliated bacteria. Type 1 piliated mutant, although they dampened activation of T cells in vitro, still induced production of IgM antibodies, which are the first antibodies to be secreted in large numbers during an infection, but they are less strongly produced during a second or recurring infection (Chaplin 2010). Interestingly, type 1 piliated bacteria did not induce production of IgG or IgA antibodies over the baseline level. A reason could be that IgG antibodies are usually only produced in higher numbers after 10-14 days of infection and are also the predominant antibody in secondary infections (Chaplin 2010). IgA antibodies are usually produced around the same time as IgM antibodies, but they are considered the main humoral defense of the mucosa (Caruso et al. 2020). Strikingly, non-piliated mutants did not increase production of IgM antibodies over the baseline levels and they actively dampened secretion of IgG and IgA antibodies. This was quite the contrary to what we expected. We expected that type 1 piliated UPEC decrease the humoral immune response after decreasing T cell activation. However, we found non-piliated UPEC to silent or even dampen the humoral immunity. The underlying mechanism for this silencing by non-piliated UPEC remains to be studied.

3.4 Methods

DCs differentiation, growth of bacteria and general infection assays were performed as described in chapter two of this thesis.

3.4.1 Ex vivo Crawl in ear assay

Ear crawl in assays were performed similar as published previously (Leithner et al. 2016). In brief, ears from 5-week-old female C57BL/6J mice were split as described above. WT DCs stimulated with CFT073 locked-ON (KT179) or OFF (KT180) were labelled with 10 µM TAMRA or 3 µM Oregon green, respectively, or vice versa, and either used individually or mixed at a

1:1 ratio. 6x 10^4 cells were allowed to invade the ear tissue for 30 min. Non-invaded cells were washed off and ears were incubated at 37 °C for 6 h. Ears were fixed and lymphatics were stained using rat anti-Lyve-1 and anti-rat F(ab')$_2$-AF647 antibody. Ears were fixed on cover slips with ventricles facing up using cover glasses. 10 µm z-stacks were taken on inverted LSM800 confocal microscope with 488 and 640 nm LED-laser light source. Images were taken from 3 biological replicates analyzing 2 field of views each. Maximum intensity projections images were processed with Fiji. Images were analyzed using costume-made scripts in Fiji. Pre-processing was done using lymphatics script and analysis using LVmeanDCarea script.

3.4.2 In vivo migration

In vivo migration assays were performed similar as published previously (Leithner et al. 2018). In brief, DCs stimulated with CFT073 locked-ON (KT179) or OFF (KT180) were labelled with 10 µM TAMRA or 3 µM Oregon green respectively, and vice versa. In total, 10^6 cells – either ON or OFF stimulated DCs separately or ON and OFF stimulated DCs mixed in a 1:1 ratio – were suspended in 25 µl PBS and injected subcutaneously into the hind footpad of 4-6 week old C57BL/6J or Pep Boy (B6 CD45.1, B6.SJL-*Ptprc*^{a} *Pepc*^{b}/BoyJ) mice. 48 h later, mice were sacrificed and the popliteal lymph nodes were collected. Lymph nodes were ripped open and digested for 30 min at 37 °C in complete DMEM supplemented with 2 % FCS, 100 U/ml Penicillin, 100 µg/ml Streptomycin, 3 mM $CaCl_2$, 0.5 mg/ml collagenase D and 40 µg/ml DNAseI. After blocking in Fc-block, cells were stained against CD11c, MHCII, CD86 and CD45.2. The exact ratio of injected cells was quantified by analyzing the injection mixture prior to footpad injection.

3.4.3 Proteome profiler

Differences in secreted cytokines after CFT073 locked-ON (KT179) or OFF (KT180) stimulation were analyzed using a membrane-based antibody array (Proteom Profiler Mouse Cytokine Array Kit, R&D). The assay was carried out according to the manufacturers protocol, using 1 ml of cell culture supernatant.

3.4.4 Total RNA isolation

Total RNA from 3*10^5 DCs stimulated with either CFT073 locked-ON (KT179) or OFF (KT180) was extracted using RNeasy extraction kit (Qiagen). RNA purity and concentration was estimated using a NanoDrop spectrophotometer. RNA integrity was analyzed by denaturing agarose gel electrophoresis. RNAseq analysis was performed using Illumina TruSeq standard mRNA-Seq workflow with polyA enrichment and 50 bp single-reads on a HiSeq3000 (CeMM, Vienna).

3.4.5 In vivo T cell assay

T cell assays were performed as described previously (Leithner et al. 2020). In brief, primary naïve CD4$^+$ T cells were isolated from the spleen of OT-II mice (B6.Cg-Tg(TcraTcrb)425Cbn/J) using EasySep Mouse CD4$^+$ T cell isolation kit after homogenization with a 70 µm cell strainer and resuspending the cells in PBS supplemented with 2 % FCS and 1 mM EDTA. T cells were stained with 5 µM CFSE stain in 5 % FCS in PBS for 5 min at RT. After 30 min recovery in R10 medium at 37 °C, cells were routinely checked for fluorescence. 1*10^6 CFSE labeled CD4$^+$ T-cells were injected retro-orbital into 4-6 week old Pep Boy (B6 CD45.1, B6.SJL-*Ptprc*^{a} *Pepc*^{b}/BoyJ) mice. 24 h later 2.5*10^5 CFT073 locked-ON (KT179) or OFF (KT180) stimulated DCs, pre-loaded with 0.1 µg/ml OVA for 1 h, in 25 µl PBS were injected subcutaneously into

the hind footpad. 72 h after injecting the T cells, mice were sacrificed and the popliteal lymph nodes were collected. Lymph nodes were ripped open and digested for 30 min at 37 °C in complete DMEM supplemented with 2 % FCS, 100 U/ml Penicillin, 100 µg/ml Streptomycin, 3 mM $CaCl_2$, 0.5 mg/ml collagenase D and 40 µg/ml DNAseI. After blocking in Fc-block, cells were stained against CD4 and CD45.2. The amount of T cells in proliferation was analyzed by FlowJo software.

3.4.6 B cell helper assay

Primary naïve $CD4^+$ T cells were isolated and stained as described above. T cells were co-cultured with DCs stimulated with CFT073 locked-ON (KT179) or OFF (KT180) at a ratio of 5:1 ($5*10^4$ T cells:$1*10^4$ DCs) in 96-well round bottom well plates in R10 medium and 0.1 µg/ml ovalbumin. On day 4 of co-culture of DCs and T cells, B cells were isolated from the spleen of WT mice using EasySep Mouse B cell enrichment kit (Stemcell Technologies, 19754). T cells were gated on CD4 and CD45.2 expression and proliferating T cells were sorted according to their CFSE signal, omitting non-proliferating cells. B cells and proliferated T cells were co-cultured in a 10:1 ratio ($5*10^5$ B cells:$5*10^4$ T cells) in 96-well round bottom well plates in R10 medium for 10 days. Baseline antibody production of B cells was detected after co-culture with naïve T cells. Subsequent IgM (Invitrogen, 88-50470-22), IgG (Invitrogen, 88-50400-22) and IgA (Invitrogen, 88-50450-22) antibody levels were detected with ELISA on day 10. For IgM ELISA the supernatant was diluted 1:10 in assay buffer, whereas for IgG and IgA ELISA the supernatant was not diluted.

3.4.7 Co-culture flow cytometry assay

WT and *cd14* $^{-/-}$ DCs were mixed 1:1 and stimulated with CFT073 ON (KT179) at an MOI of 10. 1 h post infection (pi) gentamicin was added at 7.5 µg/ml to prevent extracellular growth of bacteria. 18-20 h pi DCs were collected and incubated in FACS buffer (1x PBS, 2 mM EDTA, 1 % BSA; RT) with Fc receptor block for 20 min. Cells were stained for 30 min with antibodies in presence of Fc-block. Cells were washed twice with PBS and resuspended in FACS buffer for analysis on FACS Canto II (BD). 10,000 events gated on FSC-A and SSC-A to exclude debris were recorded at medium flow rate. Data were analyzed using FlowJo software by excluding doublets. WT DCs were gated on their CD14 expression, whereas *cd14*$^{-/-}$ lack expression.

3.4.8 Quantification and Statistical Analysis

Data are represented as means ± standard deviations. Statistics were performed using GraphPad Prism version 9.0.2 for Windows. Statistical details for each experiment can be found in the respective Figure legends. Significance was defined as follows: * $p<0.1$, ** $p<0.05$, *** $p<0.01$, **** $p<0.001$.

4 FimH is necessary, but not sufficient

The results in this chapter are not published.

4.1 Introduction

The data presented in chapter two of this thesis add to the understanding how pathogenic UPECs establish persistent or recurring infections using type 1 pili. Interestingly, type 1 pili are not only encoded in the genome of *E. coli* strains, but also other bacteria, such as *Klebsiella* (Struve et al. 2008). Hence, I was interested if other pathogens expressing type 1 pili would affect behavior of DCs the same way, or if this is a pure UPEC related phenomenon or even an inherent feature of the UPEC strain CFT073, which was isolated from the blood of a patient with acute pyelonephritis (Welch et al. 2002). I therefore generated phase-locked mutants of two additional UPEC strains: UTI89, which was isolated from the urine of a patient with cystitis (Chen et al. 2006) and 536, which was isolated from a patient with acute pyelonephritis (Hochhut et al. 2006). Additionally, I generated phase-locked mutants of the *K. pneumonia* strain 625, which was isolated from a patient carrying a permanent catheter (Shueb Mussa 2009).

However, although type 1 pili are encoded in the genome of almost all *E. coli* strains, irrespective of their pathogenicity, we did not find (pathogenic) FimH to be sufficient to cause the above mentioned modulation of the immune response in an otherwise non-pathogenic background (Supplementary Figure 4). I therefore aimed to identifying the "other factor(s)" expressed by the UPEC strain CFT073 contributing to the observed immune modulatory effects. Various genes, apart from type 1 pili, were shown to be important virulence factors to establish persistent infections. For example, many UPECs encode several type V secreted toxins exhibiting serine protease activities – so called autotransporters, such as Vat (vacuolating autotransporter toxin) and Sat (secreted autotransporter toxin) (Henderson et al. 2004). Both, Vat and Sat induce cytopathic effects in host cells (Wiles et al. 2008). Additionally, the secreted toxin HlyA (α-Hemolysin) complexes with LPS on the membrane of pathogenic *E. coli* and interacts with TLR4 receptor, to come into close contact with the host cell (Månsson et al. 2007). At high concentrations, HlyA forms pores in the membrane of host cells leading ultimately to cell death, whereas at sub-lytic concentrations, HlyA induces oscillatory change of intracellular calcium concentration. This has been shown to impact signal transduction pathways inside the cell (Uhlén et al. 2000).

4.2 Results

4.2.1 The genetic background of the pathogen plays an important role

Since the pathogenic potential of UPECs, compared to non-pathogenic *E. coli*, is not the result of a fixed group of virulence genes but rather a collection of different factors (Touchon et al. 2009) and since also other pathogens causing UTIs express type 1 pili (Struve et al. 2008), I was interested how the type 1 piliation status of other UPEC strains and a *Klebsiella* isolate would affected adhesion and expression of co-stimulatory molecules on DCs.

First, it had to be established if type 1 pili of *Klebsiella* mediate binding to CD14 at all. Because, although the FimH proteins of *E. coli* and *K. pneumonia* display a relatively high homology of 85% similarity in their amino acid sequence (Gerlach et al. 1989), this could still alter binding of *Klebsiella* type 1 pili to CD14. The bead binding assay using ON and OFF mutants of the *K. pneumonia* strain 625 confirmed that type 1 pili of this pathogen also highly specifically bind to CD14, since the presence of type 1 pili, and therefore the presence of FimH, are necessary for the bacteria to bind to CD14-coupled beads (Figure 4-1).

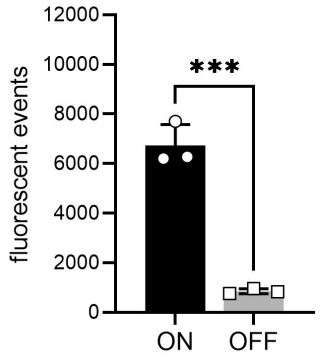

Figure 4-1: *Type 1 pili of K. pneumonia mediate binding to CD14.*

Flow cytometry analysis of bead binding assay. Quantification of fluorescent events in the bacterial gate. ON mutants (black) and OFF mutants (grey) bound to CD14-coupled beads.

Next, the immune modulatory effect of the three different UPEC strains, CFT073, UTI89 and 536, as well as the *K. pneumonia* strain 625 on the DCs were compared. Adhesion of DCs was increased after stimulation with all UPEC ON mutants, although to different extend (Figure 4-2, A-C). Interestingly, the piliation status of the *K. pneumonia* isolate did not affect the adhesion properties of DCs (Figure 4-2, D).

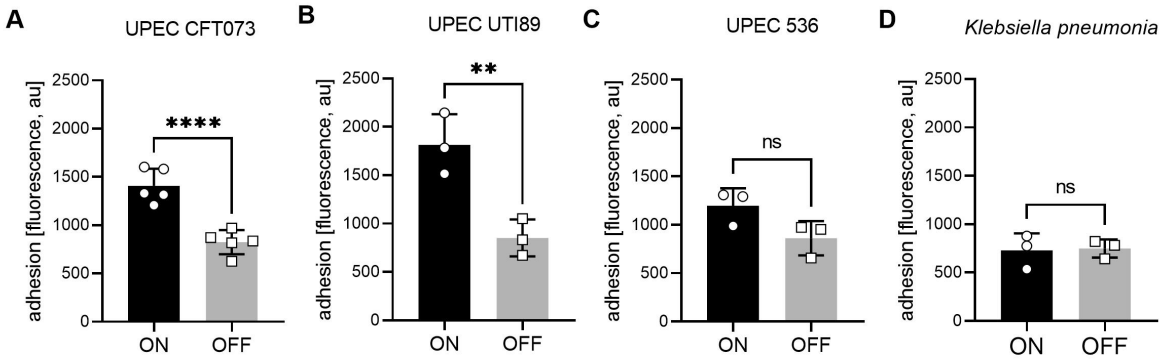

Figure 4-2: *Not every pathogen increases adhesion of DCs.*

*Quantification of fluorescence signals, proxy for adherent DCs, after ON (black) and OFF (grey) stimulation with the UPEC strains **A.** CFT073 (pyelonephritis isolate), **B.** UTI89 (cystitis isolate), **C.** 536 (pyelonephritis isolate) and **D.** the K. pneumonia strain 625 (catheter-isolate).*

Analyzing the expression of co-stimulatory molecules after stimulation with the different UTI causing pathogens showed the following: only ON mutant of CFT073 decreased the expression of all co-stimulatory molecules on DCs, whereas the other UPEC strains only affected expression of CD86 (Figure 4-3). As for the adhesion, the ON mutant of *K. pneumonia* did not affect expression of co-stimulatory molecules, compared to the respective OFF mutant.

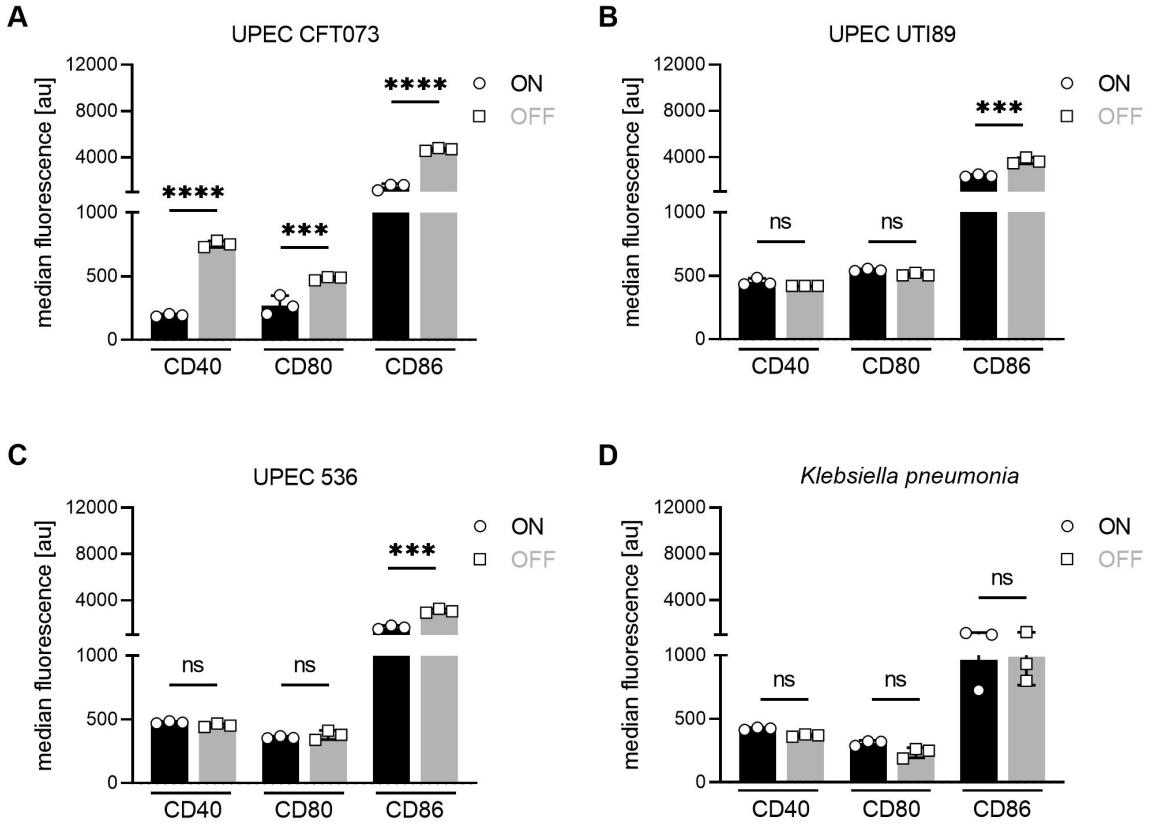

Figure 4-3: *Not every pathogen decreases expression of co-stimulatory molecules on DCs.*

Quantification of the median fluorescence signal of co-stimulatory molecules (CD40, CD80, CD86) on the membrane of DCs after stimulation with ON (black) and OFF mutants (grey) of the UPEC strains ***A.*** *CFT073 (pyelonephritis isolate),* ***B.*** *UTI89 (cystitis isolate),* ***C.*** *536 (pyelonephritis isolate) and* ***D.*** *the K. pneumonia strain 625 (catheter-isolate).*

It therefore seems that the specific genetic background of the pyelonephritis strain CFT073 isolated from blood is necessary for the striking immune modulatory effects observed on DCs.

4.2.2 An effort to identify the "other factor(s)" unique to CFT073

In an effort to identify the unique pathogenic properties of CFT073 compared to the other UPEC strains, three potential genes were identified that could affect DCs behavior after stimulation with the bacteria: the autotransporters *vat* and *sat* – which express for exotoxins, and *hemolysin* A – expressing an endotoxin. The genes *hlyA* and *sat* seemed most promising to contribute to the immune modulating effect of CFT073 and therefore those genes were deleted from CFT073 locked-ON mutants and the effect on expression of co-stimulatory molecules on DCs was analyzed.

Comparing expression of co-stimulatory molecules on DCs after stimulation with CFT073 ON and ON Δ*fimH* with the newly generated mutants showed that both, *sat* and *hlyA*, seem to be partially responsible for decreasing expression of co-stimulatory molecules after ON stimulation, but none of them seem the other factor necessary next to FimH since expression of co-stimulatory molecules is not fully restored in the *sat* and *hlyA* mutants (Figure 4-4).

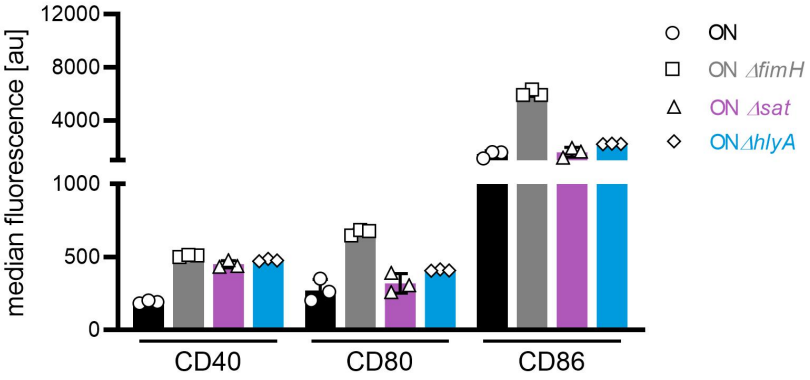

Figure 4-4: *Neither sat nor hlyA seem the additional factor necessary.*

Quantification of the median fluorescence signal of co-stimulatory molecules (CD40, CD80, CD86) on the membrane of DCs after stimulation with CFT073 ON (black), CFT073 ON ΔfimH (grey), CFT073 ON Δsat (purple) and CFT073 ON ΔhlyA (blue) mutants.

Since neither the endotoxin HlyA nor the exotoxin Sat seem to be the only "other factor" needed, I was wondering if a very simple assay could reveal if the observed effects are either based on endotoxins or exotoxins. Therefore, adhesion of DCs after stimulated with CFT073 ON mutants was compared to (i) adhesion after stimulation with the non-pathogenic *E. coli* W mutant expressing *fimH* from CFT073 (see also chapter 2 of the thesis) – which would report on an endotoxin-based mediator as the "other factor", or (ii) adhesion after stimulation with supernatant from CFT073 ON mutants – which would report on an exotoxin-based mediator as the "other factor" (Figure 4-5, A and B). Interestingly, in both cases adhesion of DCs was not increased, compared to stimulation with CFT073 ON mutants, although the presence of bacteria in general seem to increased adhesion of DCs compared to stimulation with bacterial supernatant only. Since recombinant LPS is used to stimulate DCs in the absence of bacteria, I was finally wondering if overstimulation of DCs with recombinant LPS as kind of an "endotoxin overload" would rescue adhesion of DCs after stimulation with CFT073 ON mutants (Figure 4-5, C). However, excessive amounts of LPS are not able to overcome the adverse effects after ON stimulation.

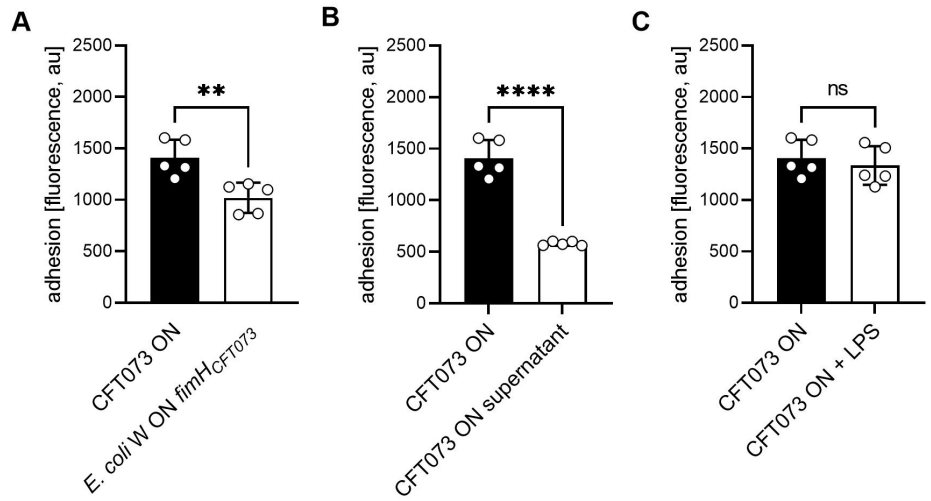

Figure 4-5: *Adhesion of DCs depends on presence of CFT073 ON mutants and the adverse effects can not be overruled with excessive amounts of LPS.*

Quantification of fluorescence signals, proxy for adherent DCs, after stimulation with CFT073 ON (black) and ***A.*** *the non-pathogenic E. coli W ON mutant expressing fimH from CFT073,* ***B.*** *supernatant of CFT073 ON mutants with 200 ng/ml LPS and* ***C.*** *CFT073 ON mutants with 200 ng/ml LPS.*

4.3 Discussion

E. coli causes the vast majority of UTIs and several strains displaying a great genetic diversity were isolated. However, also other bacteria such as *Klebsiella* were isolated from patients suffering from UTIs. Interestingly, analyzing the immune modulatory potential of three different clinical UPEC isolates (Welch et al. 2002; Chen et al. 2006; Hochhut et al. 2006) and one *K. pneumonia* isolate (Shueb Mussa 2009) revealed that all UPEC strains increased adhesion of DCs, although to very different extend, but only the pyelonephritis strain CFT073 decreased expression of all co-stimulatory molecules tremendously. Additionally, the *K. pneumonia* strain 625 isolated from a catheterized patient did not affect adhesion nor expression of co-stimulatory molecules. It therefore seems that the bacterial pathogens have evolved distinct pathogenic potential maybe related to the pressure generated by the immune system in the very host niche the pathogens were isolated from: the pyelonephritis strain CFT073 isolated from blood most likely faced the strongest selection by the immune system and thus acquired additional virulence factors to subvert the action of the immune response.

Although UPEC isolates share many properties, the very genomic features that are specifically unique to those pathogenic *E. coli* have not yet been identified to their fullest (Wiles et al. 2008). All three tested UPEC strains for example express the autotransporter Val, but only CFT073 expresses the autotransporter Sat; and all three strains express the *hemolysin* operon, but strains CFT073 and UTI89 each express one copy of the operon, whereas strain 536 expresses two copies (Wiles et al. 2008). However, neither the uniquely expressed autotransporter Sat of CFT073, known to induce cytopathic effects (Wiles et al. 2008), nor HlyA, known to impact signal transduction pathways by inducing calcium oscillations (Uhlén et al. 2000), were sufficient to affect expression of the co-stimulatory molecules on DCs similarly to FimH. Interestingly, all three tested UPEC strains express pap pili, important for

adhesion to kidney epithelial cells and therefore important to cause pyelonephritis (Wiles et al. 2008). Therefore the strain specific effect observed on adhesion and expression on co-stimulatory molecules seem independent on P pili expression. This still leaves the question open about the additional factor necessary in the UPEC strain CFT073 apart from FimH. However, given the complexity of the CFT073 genome (Kao et al. 1997; Guyer et al. 1998) it could even be a combination of several factors which cause the observed immune modulatory effects on the innate immune cells. Therefore, further genomic analysis of the different UPEC isolates in comparison to the pyelonephritis strain CFT073 could help in identifying the "other factor(s)".

4.4 Methods

DCs differentiation, growth of bacteria, general infection assays, the adhesion assay and staining of co-stimulatory molecules on DCs were performed as described in chapter two of this thesis. For the adhesion assay using supernatant of CFT073 ON mutants, the bacteria were removed by spinning and filtration (1x 0.45 µm and 1x 0.2 µm) and 200 ng/ml recombinant LPS was added.

4.4.1 Bacterial strain construction

4.4.1.1 Locked mutants

UPEC locked-ON and locked-OFF mutants were generated as described in chapter two. Clinical UPEC isolates CFT073 ((Welch et al. 2002); ATCC 7000928), UTI89 (Chen et al. 2006), 536 (Hochhut et al. 2006) were kindly provided by Ulrich Dobrindt. Resulting UPEC locked mutants were: CFT073 locked-ON – KT179, CFT073 locked-OFF – KT180, UTI89 locked-ON – KT177, UTI89 locked-OFF – KT178, 536 locked-ON – KT280 and 536 locked-OFF – KT281.

Klebsiella locked-ON and locked-OFF mutants were generated similarly, but using different primers. The clinical isolate of *Klebsiella pneumonia* strain 625 (Shueb Mussa 2009) was kindly provided by Ulrich Dobrindt. The *fimS* region was amplified either in the ON (primers 324 and 325) or OFF (primers 326 and 327) orientation from the chromosome of the wild type strain but omitting the 9 bp recognition site on the left site. The FRT-removable chloramphenicol resistance marker was assembled left of the amplified *fimS* regions using NEBuilder assembly kit. The assembled DNA fragments were PCR amplified using primers 328 and 329 and integrated into the chromosome instead of the endogenous *fimS* using lambda red recombination. The resulting mutants were: *K. pneumonia* locked-ON – KT276 and *K. pneumonia* locked-OFF – KT277. Since the *Klebsiella* strain got ampicillin resistant by spontaneous mutation, it was not possible to cure the generated mutants from the chloramphenicol resistance marker on the chromosome using pCP20.

4.4.1.2 *HlyA* and *sat* deletion mutants

hlyA and *sat* genes from CFT073 locked-ON mutants (KT179) were deleted by lambda red recombination. The FRT-flanked chloramphenicol resistance marker from pKD3 plasmid was amplified using either primers 314 and 315 for *hlyA* deletion or primers 336 and 337 for *sat* deletion and integrated into the chromosome of KT179 strain. Successful deletion was confirmed by PCR (primers 316 and 317 for *hlyA*, primers 338 and 339 for *sat*). Resistance was

flipped using pCP20 plasmid resulting in CFT073 locked-ON *ΔhlyA* mutant – KT274 and CFT073 locked-ON *Δsat* mutant – KT283.

4.4.2 Bead binding assay

Bead binding assay was performed as mentioned in chapter two of this thesis. However, since the *Klebsiella* phase-locked mutants generated became spontaneously resistant to ampicillin, no further genetic modification with the current plasmids at hand were possible. Therefore, in order to visualize bound bacteria to the CD14-coupled beads, the bead-bound bacteria were stained with thiazole orange at 10.5 µM final concentration for 5 min in the dark after having unbound bacteria washed off.

4.4.3 Quantification and Statistical Analysis

Data are represented as means ± standard deviations. Statistics were performed using GraphPad Prism version 9.0.2 for Windows. Statistical details for each experiment can be found in the respective Figure legends. Significance was defined as follows: * $p<0.1$, ** $p<0.05$, *** $p<0.01$, **** $p<0.001$.

5 Conclusions

In this thesis, I demonstrate experimentally how opportunistic pathogens modulate the innate and adaptive immune response by using adhesion filaments encoded in the genome of almost all *E. coli* strains. The immune modulating effects can be visualized as a cascade of events happening along the immune system network (Figure 5-1): Once type 1 piliated bacteria bind to CD14 receptor on DCs with the FimH protein located on the tip of the pili, this interaction modulates functional keystones of the innate immune cells. First, migration of DCs towards the lymph node is reduced. Second, DCs secrete immuno-modulating cytokines affecting other immune cells in trans. Finally, even if some DCs manage to migrate to the lymph node, the physical interaction with T cell and the ability to activate and prime T cells might be affected. (It should be noted that the efficiency between in vitro and in vivo T cell priming differ, most likely due to the non-tolerogenic environment inside the mouse). However, this skewed T cell response does not affect the humoral immune response: Type 1 piliated bacteria induce robust IgM antibody production, whereas non-piliated bacteria seem to actively dampen production of IgG and IgA antibodies. Thus, it seems that the pathogens as a population, meaning piliated but also non-piliated bacteria together, modulate the whole immune response cascade, leading to dampened innate and adaptive immunity.

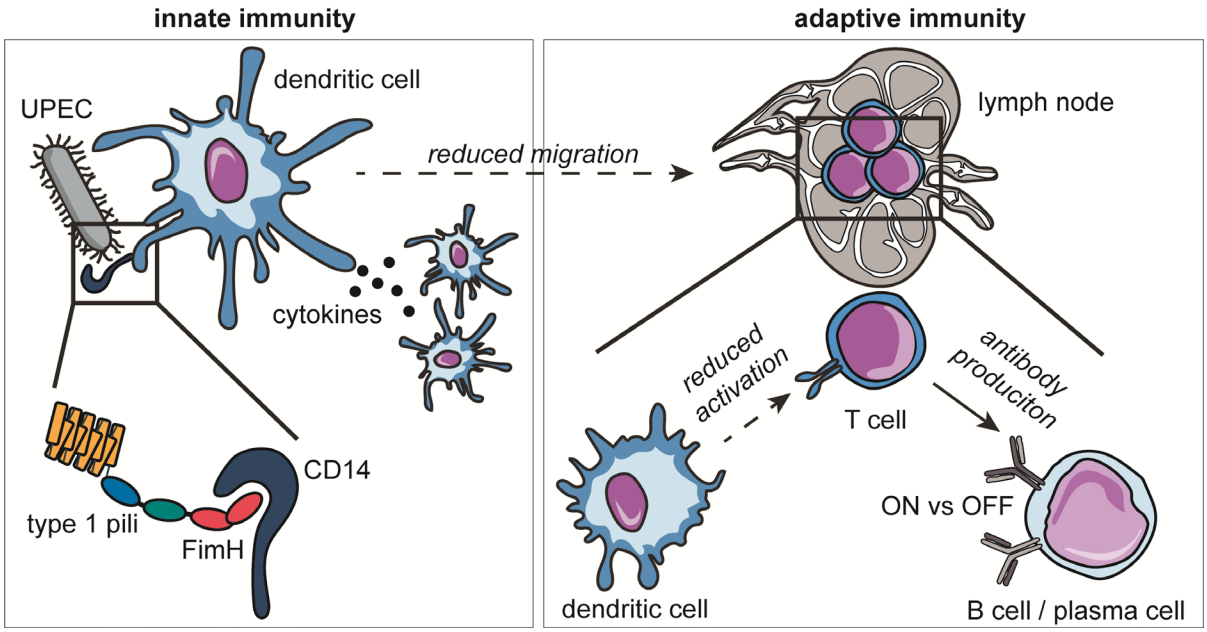

Figure 5-1**:** *Type 1 piliated uropathogenic E. coli modulate innate and adaptive immune response.*

UPEC bind to CD14 receptor on DCs with the FimH protein on the tip of type 1 pili. DCs secret immuno-modulating cytokines affecting other cells in trans. Migration of DCs to the lymph node is reduced. Even if some DCs manage to migrate to the lymph node, activation of T cells is dampened. The few activated T cells after stimulation with type 1 piliated UPEC lead to differentiation of B cells into plasma cells and robust production of IgM antibodies. However, non-piliated bacteria seem to dampen activation of antibody production.

5.1 (Cell-cell) context and (genomic) complexity – two built-in functions of host-pathogen evolution

In chapter three of this thesis a strong non-cell autonomous effect was observed. This non-cell autonomous effect was not only modulating behavior of DCs stimulated with non-piliated bacteria in the presence of cells stimulated with type 1 piliated bacteria, but also the other way around. Even in the non-tolerogenic environment of the mouse, this non-cell autonomous effect affected DCs stimulated with type 1 piliated bacteria, as enough DCs migrated into the lymph node, regained expression of co-stimulatory molecules and thus managed to efficiently activate T cells. It would be interesting to know if and how this non-cell autonomous effect would take place during an infection model where the bacteria are introduced into the host and interact with all cell types throughout the whole infection process in order to keep the biological context of cell-cell interactions. Such an infection model would also better reflect the actual antibody response towards type 1 piliated and non-piliated bacteria. However, given the complexity of such infection models they require well trained personnel and proper controls in order to extract valuable results.

In chapter four the beauty of evolution of pathogens to specific host niches could almost be observed in action: two different bacterial species causing UTIs, *E. coli* and *Klebsiella*, and three distinct UPEC isolates affected behavior of DCs very differently. This diverse effect on the innate immune cells most likely reflects the evolution of the pathogen towards the pressure of the host immune response and the very combination of virulence factors of the pathogen. Unfortunately, the "other factor" making the pyelonephritis strain CFT073 very potent in modulating DCs behavior was not identified entirely, although both tested genes, the autotransporter *sat* and *hemolysin* A, had certain effect on DCs behavior. However, most likely it would be more accurate to think about the "other factor**(s)**" necessary apart from FimH, as most likely a combination of genes or virulence factors generates the pathogenic potential of a bacterium.

Bacteria populated Earth long before humans did and they are also residing on and within humans in various niches. Some bacteria are beneficial to the health of the host and the host lives with them in symbiosis – these are the commensals. Whereas other bacteria are a threat to the health and life of the host – these are the pathogens. However, things are not always as black and white as it seems from this description or from simplified in vitro experiments. Commensal bacteria can evolve to become truly pathogenic and some commensals might only accidentally act like pathogens once they end up in a wrong host niche. Hence, it is not surprising that the host immune system faces a conundrum of having to distinguish commensal from pathogenic bacteria in vivo. Sometimes the host confuses commensal bacteria, for example as part of the microbiota, with pathogens, resulting in aberrant immune responses and the establishment of inflammatory diseases. Luckily, generally the immune system does not attack commensal bacteria. However, pathogenic bacteria might also abuse this dampened response of the immune system to "go undercover" among the commensals to persist prolonged times inside the host without electing a proper immune response. In this thesis I've uncovered exactly such a mechanism of pathogens abusing per-se non virulent adhesion filaments to actively dampen the innate and adaptive immune response with the goal to persist for prolong times inside the host.

Taking one step back from this narrow view on bacteria-host or pathogen-host interaction, which is a continual trade-off between benefit and risk, we might appreciate the following: these interactions cannot be seen solely in isolation, which is especially reflected in the data presented in chapter three of this thesis – the non-cell autonomous effect. Not only the host undergoes continues interactions with commensal **and** pathogenic bacteria at a time, each host cell interacts with many other cells, as well as commensal and pathogenic bacteria interact with each other. Each node and each edge in this big and complex interaction network are crucial for the outcome of the very interaction. Thus, the complexity of this *"interactome"* needs to be understood in context. Context & complexity – the dancing couple we all fall for in science.

References

Abraham, Soman N.; Miao, Yuxuan (2015): The nature of immune responses to urinary tract infections. In Nat Rev Immunol 15 (10), pp. 655–663. DOI: 10.1038/nri3887.

Alton, Gordon; Kjaergaard, Susanne; Etchison, James R.; Skovby, Flemming; Freeze, Hudson H. (1997): Oral Ingestion of Mannose Elevates Blood Mannose Levels: A First Step toward a Potential Therapy for Carbohydrate-Deficient Glycoprotein Syndrome Type I. In Biochemical and Molecular Medicine 60 (2), pp. 127–133. DOI: 10.1006/bmme.1997.2574.

Archer, Colin T.; Kim, Jihyun F.; Jeong, Haeyoung; Park, Jin Hwan; Vickers, Claudia E.; Lee, Sang Yup; Nielsen, Lars K. (2011): The genome sequence of E. coli W (ATCC 9637): comparative genome analysis and an improved genome-scale reconstruction of E. coli. In BMC Genomics 12, p. 9. DOI: 10.1186/1471-2164-12-9.

Axtelle, T.; Pribble, J. (2001): IC14, a CD14 specific monoclonal antibody, is a potential treatment for patients with severe sepsis. In Journal of endotoxin research 7 (4), pp. 310–314.

Banchereau, J.; Steinman, R. M. (1998): Dendritic cells and the control of immunity. In Nature 392 (6673), pp. 245–252. DOI: 10.1038/32588.

Bayliss, Christopher D. (2009): Determinants of phase variation rate and the fitness implications of differing rates for bacterial pathogens and commensals. In FEMS Microbiol Rev 33 (3), pp. 504–520. DOI: 10.1111/j.1574-6976.2009.00162.x.

Beutler, Bruce (2016): Pathogens, Commensals, and Immunity: From the Perspective of the Urinary Bladder. In Pathogens 5 (1), p. 5. DOI: 10.3390/pathogens5010005.

Bien, Justyna; Sokolova, Olga; Bozko, Przemyslaw (2012): Role of Uropathogenic Escherichia coli Virulence Factors in Development of Urinary Tract Infection and Kidney Damage. In International Journal of Nephrology 2012 (3), pp. 1–15. DOI: 10.1155/2012/681473.

Boucher, Helen W.; Talbot, George H.; Bradley, John S.; Edwards, John E.; Gilbert, David; Rice, Louis B. et al. (2009): Bad bugs, no drugs: no ESKAPE! An update from the Infectious Diseases Society of America. In Clinical infectious diseases : an official publication of the Infectious Diseases Society of America 48 (1), pp. 1–12. DOI: 10.1086/595011.

Bousso, Philippe (2008): T-cell activation by dendritic cells in the lymph node: lessons from the movies. In Nat Rev Immunol 8 (9), pp. 675–684. DOI: 10.1038/nri2379.

Bouvet, Odile; Bourdelier, Emmanuelle; Glodt, Jeremy; Clermont, Olivier; Denamur, Erick (2017): Diversity of the auxotrophic requirements in natural isolates of Escherichia coli. In Microbiology (Reading, England) 163 (6), pp. 891–899. DOI: 10.1099/mic.0.000482.

Caruso, Roberta; Lo, Bernard C.; Núñez, Gabriel (2020): Host–microbiota interactions in inflammatory bowel disease. In Nat Rev Immunol 20 (7), pp. 411–426. DOI: 10.1038/s41577-019-0268-7.

Chait, Remy; Ruess, Jakob; Bergmiller, Tobias; Tkačik, Gašper; Guet, Călin C. (2017): Shaping bacterial population behavior through computer-interfaced control of individual cells. In Nat Comms, p. 1535. DOI: 10.1038/s41467-017-01683-1.

Chan, Cheryl Y.; St John, Ashley L.; Abraham, Soman N. (2013): Mast cell interleukin-10 drives localized tolerance in chronic bladder infection. In Immunity 38 (2), pp. 349–359. DOI: 10.1016/j.immuni.2012.10.019.

Chaplin, David D. (2010): Overview of the immune response. In The Journal of allergy and clinical immunology 125 (2 Suppl 2), S3-23. DOI: 10.1016/j.jaci.2009.12.980.

Chen, S. L.; Hung, C.-S.; Xu, J.; Reigstad, C. S.; Magrini, V.; Sabo, A. et al. (2006): Identification of genes subject to positive selection in uropathogenic strains of Escherichia coli: A comparative genomics approach. In Proceedings of the National Academy of Sciences 103 (15), pp. 5977–5982. DOI: 10.1073/pnas.0600938103.

Chen, Swaine L.; Hung, Chia S.; Pinkner, Jerome S.; Walker, Jennifer N.; Cusumano, Corinne K.; Li, Zhaoli et al. (2009): Positive selection identifies an in vivo role for FimH during urinary tract infection in addition to mannose binding. In Proceedings of the National Academy of Sciences of the United States of America 106 (52), pp. 22439–22444. DOI: 10.1073/pnas.0902179106.

Cherepanov, P. P.; Wackernagel, W. (1995): Gene disruption in Escherichia coli: TcR and KmR cassettes with the option of Flp-catalyzed excision of the antibiotic-resistance determinant. In Gene 158 (1), pp. 9–14.

Choudhury, D.; Thompson, A.; Stojanoff, V.; Langermann, S.; Pinkner, J.; Hultgren, S. J.; Knight, S. D. (1999): X-ray structure of the FimC-FimH chaperone-adhesin complex from uropathogenic Escherichia coli. In Science 285 (5430), pp. 1061–1066. DOI: 10.1126/science.285.5430.1061.

Chutipongtanate, Somchai; Thongboonkerd, Visith (2010): Systematic comparisons of artificial urine formulas for in vitro cellular study. In Analytical biochemistry 402 (1), pp. 110–112. DOI: 10.1016/j.ab.2010.03.031.

Croxen, Matthew A.; Finlay, B. Brett (2010): Molecular mechanisms of Escherichia coli pathogenicity. In Nature reviews. Microbiology 8 (1), pp. 26–38. DOI: 10.1038/nrmicro2265.

Datsenko, K. A.; Wanner, B. L. (2000): One-step inactivation of chromosomal genes in Escherichia coli K-12 using PCR products. In Proceedings of the National Academy of Sciences 97 (12), pp. 6640–6645. DOI: 10.1073/pnas.120163297.

Datta, Simanti; Costantino, Nina; Court, Donald L. (2006): A set of recombineering plasmids for gram-negative bacteria. In Gene 379, pp. 109–115. DOI: 10.1016/j.gene.2006.04.018.

Domogalla, Matthias P.; Rostan, Patricia V.; Raker, Verena K.; Steinbrink, Kerstin (2017): Tolerance through Education: How Tolerogenic Dendritic Cells Shape Immunity. In Frontiers in immunology 8, p. 1764. DOI: 10.3389/fimmu.2017.01764.

Donnenberg, Michael S. (2013): Escherichia coli. Pathotypes and principles of pathogenesis / edited by Michael S. Donnenberg. Second edition. Amsterdam: Academic Press.

Eldridge, Gary R.; Hughey, Heidi; Rosenberger, Lois; Martin, Steven M.; Shapiro, Andrew Marc; D'Antonio, Elizabeth et al. (2020): Safety and immunogenicity of an adjuvanted Escherichia coli adhesin vaccine in healthy women with and without histories of recurrent urinary tract infections: results from a first-in-human phase 1 study. In Human vaccines & immunotherapeutics, pp. 1–9. DOI: 10.1080/21645515.2020.1834807.

Fric, Jan; Zelante, Teresa; Wong, Alicia Y. W.; Mertes, Alexandra; Yu, Hong-Bing; Ricciardi-Castagnoli, Paola (2012): NFAT control of innate immunity. In Blood 120 (7), pp. 1380–1389. DOI: 10.1182/blood-2012-02-404475.

Gamble, J. R.; Elliott, M. J.; Jaipargas, E.; Lopez, A. F.; Vadas, M. A. (1989): Regulation of human monocyte adherence by granulocyte-macrophage colony-stimulating factor. In Proc Natl Acad Sci USA 86 (18), pp. 7169–7173. DOI: 10.1073/pnas.86.18.7169.

Gerlach, G. F.; Clegg, S.; Allen, B. L. (1989): Identification and characterization of the genes encoding the type 3 and type 1 fimbrial adhesins of Klebsiella pneumoniae. In Journal of Bacteriology 171 (3), pp. 1262–1270. DOI: 10.1128/jb.171.3.1262-1270.1989.

Grant, Sarah Schmidt; Hung, Deborah T. (2013): Persistent bacterial infections, antibiotic tolerance, and the oxidative stress response. In Virulence 4 (4), pp. 273–283. DOI: 10.4161/viru.23987.

Greene, Sarah E.; Hibbing, Michael E.; Janetka, James; Chen, Swaine L.; Hultgren, Scott J. (2015): Human Urine Decreases Function and Expression of Type 1 Pili in Uropathogenic Escherichia coli. In mBio 6 (4), e00820. DOI: 10.1128/mBio.00820-15.

Guyer, Debra M.; Kao, Jyh-Shyang; Mobley, Harry L. T. (1998): Genomic Analysis of a Pathogenicity Island in Uropathogenic Escherichia coli CFT073: Distribution of Homologous Sequences among Isolates from Patients with Pyelonephritis, Cystitis, and CatheterAssociated Bacteriuria and from Fecal Samples. In Infection and immunity 66 (9), pp. 4411–4417.

Haldimann, A.; Wanner, B. L. (2001): Conditional-replication, integration, excision, and retrieval plasmid-host systems for gene structure-function studies of bacteria. In Journal of Bacteriology 183 (21), pp. 6384–6393. DOI: 10.1128/JB.183.21.6384–6393.2001.

Han, Zhenfu; Pinkner, Jerome S.; Ford, Bradley; Obermann, Robert; Nolan, William; Wildman, Scott A. et al. (2010): Structure-based drug design and optimization of mannoside bacterial FimH antagonists. In Journal of medicinal chemistry 53 (12), pp. 4779–4792. DOI: 10.1021/jm100438s.

Harokopakis, Evlambia; Hajishengallis, George (2005): Integrin activation by bacterial fimbriae through a pathway involving CD14, Toll-like receptor 2, and phosphatidylinositol-3-kinase. In Eur. J. Immunol. 35 (4), pp. 1201–1210. DOI: 10.1002/eji.200425883.

Henderson, Ian R.; Navarro-Garcia, Fernando; Desvaux, Mickaël; Fernandez, Rachel C.; Ala'Aldeen, Dlawer (2004): Type V protein secretion pathway: the autotransporter story. In Microbiology and molecular biology reviews : MMBR 68 (4), pp. 692–744. DOI: 10.1128/MMBR.68.4.692-744.2004.

Hochhut, Bianca; Wilde, Caroline; Balling, Gudrun; Middendorf, Barbara; Dobrindt, Ulrich; Brzuszkiewicz, Elzbieta et al. (2006): Role of pathogenicity island-associated integrases in the genome plasticity of uropathogenic Escherichia coli strain 536. In Mol Microbiol 61 (3), pp. 584–595. DOI: 10.1111/j.1365-2958.2006.05255.x.

Hooper, Lora V.; Macpherson, Andrew J. (2010): Immune adaptations that maintain homeostasis with the intestinal microbiota. In Nat Rev Immunol 10 (3), pp. 159–169. DOI: 10.1038/nri2710.

Hou, Tingjun; Wang, Junmei; Li, Youyong; Wang, Wei (2011): Assessing the performance of the MM/PBSA and MM/GBSA methods. 1. The accuracy of binding free energy calculations based on molecular dynamics simulations. In Journal of chemical information and modeling 51 (1), pp. 69–82. DOI: 10.1021/ci100275a.

Hsu, Peter; Santner-Nanan, Brigitte; Hu, Mingjing; Skarratt, Kristen; Lee, Cheng Hiang; Stormon, Michael et al. (2015): IL-10 Potentiates Differentiation of Human Induced Regulatory T Cells via STAT3 and Foxo1. In Journal of immunology (Baltimore, Md. : 1950) 195 (8), pp. 3665–3674. DOI: 10.4049/jimmunol.1402898.

Hung, Chia-Suei; Bouckaert, Julie; Hung, Danielle; Pinkner, Jerome; Widberg, Charlotte; DeFusco, Anthony et al. (2002): Structural basis of tropism of Escherichia coli to the bladder during urinary tract infection. In Mol Microbiol 44 (4), pp. 903–915. DOI: 10.1046/j.1365-2958.2002.02915.x.

Hung, Chia-Suei; Dodson, Karen W.; Hultgren, Scott J. (2009): A murine model of urinary tract infection. In Nature protocols 4 (8), pp. 1230–1243. DOI: 10.1038/nprot.2009.116.

Hunstad, David A.; Justice, Sheryl S. (2010): Intracellular Lifestyles and Immune Evasion Strategies of Uropathogenic Escherichia coli. In Annu. Rev. Microbiol. 64 (1), pp. 203–221. DOI: 10.1146/annurev.micro.112408.134258.

Inaba, K.; Turley, S.; Yamaide, F.; Iyoda, T.; Mahnke, K.; Inaba, M. et al. (1998): Efficient presentation of phagocytosed cellular fragments on the major histocompatibility complex class II products of dendritic cells. In The Journal of experimental medicine 188 (11), pp. 2163–2173. DOI: 10.1084/jem.188.11.2163.

Ingersoll, Molly A.; Kline, Kimberly A.; Nielsen, Hailyn V.; Hultgren, Scott J. (2008): G-CSF induction early in uropathogenic Escherichia coli infection of the urinary tract modulates host immunity. In Cell Microbiol 10 (12), pp. 2568–2578. DOI: 10.1111/j.1462-5822.2008.01230.x.

Jones, C. H.; Pinkner, J. S.; Roth, R.; Heuser, J.; Nicholes, A. V.; Abraham, S. N.; Hultgren, S. J. (1995): FimH adhesin of type 1 pili is assembled into a fibrillar tip structure in the

Enterobacteriaceae. In Proceedings of the National Academy of Sciences of the United States of America 92 (6), pp. 2081–2085.

Kalas, Vasilios; Pinkner, Jerome S.; Hannan, Thomas J.; Hibbing, Michael E.; Dodson, Karen W.; Holehouse, Alex S. et al. (2017): Evolutionary fine-tuning of conformational ensembles in FimH during host-pathogen interactions. In Science advances 3 (2), e1601944. DOI: 10.1126/sciadv.1601944.

Kao, J. S.; Stucker, D. M.; Warren, J. W.; Mobley, H. L. (1997): Pathogenicity island sequences of pyelonephritogenic Escherichia coli CFT073 are associated with virulent uropathogenic strains. In Infection and immunity 65 (7), pp. 2812–2820.

Kaukonen, Riina; Jacquemet, Guillaume; Hamidi, Hellyeh; Ivaska, Johanna (2017): Cell-derived matrices for studying cell proliferation and directional migration in a complex 3D microenvironment. In Nature protocols 12 (11), pp. 2376–2390. DOI: 10.1038/nprot.2017.107.

Kavčič, Bor; Tkačik, Gašper; Bollenbach, Tobias (2020): Mechanisms of drug interactions between translation-inhibiting antibiotics. In Nat Comms 11 (1), p. 4013. DOI: 10.1038/s41467-020-17734-z.

Kelley, Stacy L.; Lukk, Tiit; Nair, Satish K.; Tapping, Richard I. (2013): The crystal structure of human soluble CD14 reveals a bent solenoid with a hydrophobic amino-terminal pocket. In Journal of immunology (Baltimore, Md. : 1950) 190 (3), pp. 1304–1311. DOI: 10.4049/jimmunol.1202446.

Kim, Jung-In; Lee, Chang Jun; Jin, Mi Sun; Lee, Cherl-Ho; Paik, Sang-Gi; Lee, Hayyoung; Lee, Jie-Oh (2005): Crystal structure of CD14 and its implications for lipopolysaccharide signaling. In J. Biol. Chem. 280 (12), pp. 11347–11351. DOI: 10.1074/jbc.M414607200.

Kim, Minsoo; Ogawa, Michinaga; Fujita, Yukihiro; Yoshikawa, Yuko; Nagai, Takeshi; Koyama, Tomohiro et al. (2009): Bacteria hijack integrin-linked kinase to stabilize focal adhesions and block cell detachment. In Nature 459 (7246), pp. 578–582. DOI: 10.1038/nature07952.

Klemm, P.; Christiansen, G. (1987): Three fim genes required for the regulation of length and mediation of adhesion of Escherichia coli type 1 fimbriae. In Molecular & general genetics : MGG 208 (3), pp. 439–445. DOI: 10.1007/BF00328136.

Kolenda, Rafal; Ugorski, Maciej; Grzymajlo, Krzysztof (2019): Everything You Always Wanted to Know About Salmonella Type 1 Fimbriae, but Were Afraid to Ask. In Front. Microbiol. 10, p. 1017. DOI: 10.3389/fmicb.2019.01017.

Kopf, Aglaja; Renkawitz, Jörg; Hauschild, Robert; Girkontaite, Irute; Tedford, Kerry; Merrin, Jack et al. (2020): Microtubules control cellular shape and coherence in amoeboid migrating cells. In The Journal of cell biology 219 (6). DOI: 10.1083/jcb.201907154.

Lämmermann, Tim; Bader, Bernhard L.; Monkley, Susan J.; Worbs, Tim; Wedlich-Söldner, Roland; Hirsch, Karin et al. (2008): Rapid leukocyte migration by integrin-independent flowing and squeezing. In Nature 453 (7191), pp. 51–55. DOI: 10.1038/nature06887.

Lane, M. Chelsea; Simms, Amy N.; Mobley, Harry L. T. (2007): complex interplay between type 1 fimbrial expression and flagellum-mediated motility of uropathogenic Escherichia coli. In Journal of Bacteriology 189 (15), pp. 5523–5533. DOI: 10.1128/JB.00434-07.

Leithner, Alexander; Altenburger, Lukas M.; Hauschild, Robert; Assen, Frank; Rottner, Klemens; Stradal, Theresia E.B. et al. (2020): Dendritic cell actin dynamics controls T cell priming efficiency at the immunological synapse (162).

Leithner, Alexander; Altenburger, Lukas M.; Hauschild, Robert; Assen, Frank P.; Rottner, Klemens; Stradal, Theresia E. B. et al. (2021): Dendritic cell actin dynamics control contact duration and priming efficiency at the immunological synapse. In The Journal of cell biology 220 (4). DOI: 10.1083/jcb.202006081.

Leithner, Alexander; Eichner, Alexander; Müller, Jan; Reversat, Anne; Brown, Markus; Schwarz, Jan et al. (2016): Diversified actin protrusions promote environmental exploration but are dispensable for locomotion of leukocytes. In Nature cell biology 18 (11), pp. 1253–1259. DOI: 10.1038/ncb3426.

Leithner, Alexander; Renkawitz, Joerg; Vries, Ingrid de; Hauschild, Robert; Häcker, Hans; Sixt, Michael (2018): Fast and efficient genetic engineering of hematopoietic precursor cells for the study of dendritic cell migration. In Eur. J. Immunol. 48 (6), pp. 1074–1077. DOI: 10.1002/eji.201747358.

Lim, J. K.; Gunther, N. W.; Zhao, H.; Johnson, D. E.; Keay, S. K.; Mobley, H. L. (1998): In vivo phase variation of Escherichia coli type 1 fimbrial genes in women with urinary tract infection. In Infection and immunity 66 (7), pp. 3303–3310.

Lindquist, Randall L.; Shakhar, Guy; Dudziak, Diana; Wardemann, Hedda; Eisenreich, Thomas; Dustin, Michael L.; Nussenzweig, Michel C. (2004): Visualizing dendritic cell networks in vivo. In Nature immunology 5 (12), pp. 1243–1250. DOI: 10.1038/ni1139.

Lloyd, A. L.; Rasko, D. A.; Mobley, H. L. T. (2007): Defining Genomic Islands and Uropathogen-Specific Genes in Uropathogenic Escherichia coli. In Journal of Bacteriology 189 (9), pp. 3532–3546. DOI: 10.1128/JB.01744-06.

Magalhaes, Joao G.; Tattoli, Ivan; Girardin, Stephen E. (2007): The intestinal epithelial barrier: how to distinguish between the microbial flora and pathogens. In Seminars in Immunology 19 (2), pp. 106–115. DOI: 10.1016/j.smim.2006.12.006.

Maiguel, Dony; Faridi, Mohd Hafeez; Wei, Changli; Kuwano, Yoshihiro; Balla, Keir M.; Hernandez, Dayami et al. (2011): Small molecule-mediated activation of the integrin CD11b/CD18 reduces inflammatory disease. In Science signaling 4 (189), ra57. DOI: 10.1126/scisignal.2001811.

Månsson, Lisa E.; Kjäll, Peter; Pellett, Shahaireen; Nagy, Gábor; Welch, Rodney A.; Bäckhed, Fredrik et al. (2007): Role of the lipopolysaccharide-CD14 complex for the activity of hemolysin from uropathogenic Escherichia coli. In Infect. Immun. 75 (2), pp. 997–1004. DOI: 10.1128/IAI.00957-06.

Martinez, J. J.; Mulvey, M. A.; Schilling, J. D.; Pinkner, J. S.; Hultgren, S. J. (2000): Type 1 pilus-mediated bacterial invasion of bladder epithelial cells. In The EMBO journal 19 (12), pp. 2803–2812. DOI: 10.1093/emboj/19.12.2803.

Maurer, Lisa; Orndorff, Paul E. (1985): A new locus, pilE, required for the binding of type 1 piliated Escherichia coli to erhythrocytes. In FEMS Microbiology Letters 30 (1-2), pp. 59–66. DOI: 10.1111/j.1574-6968.1985.tb00985.x.

Mayer, Christian Thomas; Ghorbani, Peyman; Nandan, Amrita; Dudek, Markus; Arnold-Schrauf, Catharina; Hesse, Christina et al. (2014): Selective and efficient generation of functional Batf3-dependent CD103+ dendritic cells from mouse bone marrow. In Blood 124 (20), pp. 3081–3091. DOI: 10.1182/blood-2013-12-545772.

McArdel, Shannon L.; Terhorst, Cox; Sharpe, Arlene H. (2016): Roles of CD48 in regulating immunity and tolerance. In Clinical immunology (Orlando, Fla.) 164, pp. 10–20. DOI: 10.1016/j.clim.2016.01.008.

Medzhitov, Ruslan (2007): Recognition of microorganisms and activation of the immune response. In Nature 449 (7164), pp. 819–826. DOI: 10.1038/nature06246.

Mellman, I.; Steinman, R. M. (2001): Dendritic cells: specialized and regulated antigen processing machines. In Cell 106 (3), pp. 255–258.

Merad, Miriam; Sathe, Priyanka; Helft, Julie; Miller, Jennifer; Mortha, Arthur (2013): The Dendritic Cell Lineage: Ontogeny and Function of Dendritic Cells and Their Subsets in the Steady State and the Inflamed Setting. In Annu. Rev. Immunol. 31 (1), pp. 563–604. DOI: 10.1146/annurev-immunol-020711-074950.

Mittal, Sharad K.; Roche, Paul A. (2015): Suppression of antigen presentation by IL-10. In Current Opinion in Immunology 34, pp. 22–27. DOI: 10.1016/j.coi.2014.12.009.

Mora-Bau, Gabriela; Platt, Andrew M.; van Rooijen, Nico; Randolph, Gwendalyn J.; Albert, Matthew L.; Ingersoll, Molly A. (2015): Macrophages Subvert Adaptive Immunity to Urinary Tract Infection. In PLoS pathogens 11 (7), e1005044. DOI: 10.1371/journal.ppat.1005044.

Mossman, K. L.; Mian, M. F.; Lauzon, N. M.; Gyles, C. L.; Lichty, B.; Mackenzie, R. et al. (2008): Cutting Edge: FimH Adhesin of Type 1 Fimbriae Is a Novel TLR4 Ligand. In The Journal of Immunology 181 (10), pp. 6702–6706. DOI: 10.4049/jimmunol.181.10.6702.

Mydock-McGrane, Laurel K.; Cusumano, Zachary T.; Janetka, James W. (2016): Mannose-derived FimH antagonists: a promising anti-virulence therapeutic strategy for urinary tract infections and Crohn's disease. In Expert opinion on therapeutic patents 26 (2), pp. 175–197. DOI: 10.1517/13543776.2016.1131266.

Nikolic, Nela; Bergmiller, Tobias; Vandervelde, Alexandra; Albanese, Tanino G.; Gelens, Lendert; Moll, Isabella (2018): Autoregulation of mazEF expression underlies growth heterogeneity in bacterial populations. In Nucleic acids research 46 (6), pp. 2918–2931. DOI: 10.1093/nar/gky079.

Ohto, Umeharu; Fukase, Koichi; Miyake, Kensuke; Shimizu, Toshiyuki (2012): Structural basis of species-specific endotoxin sensing by innate immune receptor TLR4/MD-2. In Proceedings of the National Academy of Sciences of the United States of America 109 (19), pp. 7421–7426. DOI: 10.1073/pnas.1201193109.

Oxvig, Claus; Lu, Chafen; Springer, Timothy A. (1999): Conformational changes in tertiary structure near the ligand binding site of an integrin I domain. In Proceedings of the National Academy of Sciences of the United States of America 96 (5), pp. 2215–2220.

Redecke, Vanessa; Wu, Ruiqiong; Zhou, Jingran; Finkelstein, David; Chaturvedi, Vandana; High, Anthony A.; Häcker, Hans (2013): Hematopoietic progenitor cell lines with myeloid and lymphoid potential. In Nat Meth 10 (8), pp. 795–803. DOI: 10.1038/nmeth.2510.

Sauer, Maximilian M.; Jakob, Roman P.; Luber, Thomas; Canonica, Fabia; Navarra, Giulio; Ernst, Beat et al. (2019): Binding of the Bacterial Adhesin FimH to Its Natural, Multivalent High-Mannose Type Glycan Targets. In Journal of the American Chemical Society 141 (2), pp. 936–944. DOI: 10.1021/jacs.8b10736.

Schilling, J. D.; Mulvey, M. A.; Hultgren, S. J. (2001): Structure and function of Escherichia coli type 1 pili: new insight into the pathogenesis of urinary tract infections. In The Journal of infectious diseases 183 Suppl 1, S36-40. DOI: 10.1086/318855.

Schilling, Joel D.; Martin, Steven M.; Hung, Chia S.; Lorenz, Robin G.; Hultgren, Scott J. (2003): Toll-like receptor 4 on stromal and hematopoietic cells mediates innate resistance to uropathogenic Escherichia coli. In Proc Natl Acad Sci USA 100 (7), pp. 4203–4208. DOI: 10.1073/pnas.0736473100.

Schönemann, Wojciech; Cramer, Jonathan; Mühlethaler, Tobias; Fiege, Brigitte; Silbermann, Marleen; Rabbani, Said et al. (2019): Improvement of Aglycone π-Stacking Yields Nanomolar to Sub-nanomolar FimH Antagonists. In ChemMedChem 14 (7), pp. 749–757. DOI: 10.1002/cmdc.201900051.

Shames, Stephanie R.; Deng, Wanyin; Guttman, Julian A.; Hoog, Carmen L. de; Li, Yuling; Hardwidge, Philip R. et al. (2010): The pathogenic E. coli type III effector EspZ interacts with host CD98 and facilitates host cell prosurvival signalling. In Cell Microbiol 12 (9), pp. 1322–1339. DOI: 10.1111/j.1462-5822.2010.01470.x.

Sharma, Kunal; Dhar, Neeraj; Thacker, Vivek V.; Simonet, Thomas M.; Signorino-Gelo, Francois; Knott, Graham W.; McKinney, John D. (2021a): Dynamic persistence of UPEC intracellular bacterial communities in a human bladder-chip model of urinary tract infection. In eLife 10. DOI: 10.7554/eLife.66481.

Sharma, Kunal; Thacker, Vivek V.; Dhar, Neeraj; Clapés Cabrer, Maria; Dubois, Anaëlle; Signorino-Gelo, François et al. (2021b): Early invasion of the bladder wall by solitary bacteria protects UPEC from antibiotics and neutrophil swarms in an organoid model. In Cell reports 36 (3), p. 109351. DOI: 10.1016/j.celrep.2021.109351.

Shawki, Ali; McCole, Declan F. (2017): Mechanisms of Intestinal Epithelial Barrier Dysfunction by Adherent-Invasive Escherichia coli. In Cellular and molecular gastroenterology and hepatology 3 (1), pp. 41–50. DOI: 10.1016/j.jcmgh.2016.10.004.

Sheikh, Alaullah; Rashu, Rasheduzzaman; Begum, Yasmin Ara; Kuhlman, F. Matthew; Ciorba, Matthew A.; Hultgren, Scott J. et al. (2017): Highly conserved type 1 pili promote enterotoxigenic E. coli pathogen-host interactions. In PLoS neglected tropical diseases 11 (5), e0005586. DOI: 10.1371/journal.pntd.0005586.

Shueb Mussa (2009): Vergleich der Invasionsfähigkeit verschiedener Klebsiella Stämme im Hühnerembryonen-Modell und Etablierung des in-vivo-Modells. Dissertation. Klinik für Allgemeine Pädiatrie der Heinrich-Heine-Universität Düsseldorf.

Sivignon, Adeline; Bouckaert, Julie; Bernard, Julien; Gouin, Sebastien G.; Barnich, Nicolas (2017): The potential of FimH as a novel therapeutic target for the treatment of Crohn's disease. In Expert opinion on therapeutic targets 21 (9), pp. 837–847. DOI: 10.1080/14728222.2017.1363184.

Socinski, M. A.; Cannistra, S. A.; Sullivan, R.; Elias, A.; Antman, K.; Schnipper, L.; Griffin, J. D. (1988): Granulocyte-macrophage colony-stimulating factor induces the expression of the CD11b surface adhesion molecule on human granulocytes in vivo. In Blood 72 (2), pp. 691–697. DOI: 10.1182/blood.V72.2.691.691.

Sokurenko, E. V.; Chesnokova, V.; Dykhuizen, D. E.; Ofek, I.; Wu, X. R.; Krogfelt, K. A. et al. (1998): Pathogenic adaptation of Escherichia coli by natural variation of the FimH adhesin. In Proc Natl Acad Sci USA 95 (15), pp. 8922–8926. DOI: 10.1073/pnas.95.15.8922.

Spaulding, Caitlin N.; Klein, Roger D.; Ruer, Ségolène; Kau, Andrew L.; Schreiber, Henry L.; Cusumano, Zachary T. et al. (2017): Selective depletion of uropathogenic E. coli from the gut by a FimH antagonist. In Nature 546 (7659), pp. 528–532. DOI: 10.1038/nature22972.

Stösel, H.; Koch, F.; Romani, N. (1997): Maturation and migration of murine dendritic cells in situ. Observations in a skin organ culture model. In Advances in experimental medicine and biology 417, pp. 311–315. DOI: 10.1007/978-1-4757-9966-8_51.

Struve, Carsten; Bojer, Martin; Krogfelt, Karen Angeliki (2008): Characterization of Klebsiella pneumoniae type 1 fimbriae by detection of phase variation during colonization and infection and impact on virulence. In Infection and immunity 76 (9), pp. 4055–4065. DOI: 10.1128/IAI.00494-08.

Tomasek, Kathrin; Bergmiller, Tobias; Guet, Călin C. (2018): Lack of cations in flow cytometry buffers affect fluorescence signals by reducing membrane stability and viability of Escherichia coli strains. In Journal of biotechnology 268, pp. 40–52. DOI: 10.1016/j.jbiotec.2018.01.008.

Tomašič, Tihomir; Rabbani, Said; Jakob, Roman P.; Reisner, Andreas; Jakopin, Žiga; Maier, Timm et al. (2021): Does targeting Arg98 of FimH lead to high affinity antagonists? In European journal of medicinal chemistry 211, p. 113093. DOI: 10.1016/j.ejmech.2020.113093.

Touaibia, Mohamed; Krammer, Eva-Maria; Shiao, Tze C.; Yamakawa, Nao; Wang, Qingan; Glinschert, Anja et al. (2017): Sites for Dynamic Protein-Carbohydrate Interactions of O- and C-Linked Mannosides on the E. coli FimH Adhesin. In Molecules (Basel, Switzerland) 22 (7). DOI: 10.3390/molecules22071101.

Touchon, Marie; Hoede, Claire; Tenaillon, Olivier; Barbe, Valérie; Baeriswyl, Simon; Bidet, Philippe et al. (2009): Organised genome dynamics in the Escherichia coli species results in highly diverse adaptive paths. In PLoS genetics 5 (1), e1000344. DOI: 10.1371/journal.pgen.1000344.

Tsukamoto, Hiroki; Fukudome, Kenji; Takao, Shoko; Tsuneyoshi, Naoko; Kimoto, Masao (2010): Lipopolysaccharide-binding protein-mediated Toll-like receptor 4 dimerization enables rapid signal transduction against lipopolysaccharide stimulation on membrane-associated CD14-expressing cells. In International immunology 22 (4), pp. 271–280. DOI: 10.1093/intimm/dxq005.

Uchiya, Kei-Ichi; Kamimura, Yurie; Jusakon, Ayumi; Nikai, Toshiaki (2019): Salmonella Fimbrial Protein FimH Is Involved in Expression of Proinflammatory Cytokines in a Toll-Like Receptor 4-Dependent Manner. In Infection and immunity 87 (3). DOI: 10.1128/IAI.00881-18.

Uhlén, P.; Laestadius, A.; Jahnukainen, T.; Söderblom, T.; Bäckhed, F.; Celsi, G. et al. (2000): Alpha-haemolysin of uropathogenic E. coli induces Ca2+ oscillations in renal epithelial cells. In Nature 405 (6787), pp. 694–697. DOI: 10.1038/35015091.

Varga, Georg; Balkow, Sandra; Wild, Martin K.; Stadtbaeumer, Andrea; Krummen, Mathias; Rothoeft, Tobias et al. (2007): Active MAC-1 (CD11b/CD18) on DCs inhibits full T-cell activation. In Blood 109 (2), pp. 661–669. DOI: 10.1182/blood-2005-12-023044.

Vaure, Céline; Liu, Yuanqing (2014): A comparative review of toll-like receptor 4 expression and functionality in different animal species. In Frontiers in immunology 5, p. 316. DOI: 10.3389/fimmu.2014.00316.

Velikovsky, C. Alejandro; Deng, Lu; Chlewicki, Lukasz K.; Fernández, Marisa M.; Kumar, Vinay; Mariuzza, Roy A. (2007): Structure of natural killer receptor 2B4 bound to CD48 reveals basis for heterophilic recognition in signaling lymphocyte activation molecule family. In Immunity 27 (4), pp. 572–584. DOI: 10.1016/j.immuni.2007.08.019.

Welch, R. A.; Burland, V.; Plunkett, G.; Redford, P.; Roesch, P.; Rasko, D. et al. (2002): Extensive mosaic structure revealed by the complete genome sequence of uropathogenic Escherichia coli. In Proceedings of the National Academy of Sciences 99 (26), pp. 17020–17024. DOI: 10.1073/pnas.252529799.

Weng, Gaoqi; Wang, Ercheng; Wang, Zhe; Liu, Hui; Zhu, Feng; Li, Dan; Hou, Tingjun (2019): HawkDock: a web server to predict and analyze the protein-protein complex based on computational docking and MM/GBSA. In Nucleic acids research 47 (W1), W322-W330. DOI: 10.1093/nar/gkz397.

Wiles, Travis J.; Kulesus, Richard R.; Mulvey, Matthew A. (2008): Origins and virulence mechanisms of uropathogenic Escherichia coli. In Experimental and Molecular Pathology 85 (1), pp. 11–19. DOI: 10.1016/j.yexmp.2008.03.007.

Wirth, Thierry; Falush, Daniel; Lan, Ruiting; Colles, Frances; Mensa, Patience; Wieler, Lothar H. et al. (2006): Sex and virulence in Escherichia coli: an evolutionary perspective. In Mol Microbiol 60 (5), pp. 1136–1151. DOI: 10.1111/j.1365-2958.2006.05172.x.

Wright, Kelly J.; Seed, Patrick C.; Hultgren, Scott J. (2007): Development of intracellular bacterial communities of uropathogenic Escherichia coli depends on type 1 pili. In Cellular Microbiology 9 (9), pp. 2230–2241. DOI: 10.1111/j.1462-5822.2007.00952.x.

Wright, S. D.; Ramos, R. A.; Hermanowski-Vosatka, A.; Rockwell, P.; Detmers, P. A. (1991): Activation of the adhesive capacity of CR3 on neutrophils by endotoxin: dependence on lipopolysaccharide binding protein and CD14. In The Journal of experimental medicine 173 (5), pp. 1281–1286. DOI: 10.1084/jem.173.5.1281.

Zanoni, Ivan; Granucci, Francesca (2013): Role of CD14 in host protection against infections and in metabolism regulation. In Frontiers in cellular and infection microbiology 3, p. 32. DOI: 10.3389/fcimb.2013.00032.

Zanoni, Ivan; Ostuni, Renato; Capuano, Giusy; Collini, Maddalena; Caccia, Michele; Ronchi, Antonella Ellena et al. (2009): CD14 regulates the dendritic cell life cycle after LPS exposure through NFAT activation. In Nature 460 (7252), pp. 264–268. DOI: 10.1038/nature08118.

Zeiner, Sarah A.; Dwyer, Brett E.; Clegg, Steven (2012): FimA, FimF, and FimH are necessary for assembly of type 1 fimbriae on Salmonella enterica serovar Typhimurium. In Infection and immunity 80 (9), pp. 3289–3296. DOI: 10.1128/IAI.00331-12.

A. Appendix: Supplementary Information

Oligonucleotide	Sequence
110	ATATGCATGCCAAAAGATGAAACATATATCATAAATAAGTTACGT
112	ATATGCATGCCAAAAGATGAAACATTCATAGAGGAAAGCATCG
119	CAGTAATGCTGCTCGTTTTGCCG
120	GACAGAGCCGACAGAACAAC
128	TGTGTAGGCTGGAGCTGCTTC
130	AAAAGAGAAGAGGTTTGATTTAACTTATTGATAATAAAGTTAAAAAAACAC TGCTTCGAAGTTCC
131	CACTTTGTTTTGTAAACGAGTTTGACTGCCAACACTGCACAGTTTTCCCCCA AAAGATGAAACAT
132	ATTCATATGGAATAAATACAAGACAATCATAGAGGAAAGCATC
133	ATTCATATGGAATAAATACAAGACAAATATCATAAATAAGTTACGTATTTTT TCTCAAGCATAAAAATATTAAAAAACGAC
134	TTGTATTTATTCCATATGAATATCCTCCTTAGTTCCTATTCC
146	TAGCTTCAGGTAATATTGCGTACCTGCATTAGCAATGCCCTGTGATTTCTCC ATATGAATATCCTCCTTAGTTCC
148	AGTGATTAGCATCACCTATACCTACAGCTGAACCCAAAGAGATGATTGTAT GTGTAGGCTGGAGCTGCTTCG
157	AGCATCACCTATACCTACAGCTG
158	AGCTTCAGGTAATATTGCGTACC
198	AGTGATTAGCATCACCTATACCTACAGCTGAACCCGAAGAGATGATTGTAA TGAAACGAGTTATTACC
276	TAGCTTCAGGTAATATTGCGTACCTGCATTAGCAATGCCCTGTGATTTCTTT ATTGATAAACAAA
296	AGTGATTAGCATCACCTATACCTACAGCTGAACCCGAAGAGATGATTGTAT TGACGGCTAGCTCAGTCCTAGGTA
297	TAGCTTCAGGTAATATTGCGTACCTGCATTAGCAATGCCCTGTGATTTCTTC AGCACTGTCCTGCTCCTTGTGAT
314	ACGAGTTAATAACTGAAGTAAAAAACAAGACAGATTTCAATTTTTCATTAAC AGGTTAAGAGATAATTAATGTGTAGGCTGGAGCTG
315	TATGACTCCAAAAAAATAGCAATCTTATGTGGCACAGCCCAGTAAGATTGC TATTATTTAAATTAATAAACCATATGAATATCCTCCTTAGTTCC
316	ACTGGATTGCTCCTTTCGGG
317	TTCCCAGTTCATCTGCCGTC
324	TTCATATGGAATAAATACAAAATAACGAACAGGTCAATTTTGACTCGTTGG GATAAATG
325	GAGACAATTGGGGCCAAAC
326	TTCATATGGAATAAATACAAAATAACGAACAGGTCAAAACTGTTTATATCAT AAAAATGTTTTGACATATTTTG
327	GAGACAATTGGGGCCATTTTG
328	GACCAGAAGACGAAAAATGAAATAACAGATTGATTTTAAAGAATTAAAAAC TGCTTCGAAGTTCC
329	TCAGCCGAGTGGTCCGGCTGCCGGCTCTGCACAGTTTTCGCCCAACCGATG AGACAATTGGGGCC

336	ACATATTCTCTCCGGTAGAAGAAGGGCCGCAAACGCGGCCCGGGCTGTTATGTGTAGGCTGGAGCTGCTTCG
337	ATTTTAATTCTTAATACTTTGTTCATTCAATAAATGAGTTGAGAGAATATCCATATGAATATCCTCCTTAGTTCC
338	TGTTACGTCTGTTGCTCCGG
339	CGCACAAAGGAAACGGTCTG
3_SphI_pKD3_test	TGAATACCACGACGATTTCC
cam_test_R	CAACGGTGGTATATCCAGTGA
FarChro galK UO	GTTAATTATCATTTTGCACCGCGTC
galK-KpnI-r	CCGGGTACCTCAGCACTGTCCTGCTCC
galK-ver-F	CCTACTCTATGGGCTGGCAC
galk-ver-R	GGAAAGTAAAGTCGCACCCC

Table 1: *Primers used for cloning.*

Reagent or Resource	Source	Identifyer
Antibodies		
Rat anti-MHC II (I-A/I-E) eFluor450 (clone M5/114.15.2)	eBioscience	48-5321-82
Armenian hamster anti-CD11c APC (clone N418)	eBioscience	17-0114-82
Rat anti-CD18 PE (clone C71/16)	BD	553293
Rat anti-CD11b FITC (clone M1/70)	eBioscience	11-0112-82
Mouse anti-human CD11b (active epitope) APC (clone CBRM1/5)	eBioscience	17-0113-41
Rat anti-CD86 biotin (clone GL1)	eBioscience	13-0862-85
Armenian hamster anti-CD80 (clone 16-10A1)	eBioscience	13-0801-85
Rat anti-CD40 (clone 1C10)	Biolegend	102802
Armenian Hamster anti-CD103 Brilliant Violet 421 (clone 2E7)	Biolegend	121421
Rat anti-CD14 Brilliant Violet 421 (clone Sa14-2)	Biolegend	123329
Rat anti-CD4 eFluor450 (clone GK1.5)	eBioscience	48-0042-82
Armenian Hamster anti-CD69 APC-eFluor780 (clone H1.2F3)	eBioscience	47-0691-82
Rat anti-CD62-L PE (clone MEL-14)	eBioscience	12-0621-82
Rat IgG2b kappa Isotype Control eFluor450 (clone eB146/10H5)	eBioscience	48-4031-82
Armenian Hamster IgG Isotype Control APC (clone eBio299Arm)	eBioscience	14-4888-81
Rat IgG2a kappa Isotype Control PE (clone eBR2a)	eBioscience	12-4321-81
Rat IgG2b kappa Isotype Control FITC (clone eB149/10H5)	eBioscience	11-4031-82
Rat IgG1 kappa Isotype Control APC (clone eBRG1)	eBioscience	17-4301-82
Armenian Hamster IgG Brilliant Violet 421 (clone HTK888)	Biolegend	400936
Rat IgG2a kappa Isotype Control Biotin (clone RTK2758)	Stemcell Technologies	60076
Armenian Hamster IgG Isotype Control Biotin (clone eBio299Arm)	eBioscience	13-4888-81
Rat IgG2a kappa Isotype Control (clone RTK2758)	Stemcell Technologies	60076
Alexa Fluor 647-conjugated Streptavidin	Jackson ImmunoResearch	016-600-084
Donkey anti-rat IgG H+L Alexa Fluor488 AffiniPure F(ab')2 Fragment	Jackson ImmunoResearch	712-546-150
Goat anti-rabbit Alexa Fluor488	Invitrogen	A11008
Rat anti-CD29 (clone 9EG7)	BD	553715
Armenian Hamster anti-CD29 PE (clone HMβ1-1)	Biolegend	102207
Armenian Hamster IgG Isotype Control PE (clone HTK888)	Biolegend	400907
M14-23 (anti-mouse CD14 antibody)	Biolegend	150102
Strep-Tactin HRP	iba-lifesciences	2-1502-001

Fc receptor block	eBioscience	14-9161-73
Bacterial and Virus Strains		
E. coli W	Archer et al 2011	ATCC 9637
CFT073 O6:K2:H1	Welch et al 2002	ATCC 700928
UTI89 O18:K1:H7	Chen et al 2006	N/A
536 O6:K15:H31	Hochhut et al 2006	N/A
Klebsiella pneumonia 625	Shueb	N/A
KT177 (UTI89 lcoked-ON::FRT)	this thesis	N/A
KT178 (UTI89 locked-OFF::FRT)	this thesis	N/A
KT179 (CFT073 locked-ON::FRT)	this thesis	N/A
KT180 (CFT073 locked-OFF::FRT)	this thesis	N/A
KT193 (CFT073 locked-ON::FRT *ΔfimH*::FRT)	this thesis	N/A
KT232 (E. coli W locked-ON::FRT)	this thesis	N/A
KT257 (CFT073 locked-ON::FRT *ΔfimH attλ* P_R-*mVenus*::FRT)	this thesis	N/A
KT260 (CFT073 locked-ON::FRT *ΔgalK*::FRT *fimH*::*fimH*$_{Y48A\ R98A\ T99A}$)	this thesis	N/A
KT261 (CFT073 locked-ON::FRT *ΔgalK*::FRT *fimH*::*fimH*$_{Y48A}$)	this thesis	N/A
KT262 (CFT073 locked-ON::FRT *ΔgalK*::FRT *fimH*::*fimH*$_{R98A}$)	this thesis	N/A
KT263 (CFT073 locked-ON::FRT *ΔgalK*::FRT *fimH*::*fimH*$_{T99A}$)	this thesis	N/A
KT274 (CFT073 locked-ON::FRT *ΔhlyA*::FRT)	this thesis	N/A
KT276 (Klebsiella pneumonia 625 locked-ON::*chlor*)	this thesis	N/A
KT277 (Klebsiella pneumonia 625 locked-ON::*chlor*)	this thesis	N/A
KT280 (536 locked-ON::FRT)	this thesis	N/A
KT281 (536 locked-OFF::FRT)	this thesis	N/A
KT283 (CFT073 locked-ON::FRT *Δsat*::FRT)	this thesis	N/A
MG002 (E. coli W locked-ON::FRT *ΔgalK*::FRT *fimH*::*fimH*$_{CFT073}$)	this thesis	N/A
VG003 (CFT073 locked-ON::FRT *attλ* P_R-*mVenus*::FRT)	this thesis	N/A
Hoxb8-MSCV retrovirus	Redecke et al 2013	N/A
Chemicals, Peptides, and Recombinant Proteins		
CCL19	RND Systems	440-M3-025
CCL21	RND Systems	457-6c-025
Recombinant Mouse CD14 Fc Chimera	RND Systems	982-CD-100
M4284	medchemexpress	HY-120568
Critical Commercial Assays		
EasySep Mouse Pan-DC Enrichment Kit	Stemcell Technologies	19763
EZ-Link Sulfo NHS-LC-LC-Biotin kit	Thermofisher	A35358

EasySep Mouse CD4$^+$ T cell isolation kit	Stemcell Technologies	19852
Experimental Models: Cell Lines		
HoxB8 precursor cells	Redecke et al 2013	N/A
GM-CSF hybridoma cells	lab resource	N/A
Flt3 hybridoma cells	Redecke et al 2013	N/A
3T3 mouse fibroblasts	ATCC	ATCC CRL-1658
Experimental Models: Organisms/Strains		
mouse: C57BL/6J	The Jackson Laboratory	000664
mouse: *β2*$^{-/-}$ (B6.129S7-*Itgb2*^{tm1Bay}/J)	The Jackson Laboratory	002128
mouse: *tlr4*$^{-/-}$ (B6(Cg)-*Tlr4*$^{tm1.2Karp}$/J)	The Jackson Laboratory	029015
mouse: *cd14*$^{-/-}$ (B6.129S4-*Cd14*^{tm1Frm}/J)	The Jackson Laboratory	003726
mouse: OT-II (B6.Cg-Tg(TcraTcrb)425Cbn/J)	The Jackson Laboratory	004194
Recombinant DNA		
gblock: CFT073 fimH	IDT	N/A
gblock: CFT073 fimH Y48A R98A T99A	IDT	N/A
gblock: CFT073 fimH Y48A	IDT	N/A
gblock: CFT073 fimH R98A	IDT	N/A
gblock: CFT073 fimH T99A	IDT	N/A
plasmid: pSIM6 (pSC101 repA_{ts}, Amp^R)	Datta et al. 2006	N/A
plasmid: pKD3 (R6K oriR, Amp^R, Cm^R*::frt*)	Datsenko and Wanner 2000	Addgene 45604
plasmid: pKD13-PcgalK (J23100-galK, R6K oriR, Amp^R, Kan^R)	Kavčič et al. 2020	N/A
plasmid: pCP20 (FLP+, λ cI857+, λ PR Rep$_{ts}$, Amp^R, Cm^R)	Cherepanov and Wackernagel 1995	N/A
plasmid: pAH120-frt-cat (pAH120 *Δbla::frt-cat-frt*)	Nikolic et al. 2018	N/A
plasmid: pAH120-PR-mVenus-frt-cat (pAH120 P_R-mVenus *Δbla::frt-cat-frt*)	this thesis	N/A
plasmid: pInt-ts	Haldimann and Wanner 2001	Addgene 66076
Software and Algorithms		
ImageJ	Schneider et al 2012	https://imagej.nih.gov/ij/
Huygens	Scientific Volume Imaging, The Netherlands	https://svi.nl

GraphPad Prism 9.0.2.	GraphPad Prism, San Diego, California USA	https://graphpad.com

Table 2: *List of used antibodies, bacterial and virus strains, chemicals and recombinant proteins, commercial assays, cell lines and mouse lines, recombinant DNA and software.*

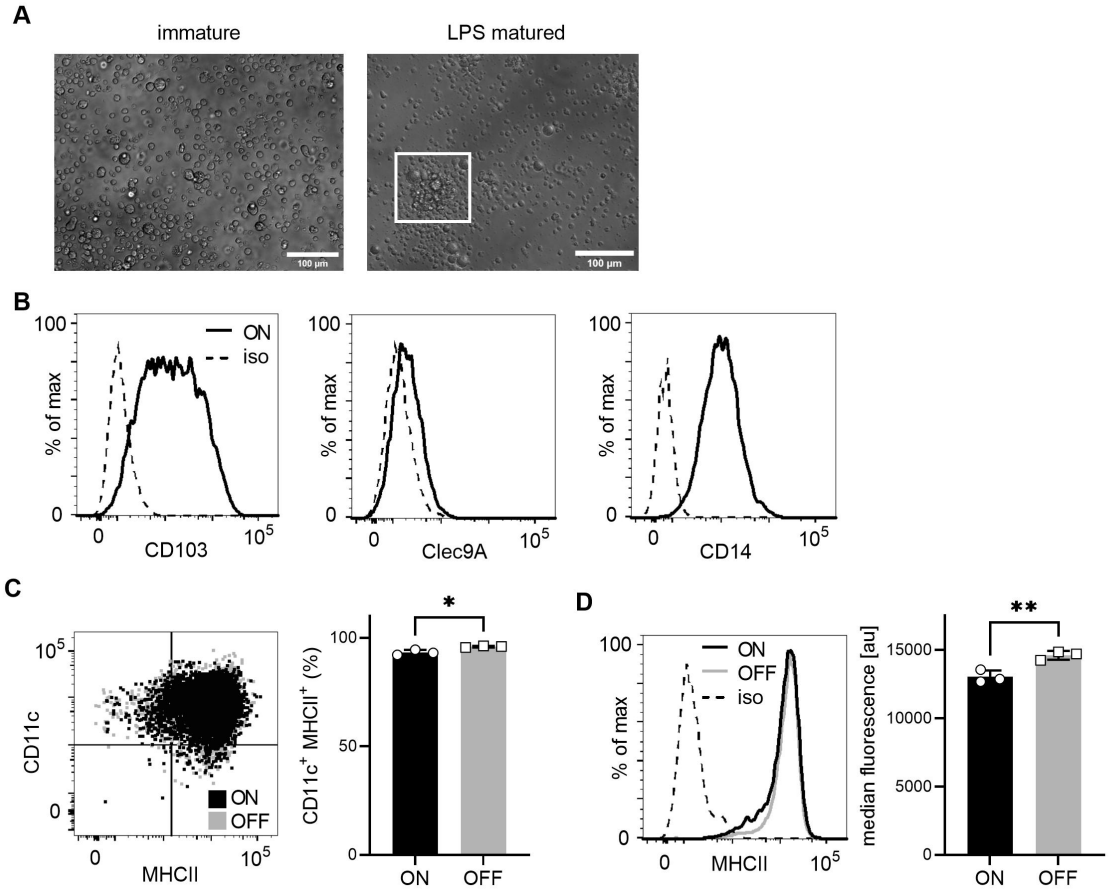

Supplementary Figure 1: *In vitro generated DCs from Hoxb8-progenitor cells resemble iCD103 DCs and differentiation of cells is not different after UPEC ON and OFF stimulation.*
A. *Upon stimulation with recombinant LPS (200 ng/ml) immature DCs change to a mature phenotype and cluster together (see cells highlighted in inlay).* ***B.*** *In vitro generated iCD103 DCs express CD103, Clec9A and CD14.* ***C.*** *Differentiated DCs after ON (black) and OFF (grey) stimulation are defined by expression of CD11c integrin (DC marker) and upregulation of MHCII (activation marker) (left panel). Quantification of differentiated DCs after ON (black) and OFF (grey) stimulation (right panel).* ***D.*** *Histograms of MHCII of WT DCs after stimulation with ON (black) and ON ΔfimH mutants (grey) (left panel; iso – isotype control). Quantification of median fluorescence values of MHCII (right panel).*

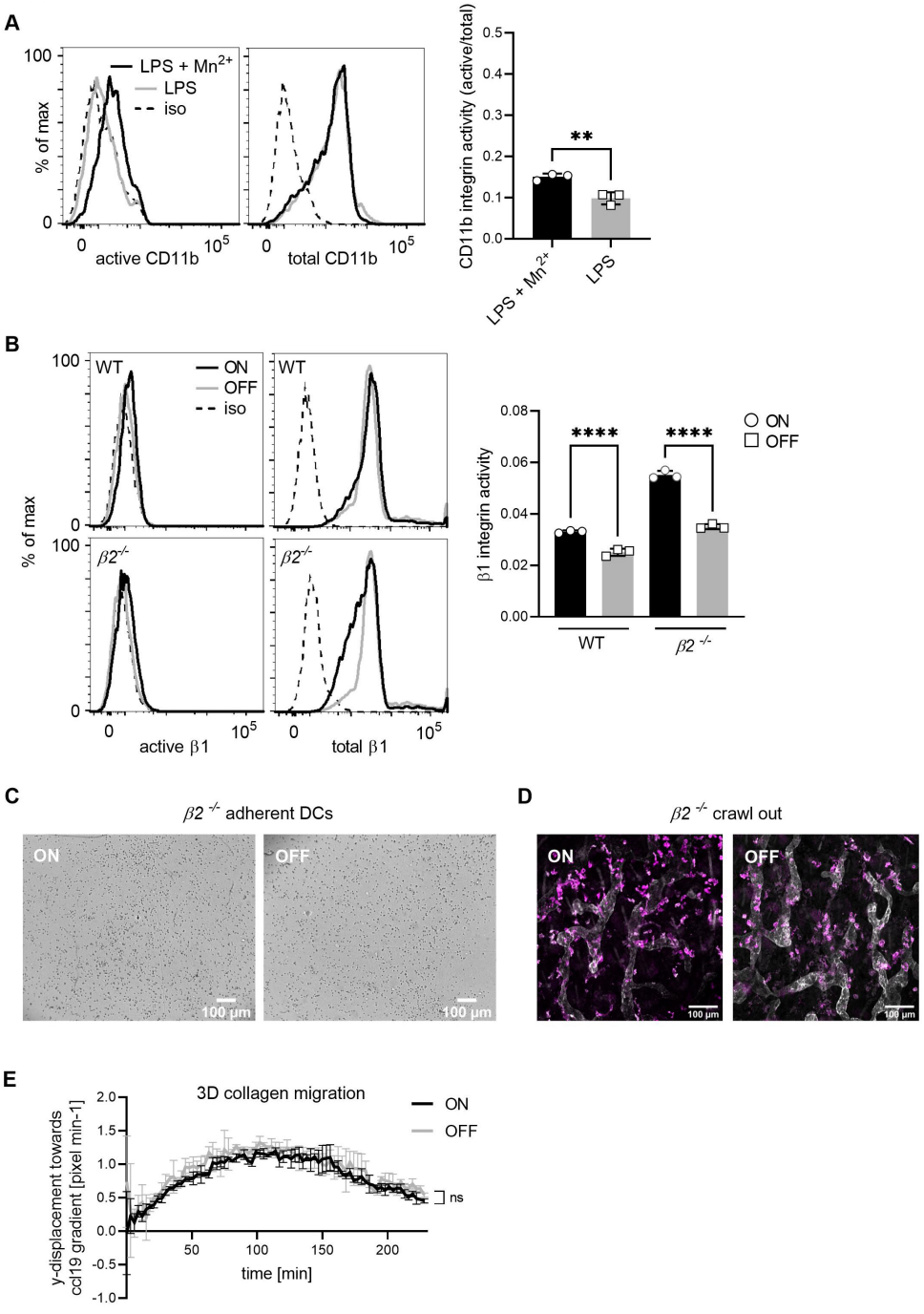

Supplementary Figure 2: *Type 1 piliated UPECs do not affect integrin-independent migration.*
A. *Expression level of active and total CD11b integrin of WT DCs after LPS plus Mn^{2+} stimulation (black) and LPS only stimulation (grey) (left panel; iso – isotype control). Quantification of CD11b integrin activity (active/total levels of CD11b) (right panel) (see also Figure 2-2B).* ***B.*** *Expression level of active and total β1 integrin after ON (black) and OFF (grey) stimulation of WT and $β2^{-/-}$ DCs (left panel; iso – isotype control). Quantification of β1 integrin activity (active/total levels of CD11b) (right panel). It should be noted, that β1 integrin activity after UPEC ON stimulation of $β2^{-/-}$ DCs might be artificially increased due to a slight decrease in total β1 integrin staining after ON stimulation.* ***C.*** *Adhesion assay of $β2^{-/-}$ DCs after ON and OFF stimulation (quantification see Figure 2-2C).* ***D.*** *Ear crawl out assay of $β2^{-/-}$ DCs after ON and OFF stimulation. Endogenous DCs stained with anti-MHCII (magenta). Lymph vessels stained with anti-LYVE-1 (white) (left panel). Quantification of cells inside over outside of lymph vessel after ON (black) and OFF (grey) stimulation $β2^{-/-}$ DCs (right panel) (3 biological replicates) (quantification see Figure 2-2E).* ***E.*** *3D collagen migration assay of WT DCs after stimulation with ON (black) and OFF (grey) mutants.*

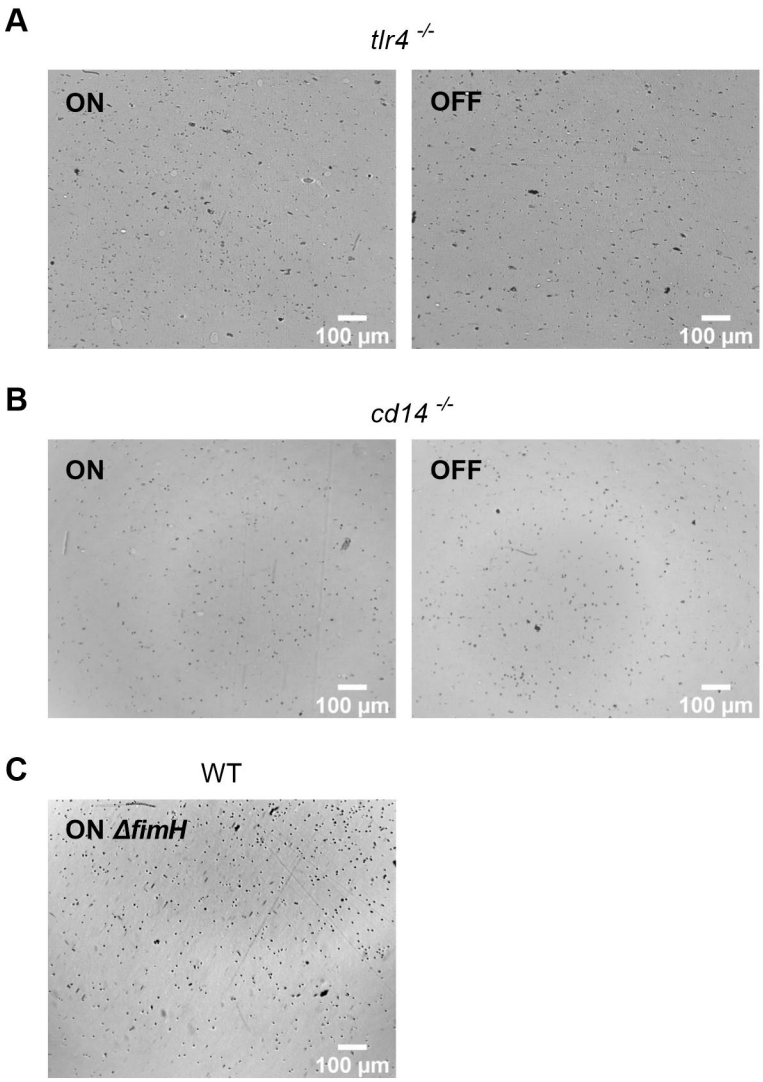

Supplementary Figure 3: *FimH and CD14, but not TLR4, are important for the observed adhesion phenotype.* ***A.*** *Adhesion assay of tlr4$^{-/-}$ DCs after ON and OFF stimulation (quantification see Figure 2-3A).* ***B.*** *Adhesion assay of cd14$^{-/-}$ DCs after ON and OFF stimulation (quantification see Figure 2-3B).* ***C.*** *Adhesion assay of WT DCs after ON ΔfimH stimulation (quantification see Figure 2-4E).*

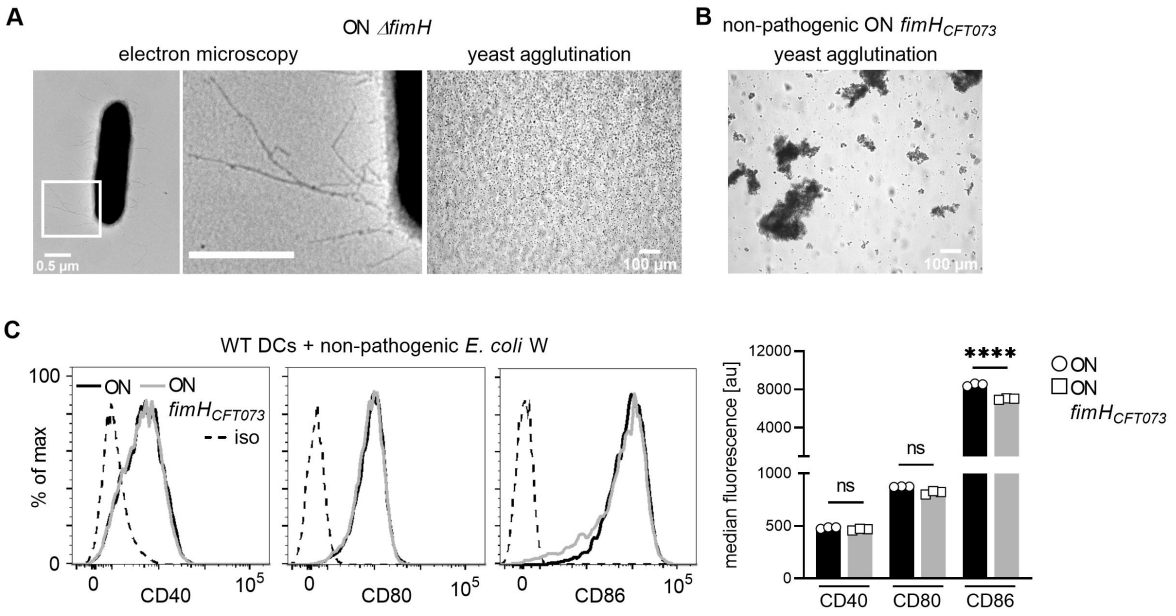

Supplementary Figure 4: *FimH is necessary, but it is not sufficient – bacteria need to have a pathogenic genetic background to cause adverse effects to DCs.*
A. *Electron microscopy images, with zoomed in regions marked in inlays, (left panel) and yeast agglutination assay (right panel) of ON ΔfimH mutant.* ***B.*** *Yeast agglutination assay non-pathogenic ON mutant with pathogenic fimH (ON fimH$_{CFT073}$).* ***C.*** *Expression levels of co-stimulatory molecules (CD40, CD80, CD86) of WT DCs after stimulation with non-pathogenic ON (black) and non-pathogenic ON fimH$_{CFT073}$ mutants (grey) (left panel; iso – isotype control). Quantification of median fluorescence values of co-stimulatory molecules (right panel).*

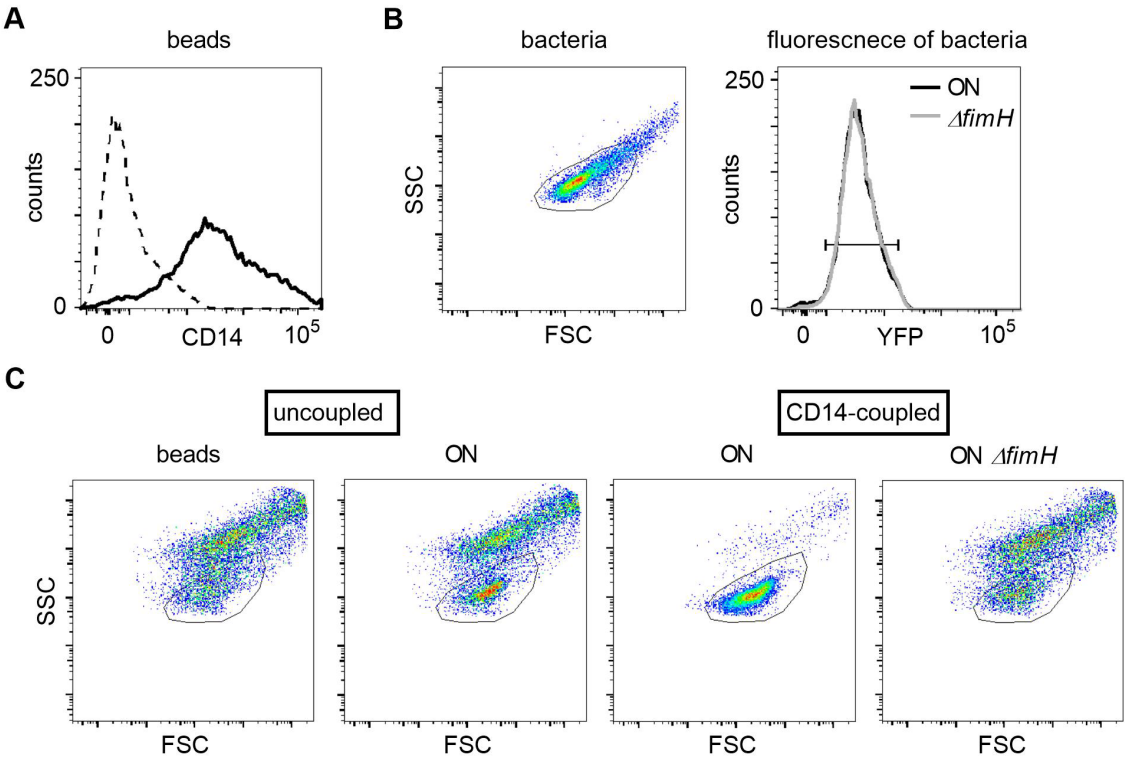

Supplementary Figure 5: *Bead assay using CD14-coupled magnetic beads.*
A. *Coupling of recombinant CD14-Fc to the magnetic Protein A beads was confirmed by staining with anti-CD14 antibody (dashed black – uncoupled beads, solid black – CD14-coupled beads).* ***B.*** *The scatter properties for the bead assay were defined by FSC and SSC properties of the bacteria (left panel). The yfp fluorescence signal of ON (black) and ON ΔfimH (grey) mutants in the bacteria gate was used to define the fluorescent properties for analysis (right panel).* ***C.*** *Events (beads ± bacteria) in FSC and SSC were recorded and are shown as dot plots. The bacteria gate as defined in A is shown.*

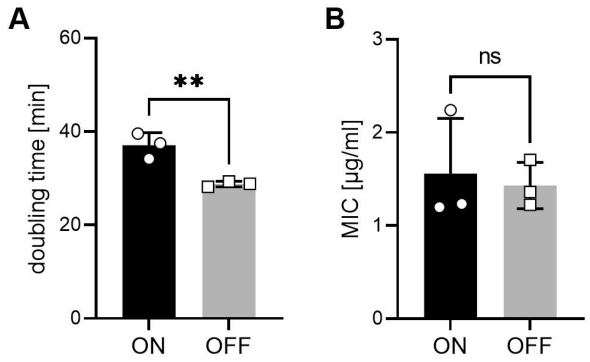

Supplementary Figure 6: *UPEC ON and OFF mutants exhibit slightly different growth rates but no difference in minimal inhibitory concentration (MIC) to gentamicin.*
A. *Doubling time of ON and OFF mutants in R10H20.* ***B.*** *MIC to gentamicin for ON and OFF mutants (MIC = 1.5 µg/ml; 5x MIC was used in the infection assays after 1 h of co-culture of bacteria and DCs).*